

THESIS ON CHEMISTRY AND CHEMICAL ENGINEERING G48

**Degradation of Persistent Micropollutants in  
Suspended-Bed Reactor by Photocatalytic  
Oxidation and Combination of Biological  
Treatment with Photocatalysis**

NATALJA PRONINA

TALLINN UNIVERSITY OF TECHNOLOGY  
School of Engineering  
Department of Materials and Environmental Technology

**This dissertation was accepted for the defence of the degree of Doctor of Philosophy in Engineering on April 19, 2017**

**Supervisor:** Senior Research Scientist Dr. Marina Kritševskaja, Department of Materials and Environmental Technology, Tallinn University of Technology

**Opponents:** Prof. Dr. Santiago Esplugas, Chemical Engineering Department, University of Barcelona, Spain

Assoc. Prof. Taavo Tenno, Chair of Colloidal and Environmental Chemistry, University of Tartu, Estonia

Defence of the thesis: June 13, 2017, 12:00  
Lecture hall: U03-103  
Tallinn University of Technology, Ehitajate tee 5,  
Tallinn

Declaration:

*Hereby I declare that this doctoral thesis, my original investigation and achievement, submitted for the doctoral degree at Tallinn University of Technology has not been submitted for doctoral or equivalent academic degree.*

Natalja Pronina



This work has been partially supported by ASTRA “TUT Institutional Development Programme for 2016-2022” graduate school “Functional materials and technologies” (2014-2020.4.01.16-0032)

Copyright: Natalja Pronina, 2017  
ISSN 1406-4776  
ISBN 978-9949-83-102-9 (publication)  
ISBN 978-9949-83-103-6 (PDF)

KEEMIA JA KEEMIASTEHNIKA G48

**Püsivate mikrosaasteainete lagundamine  
keevkihtreaktoris fotokatalüütilise oksüdatsiooniga  
ning bioloogilise oksüdatsiooni kombineerimine  
fotokatalüüsiga**

NATALJA PRONINA



## TABLE OF CONTENTS

LIST OF PUBLICATIONS .....	6
AUTHOR'S CONTRIBUTION TO THE PUBLICATIONS .....	7
INTRODUCTION.....	8
LIST OF ABBREVIATIONS AND SYMBOLS.....	9
1. LITERATURE REVIEW.....	10
1.1 Photocatalysis .....	10
1.2 Photocatalytic coatings and reactors.....	12
1.3 Micropollutants .....	13
1.4 Treatment of pharmaceuticals .....	16
1.5 Aims of the study .....	19
2. MATERIALS AND METHODS.....	19
2.1 Catalyst attachment and study of photocatalytic activity of the coatings .....	19
2.2 Evaluation of the performance of suspended-bed photocatalytic reactor .....	21
2.3 Combination of photocatalytic pre-treatment with aerobic bio-oxidation.....	22
2.4 Analytical methods .....	23
3. RESULTS AND DISCUSSION .....	26
3.1 Support material .....	26
3.2 Coatings.....	27
3.3 Performance of suspended-bed photocatalytic reactor .....	30
3.4 Combination of photocatalytic oxidation with biological treatment .....	31
CONCLUSIONS.....	33
REFERENCES.....	34
ACKNOWLEDGMENTS.....	49
ABSTRACT .....	50
KOKKUVÕTE.....	52
APPENDIX A .....	55
PAPER I.....	57
PAPER II.....	69
PAPER III .....	79
APPENDIX B .....	93
ELULOOKIRJELDUS .....	95
CURRICULUM VITAE .....	97

## LIST OF PUBLICATIONS

The present doctoral thesis is based on the following original publications:

### Paper I

Klauson, D., Poljakova, A., **Pronina, N.**, Krichevskaya, M., Moiseev, A., Dedova, T., Preis, S. Aqueous photocatalytic oxidation of doxycycline. - *Journal of Advanced Oxidation Technologies*, 2013, 16 (2), 234–243.

### Paper II

**Pronina, N.**, Klauson, D., Moiseev, A., Deubener, J., Krichevskaya, M. Titanium dioxide sol-gel-coated expanded clay granules for use in photocatalytic fluidized-bed reactor. - *Applied Catalysis B: Environmental*, 2015, 178, 117–123.

### Paper III

**Pronina, N.**, Klauson, D., Rudenko, T., Künnis-Beres, K., Kamenev, I., Kamenev, S., Moiseev, A., Deubener, J., Krichevskaya, M. Elimination of persistent emerging micropollutants in suspended-bed photocatalytic reactor: influence of operating conditions and combination with aerobic biological treatment. - *Photochemical and Photobiological Sciences*, 2016, 12, 1492–1502.

### Other publications related to the research:

Krichevskaya, M., Preis, S., Moiseev, A., **Pronina, N.**, Deubener, J. Gas-phase photocatalytic oxidation of refractory VOCs mixtures: Through the net of process limitations. - *Catalysis Today*, 2017, 280 (1), 93-98.

Klauson, D., Šakarašvili, M., **Pronina, N.**, Krichevskaja, M., Kärber, E., Mikli, V. Aqueous photocatalytic degradation of selected micropollutants by Pd-modified titanium dioxide in three photoreactor types. - *Environmental Technology*, 2017, 38 (7), 860–871.

Klauson, D., Gromyko, I., Dedova, T., **Pronina, N.**, Krichevskaya, M., Budarnaja, O., Oja Acik, I., Volobujeva, O., Sildos, I., Utt, K. Study of photocatalytic activity of zinc oxide nanoneedles, nanorods, pyramids and hierarchical structures obtained by spray pyrolysis. - *Materials Science in Semiconductor Processing*, 2015, 31 (1), 315–324.

Klauson, D., Pilnik-Sudareva, J., **Pronina, N.**, Budarnaja, O., Krichevskaya, M., Käkinen, A., Juganson, K., Preis, S. Aqueous photocatalytic oxidation of prednisolone. - *Central European Journal of Chemistry*, 2013, 11 (10), 1620–1633.

## **AUTHOR'S CONTRIBUTION TO THE PUBLICATIONS**

The contribution of the author to the papers listed below is as follows:

**Paper I:** The author carried out part of the experiments and respective analyses, analyzed obtained data and participated in writing of the paper.

**Paper II:** The author carried out the experimental work, interpreted the results and wrote the paper. She presented the results at the 8<sup>th</sup> European Meeting on Solar Chemistry and Photocatalysis (SPEA8): Environmental Applications.

**Paper III:** The author conducted part of the experiments, supervised the experimental work of three M.Sc. students, interpreted the results and wrote the paper. She presented the results at the 4th European Conference on Environmental Applications of Advanced Oxidation Processes (EAAOP-4).

## INTRODUCTION

Water is a key resource crucial for natural ecosystems and human life and that makes the ensuring of drinking water quality and appropriate wastewater decontamination an important research topic. The presence of substances resistant to conventional biological wastewater treatment systems, e.g. pharmaceuticals, is posing an increasing challenge for environmental and health protection.

To eliminate the discharge of pharmaceuticals with effluents of wastewater treatment plants into the environment, the upgrading of conventional wastewater treatment systems is required and one of the most feasible choices is to apply the advanced oxidation technologies, such as photocatalysis. Photocatalysis is relatively inexpensive technology capable of destroying variety of pharmaceutical compounds; however, its widespread implementation is limited due to major obstacles related to catalyst separation after water treatment.

The implementation of photocatalytic suspended-bed reactor, where catalyst is immobilized onto a support, allows simplifying catalyst separation while benefitting from the high light utilization and reactant-catalyst contact. However, despite all the advantages, bed material is subjected to high levels of mechanical stress causing the detachment of photocatalyst. This is the main limitation of suspended-bed reactor that could be overcome by the appropriate choice of catalyst support, attachment method and reactor operating conditions.

This research is focused on the development of catalyst immobilization procedure onto support to be applied in the photocatalytic treatment system based on fluidized-bed concept. It is also focused on the evaluation of the performance of the treatment system for the removal of pharmaceuticals and estimation of the potential of combining this system with bio-oxidation for enhanced elimination of emerging environmental micropollutants.

This study presents one of the first implementations of lightweight expanded clay aggregates as  $\text{TiO}_2$  support and the first application of sol-gel technology for coating of expanded clay granules with  $\text{TiO}_2$ . Current research supplements the discrepant results of studies on the coupling photocatalysis and bio-oxidation for removal of pharmaceuticals. The obtained knowledge contributes to the further development of the photocatalytic oxidation process and its applications in wastewater treatment.

## LIST OF ABBREVIATIONS AND SYMBOLS

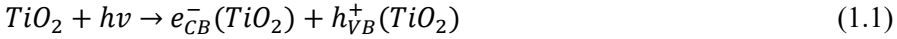
AMO	amoxicillin
AOP	advanced oxidation processes
BOD <sub>7</sub>	7-day biochemical oxygen demand
CB	conduction band
COD	chemical oxygen demand
CSTR	continuous flow stirred-tank reactor
DC	doxycycline
DNA	deoxyribonucleic acid
DOC	dissolved organic carbon
<i>E</i>	photocatalytic efficiency
<i>e</i> <sup>-</sup>	electron
<i>h</i> <sup>+</sup>	hole
HPLC-PDA-MS	high-performance liquid chromatograph with photodiode array detector and mass spectrometer
HTR	hydraulic retention time
IARC	International Agency for Research on Cancer
IC	ion chromatograph
IUPAC	International Union of Pure and Applied Chemistry
LECA	lightweight expanded clay aggregates
MLSS	mixed liquor suspended solids
MLVSS	mixed liquor volatile suspended solids
PNL	prednisolone
SEM	scanning electron microscope
SMZ	sulfamethizole
SNMS	secondary neutral mass spectrometer
sOUR	specific oxygen uptake rate
SVI	sludge volume index
TBOT	tetrabutyl orthotitanate
TC	total carbon
TEOS	tetraethyl orthosilicate
TN	total nitrogen
TTIP	titanium tetraisopropoxide
UV	ultraviolet
VB	valence band
XRD	X-ray diffraction
WWTP	wastewater treatment plant

# 1. LITERATURE REVIEW

## 1.1 Photocatalysis

Heterogeneous photocatalysis is the initiation of photochemical reactions in the presence of a semiconductor catalyst, usually  $TiO_2$ , that is activated by light radiation. Since the studies on  $TiO_2$  photocatalytic activity and generation of hydrogen have been reported in 1972 by Fujishima and Honda [1], the scientific interest in photocatalysis is year by year increasing due to a wide range of its functions [2]. Heterogeneous photocatalysis has a variety of applications ranging from modification and functionalization of a surface, assigning to it antifogging, antimicrobial and self-cleaning property, and solar energy conversion through to light-assisted hydrogen production and polluted air and water remediation [3-5].

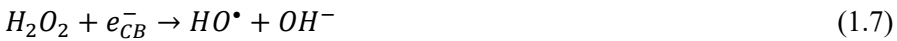
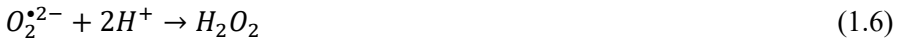
Heterogeneous photocatalysis over  $TiO_2$  irradiated with UV-A light is one of the most common photocatalytic combinations, where the process is initiated by the absorption of a photon with energy greater than the band gap of the semiconductor (ca. 3.2 eV for anatase, wavelength lower than ca. 385 nm) resulting in excitation of electron ( $e_{CB}^-$ ) and its migration from valence band (VB) to the conduction band (CB) and leaving a positive hole ( $h_{VB}^+$ ) in the valence band (Eq. 1.1) [5, 6].



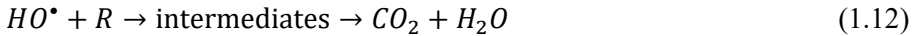
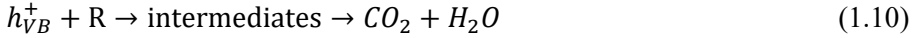
Generated electron  $e_{CB}^-$  can react with electron acceptors, such as oxygen, forming superoxide radical (Eq. 1.2).



Further reaction through numerous radical species can lead to the formation of a highly reactive hydroxyl radical,  $HO^\bullet$ , with high oxidation potential of 2.8 V (Eq. 1.3-1.9) [7, 8].



Generated in the valence band hole,  $h_{VB}^+$ , that owns oxidation potential of ca. 3 V, participates in direct oxidation of organic compounds resulting in the formation of  $CO_2$  and  $H_2O$  as end products (Eq. 1.10) or reacts with water to form hydroxyl radicals (Eq. 1.11) [5, 9]. Hydroxyl radicals can non-selectively oxidize organic molecules, eventually leading to their total mineralization [5]. Oxidation of the organic pollutant (R) via successive attacks by hydroxyl radicals is shown below (Eq. 1.12):



Both holes and electrons need to be scavenged efficiently in order to avoid their accumulation and recombination.

Besides  $TiO_2$ , various metal oxides and sulfides, such as  $ZnO$ ,  $WO_3$ ,  $Nb_2O_5$ ,  $Bi_2O_3$ ,  $SnO_2$ ,  $CdS$ ,  $ZnS$ ,  $SrTiO_3$ ,  $BiVO_4$ ,  $CeO_2$  and  $Fe_2O_3$  [10-13], were also studied for photocatalytic purposes, however  $TiO_2$  is the most widely applied due to its relatively high photocatalytic activity, chemical stability, availability and reasonable price [3, 14, 15].  $TiO_2$  exists in three crystalline phases, anatase, brookite and rutile. In general, rutile is less photocatalytically active among crystalline phases and the difference in photocatalytic performance between anatase and brookite is being debated [16-21]. Even though  $TiO_2$  is usually referred as non-toxic, nano-sized particles so often used in photocatalytic studies are not that harmless and have been reported to enter eukaryotic cells [22-24], affect a variety of cell functions [23, 25], and are classified as a possible human carcinogen (IARC, group 2B) [23, 26].

Several commercial photocatalytic water treatment systems using artificial UV-light as the irradiation source are available on the market. Some photocatalytic water treatment applications using artificial UV-light have already achieved commercial maturity but have not yet widely entered the global market. Small-scale photocatalytic wastewater treatment systems, such as *Photo-Cat*, *PhotoCREC* and *Gyrecat*<sup>®</sup>, have already been on the market for several years [27-30], whereas pilot projects for drinking water purification in developing countries have been started recently by *Panasonic* [31], and solar photocatalytic water treatment plants, such as *SOWARLA SUN* and *SOLARDETOX*<sup>®</sup>, are at a demonstration phase [32, 33].

Generally, while majority of studies on photocatalytic water treatment were conducted in lab-scale reactors, the construction of efficient intermediate and large-scale photocatalytic reactors for industrial and commercial applications is challenging due to several technical barriers. To achieve a successful and economically viable commercial large scale implementation, several key technical constraints ranging from catalyst development, reactor design and

process optimization to safe photocatalyst nanoparticle retention in photocatalytic oxidation reactors have to be overcome [34].

## 1.2 Photocatalytic coatings and reactors

Reactor configuration plays an important role in achieving commercial success as it defines the mode of use of irradiation (solar or artificial, external or immersed irradiation source) and catalyst (slurry or immobilized), as well as gives an opportunity to improve the process performance via the optimization of operational conditions.

Despite the fact that so widely studied slurry type systems are efficient in the degradation of pollutant mainly due to a large reactive surface area and superior mass-transfer properties [35], the main practical shortcoming is costly separation of the nanoscale photocatalyst particles from the liquid phase that follows treatment. To overcome limitations related to catalyst separation and recovery, reactors with catalyst immobilized on solid support could be an appropriate solution. In fixed-bed systems, despite an inherent decrease in the surface area of the catalyst available for reactions, the penetration depth of light is improved. Suspended-bed reactor, where catalyst support is fluidized, has more advantages over fixed-bed one as it exhibits enhanced mass transfer and light utilization due to better delivery of both photons and target compounds to the photocatalyst surface vicinity. To benefit from the reactor construction, the catalyst should be attached to a suitable substrate.

Selection of the support for catalyst immobilization is an important issue and must consider technological, economical and practical aspects. The substrate should meet certain requirements, although it may be difficult for a single support material to fulfil all of them [36, 37]:

- transparency to applied radiation
- strong adhesion between photocatalyst and support without adversely affecting the performance of the photocatalyst
- high specific surface area
- structure, that enables easy separation
- proper geometry to facilitate irradiation of the photocatalyst
- lightweight, to minimize energy needed for fluidization

Apart from the above mentioned criteria, support should also be inert and stable, insoluble, non-toxic and preferably inexpensive [38].

Different types of supporting materials, such as glass, quartz, silica, activated carbon, zeolites, textiles, stainless steel, ceramics, and polymers, have been studied [36-41]. However, for instance, steel and glass do not satisfy lightweight material requirement having relatively high density and resulting in higher energy demand for the fluidization of suspended bed with higher mechanical stress placed on coatings as a consequence.

The chemical composition of the substrate has been reported to affect photocatalytic activity of TiO<sub>2</sub> coatings. For example, during thermal treatment step in sol-gel synthesis, sodium or other alkali metal cations can diffuse from the substrate to the TiO<sub>2</sub> film leading to a detrimental effect on the photocatalytic activity [42]. In [43] it was concluded that sodium content influences TiO<sub>2</sub> films synthesized via sol-gel route by inhibiting the crystallization and growth of anatase phase and promoting the formation of brookite phase. The resulted poor crystallinity of TiO<sub>2</sub> film is the main reason for its lower photocatalytic activity if compared to that of the TiO<sub>2</sub> films prepared on substrates with lower sodium content.

Fluidization during suspended-bed reactor operation may reduce the lifetime of photocatalytic coatings resulting in catalyst detachment and washout from the support due to collision and attrition of the bed. Thus, the method of catalyst immobilization should be selected carefully to assure satisfactory photocatalytic activity along with mechanical stability, i.e. good adhesion and abrasion resistance of the photocatalytic coating on the bed material [44, 45].

Numerous techniques were reported for the immobilization of TiO<sub>2</sub> on support material, for instance, hydrothermal treatment, thermal treatment, chemical vapor deposition, electrodeposition, sol-spray, electron beam evaporation, reactive magnetron sputtering, spray pyrolysis, electrophoresis and sol-gel [37, 42].

The sol-gel method has been extensively reported as a simple, convenient and inexpensive pathway for TiO<sub>2</sub> immobilization with flexible applicability to a wide range of substrate sizes and shapes [42]. Sol-gel chemistry is based on the formation of an oxide network from sol through series of hydrolysis and condensation reactions of metal alkoxides [46, 47]. Dip-coating and spread-coating are two main techniques applied for the deposition of sol onto substrates [48-50]. Despite the fact that sol-gel method has low processing temperature, it requires heat treatment step after deposition to allow crystallization to occur; this step sets limitations for the selection of support material to avoid the melting of the substrate.

### **1.3 Micropollutants**

A growing body of literature broadly documents the presence of a variety of organic micropollutants in aquatic environment, including surface, ground and wastewater, as well as tap and drinking water. Micropollutants are persistent and bioaccumulative organic substances occurring in the environment in concentrations from ng L<sup>-1</sup> up to several µg L<sup>-1</sup> which have potential to cause adverse effects on the ecosystem and human health, even at such low concentrations [51-54]. These compounds usually have high rate of production and consumption, their discharge is rarely or not regulated and as a consequence of improper management of wastewater along with the diffuse source of contamination they are continuously discharged in the environment.

Emerging micropollutants are not necessarily newly occurring in water bodies; due to the rapid development of analytical methodologies for the reliable detection and quantification of these compounds in water at very low concentrations, their presence and significance has been elucidated only for last three decades [55]. The micropollutants include many substances of anthropogenic origin, arising from industry, agriculture and hospital activity, involving surfactants, flame retardants, gasoline additives, biocides, pesticides, pharmaceuticals and personal care products [54].

Among these micropollutants, pharmaceuticals are of increasing concern as they represent an overgrowing fraction of trace contaminants with multiple chemical structures, properties and modes of action that are designed to have biological effects on living organisms and are suspected to have potential to negatively affect non-target species in the environment [56-59]. More than 3000 different substances are currently in use as pharmaceuticals in Europe [60] and many of them have already been detected in environmental waters [61]. Although, it was reported that pharmaceuticals do not present acute toxic effects on aquatic organisms due to their low concentrations [62-65], concerns have been raised for chronic exposure. Despite the fact that concentrations of single pharmaceutical compounds are usually much lower than the therapeutic doses and reported to have no effect on tested aquatic organisms, it should be bear in mind that environmental water bodies receive a cocktail of pharmaceuticals and their metabolites [66] and certain specific combinations are prone to show a strong synergism that may pose a potential ecological risk for aquatic ecosystems [67-69]. Furthermore, it was also reported that pharmaceutical micropollutants can be transported via the food-chain up to secondary and tertiary consumers and impact the terrestrial higher vertebrates [70, 71, 72].

As an illustrative example of adverse effects of pharmaceuticals on non-target organisms the following evidences were reported: hyperoestrogenism in cattle, adverse effects on development, immunocompetence and disease prevalence of egg of vultures and kites, bird of prey poisonings in Canada, USA and the UK, induced hypothermia or behavioral impairment in vulture, altered immune function, changed development and behavior of adult male starlings [70].

The brief review of the pharmaceuticals used in this work is presented below.

**Amoxicillin** (AMO) is a widely consumed broad-spectrum, semisynthetic penicillin class antibiotic with bactericidal activity that acts against numerous gram-positive and gram-negative bacteria [73-76]. After administration amoxicillin is excreted unchanged in urine and feces at high rates up to 80% [74, 76] and therefore, it is likely to find trace concentrations of amoxicillin in the environment.

In addition to the risk of promotion of antibiotic resistance among pathogenic bacteria [77], a frequent exposure to this drug may produce allergic reactions [76] and has the potential to induce genomic injuries in human deoxyribonucleic acid (DNA) [78]. In aquatic environments, amoxicillin (at  $\mu\text{g L}^{-1}$  concentrations) was

reported to exhibit toxicity to the blue green algae *Synechococcus leopoliensis* [79], and trigger the changes in metabolism of the photosynthetic cyanobacteria *Microcystis aeruginosa* [80]. Furthermore, exposure to amoxicillin in mg L<sup>-1</sup> concentration range leads to abnormal development of zebrafish *Danio rerio* embryos and showed changes in the normal enzyme activity of adult fish [81]. Due to the adverse effects observed on the population parameters of rotifer species *Brachionus calyciflorus* and *Brachionus havanaensis* exposed to amoxicillin, these drugs can be considered as ecologically harmful also to zooplankton [82]. It has been also reported that continuous exposure to amoxicillin may result in accumulation of the parent compound and its metabolites in the tissues of aquatic organisms [76].

**Doxycycline (DC)** is a long-acting semi-synthetic antibiotic with bacteriostatic mechanism of action used against a wide range of gram-positive and gram-negative bacteria [83]. Due to its favorable antimicrobial properties and low cost DC possesses many advantages over other tetracycline class antibiotics and has become one of the most often used antibiotic in the therapy of human and animal infections [84].

In terms of environmental toxicity, DC has been reported to have effect on the cell permeability and growth inhibition of algae *Chlorella pyrenoidosa* and *Scenedesmus obliquus* [85]. Additionally, tetracyclines were reported to inhibit mitochondrial function across different species already at the concentration range of 0.5 to 25 mg L<sup>-1</sup> with risk of negative impact on the environment and health of non-target organisms. As a result of exposure of worms, flies, and plants to DC, a noticeable reduction and delay of growth, as well as decrease in oxygen consumption were observed [86]. At higher concentrations, that might be a case near places of industrial or hospital discharge, the drug-induced marked changes in glycogen and protein content of gills, muscle and viscera of the zebrafish *Danio rerio* were monitored [87].

**Sulfamethizole (SMZ)** is a sulfonamide antibiotic with bacteriostatic mode of action. Similarly to AMO and DC, SMZ is a wide spectrum antimicrobial applied against most of gram-positive and many gram-negative organisms. Sulfonamides are often used in aquaculture for veterinary applications and in the treatment of human respiratory and urinary tract infections [88].

Bacterial sensitivity to different sulfonamides is the same and it is enough to develop the antibiotic resistance to one of sulfonamides to be resistant to all of them, meaning that discharge into environment inducing the development of antibiotic resistance poses high threat to human health [89]. The systematic increase of the resistance of bacterial strains to sulfonamide class antibiotics has been already reported recently, being most often observed in *Escherichia coli*, *Salmonella enteric* and *Shigella spp.* bacterial strains [90].

Exposure of zebrafish *Danio rerio* to the environmentally relevant concentrations of sulfonamides demonstrated the changes in metabolism of fish and induced measurable effects on spontaneous swimming activity and heartbeat

rate [91]. While the exposure of zebrafish embryos to low concentrations of sulfonamides (ca.  $1 \mu\text{g L}^{-1}$ ) resulted in characteristic malformations, including pericardial edema, yolk sac edema, hemagglutinations, tail deformation and swim bladder defects [92]. Sulfonamides are also suspected to affect the growth and development of plants and confirmed to be toxic towards green algae *Scenedesmus vacuolatus* and duckweed *Lemna gibba* [90, 93]. Sulfonamides can also accumulate in various organisms in the food chain, and this accumulation may lead to a local increase in toxic effects induced by these drugs [94].

**Prednisolone** (PNL) is a synthetic glucocorticoid class pharmaceutical similar to the natural hormone cortisone that is widely used in the therapy of severe inflammation, autoimmune conditions, hypersensitivity reactions and organ rejection [95, 96]. PNL has been repeatedly detected in the environment [97, 98].

Studies on toxicity of PNL to aquatic organisms revealed the range of effects varying from altering early ontogeny and significantly affecting embryo behavior of zebrafish *Danio rerio* at environmentally relevant concentrations to growth inhibition of the freshwater crustacean *Ceriodaphnia dubia* at higher concentrations [96, 97, 99].

## 1.4 Treatment of pharmaceuticals

Widely used so far conventional wastewater treatment has been shown to be ineffective in complete elimination of micropollutants and results in continuous discharge of pharmaceuticals in bioactive form into environmental matrices [52, 54, 100-110]. Moreover, wastewater treatment plants (WWTPs) treating households, hospitals and industry wastewater are considered to be the main release pathway for pharmaceuticals [60].

From a legislation point of view, currently the discharge of pharmaceuticals is not regulated by the Water Framework Directive 2000/60/EC (WFD) that is aimed to protect aquatic environments and related organisms; these micropollutants are also not included in the daughter Directive 2008/105/EC (PSD) stating the List of Priority Substances. However, there are seven pharmaceutical compounds added to the watch list (Decision 2015/495/EU) to be monitored in the European Union in order “to gather monitoring data for the purpose of facilitating the determination of appropriate measures to address the risk posed by those substances” [111]. The list contains following pharmaceuticals: nonsteroidal anti-inflammatory drug diclofenac, hormones — 17-alpha-ethinylestradiol, 17-beta-estradiol and estrone, and macrolide antibiotics — erythromycin, clarithromycin and azithromycin [111, 112].

The pharmaceuticals selected for the present study have been detected in both influents and effluents of WWTPs. The highest reported concentrations in WWTP effluents that the author was able to find for these compounds were 0.72, 2000, 2.4 and  $439 \text{ ng L}^{-1}$  for PNL, AMO, SMZ and DC, respectively [113-116].

Because of limited removal of pharmaceuticals under conventional treatment applied in the WWTPs, the process improvement and implementation of additional techniques are required to eliminate pharmaceuticals from wastewater [106].

For these reasons, application of various technologies, such as membrane filtration, coagulation-flocculation, activated carbon adsorption, advanced oxidation processes (AOPs), have been investigated to achieve high quality of treated effluents [62, 109, 117]. While in membrane filtration, coagulation-flocculation and activated carbon adsorption pollutants are only transferred from one phase to another and hence regeneration and post-treatment are needed for their total elimination, in AOPs the pollutants are degraded.

AOPs are promising technologies for environmental remediation, due to their ability to mineralize or at least partially decompose a wide range of non-biodegradable or recalcitrant organic compounds into intermediates that are more biodegradable and less harmful and highly vulnerable to microbial degradation [118]. Their mode of action is based on the generation of reactive oxygen species, e.g. hydroxyl radicals, and these technologies have been proven to rapidly degrade a broad spectrum of pharmaceuticals [119-121].

Among AOPs  $\text{TiO}_2$  photocatalysis has become an attractive treatment process due to the catalyst low cost and photostability [62, 122]. Moreover, the ability of photocatalytic oxidation to degrade a variety of pharmaceutical compounds, including the ones selected for present study, has been previously confirmed [120, 123-126].

However, application of photocatalytic oxidation for complete mineralization of pollutants is generally not feasible due to relatively high energy demand (if artificial sources of irradiation are used) and low degradation rate at the current state of catalytic materials development and thus prolonged time of treatment which increase the cost [127]. Therefore, coupling photocatalytic treatment and biodegradation is a promising approach that could substantially reduce the cost and enhance the efficacy of elimination of non-biodegradable contaminants [128].

One option is to apply photocatalytic degradation as a pre-treatment to obtain biodegradable wastewaters. This can be justified if toxic, inhibitory or refractory to microorganisms compounds are converted during pre-treatment into intermediates, that microorganisms are able to degrade in a subsequent bioreactor [121].

As an example, the integrated processes involving photocatalysis as a pre-treatment coupled with a biological treatment for removal of poorly biodegradable and toxic for microorganisms antibiotics tetracycline and tylosin were studied [129]. No biodegradation was found during activated sludge treatment of tetracycline indicating no improvement in the biodegradability of its by-products forming after two hours of photocatalytic treatment. However, in case of tylosin, the same treatment conditions resulted in the formation of by-

products with significantly higher biodegradability (56% COD decrease during bio-oxidation).

Consequently, when photocatalytic oxidation is considered for application as a pre-treatment stage prior to biological processing, its performance in terms of changes in toxicity and biodegradability has to be adequately evaluated with process parameters optimized achieving enhanced biodegradability with minimal mineralization [128, 130].

The photocatalytic degradation of fluoroquinolone antibiotic moxifloxacin under UV-A irradiation resulted in almost complete oxidation of parent compound with no noticeable mineralization observed [131]. Decrease in an algal growth inhibition from 72 to 14% after 150 min of treatment indicated the reduction of solution toxicity confirming the suitability of photocatalysis as a pre-treatment process.

Another option is to apply photocatalytic oxidation as a post-treatment after biodegradation, thus allowing to remove the biodegradable fraction of wastewater pollutants first and afterwards to use the photocatalytic treatment only for remaining refractory fraction [119, 121].

Almost complete elimination of 14 pharmaceuticals in an effluent sample from the Dresden Kaditz WWTP was observed in the course of photocatalytic treatment under UV-A with  $\text{TiO}_2$  and  $\text{ZnO}$  as catalysts [62]. Moreover, no reduction in the degradation efficiency caused by the complex effluent matrix has been noticed.

Photocatalytic oxidation under solar radiation with  $\text{TiO}_2$  immobilized on sand was studied as a post-treatment process for wastewater effluent spiked with propranolol, diclofenac, carbamazepine and ibuprofen [132]. The photocatalytic treatment resulted in complete removal of propranolol and diclofenac and high removal efficiency of ca. 75% for carbamazepine and ibuprofen. In addition, after photocatalytic treatment, the toxicity of studied pharmaceuticals decreased for green and blue-green algae along with slight increase in the biodegradability of treated solution, that led authors to the conclusion that photocatalysis has the potential to improve the susceptibility of effluent to further biodegradation in the environment.

$\text{TiO}_2$  photocatalysis was applied as a post-treatment for an urban WWTP effluent containing amoxicillin, carbamazepine and diclofenac [133]. In contrast to the findings in [62], degradation rate of the pollutants in effluent matrix was less than two times slower than in distilled water; the deterioration of the oxidation process performance because of the competition of target pharmaceuticals with other oxidizable compounds and presence of radical scavengers was also observed in [119]. By the end of the treatment toxicity to *Pseudokirchneriella subcapitata* was decreased from 66 to 41%, although, having its minimum of 21% after 10 min of treatment. Generally speaking, the photocatalytic treatment did not completely eliminate the toxicity under the investigated conditions [133].

Sometimes it is even advisable to place AOPs between two biological processes to reduce the competition with other organic matter in the pre-treatment stage and degrade oxidation by-products in the post-treatment stage [117].

Anyhow, depending on the wastewater nature and properties the optimization of photocatalytic process design and operation parameters is essential in order to achieve desirable effluent quality.

## **1.5 Aims of the study**

Summarizing the review above, photocatalysis is a cost-effective and promising technology for water decontamination from emerging persistent pollutants. In theory, its combination with biological treatment will enhance the efficiency of pollutant removal and reduce the treatment cost. However, for practical use of photocatalysis the methods of the catalyst attachment and synthesis on granulated support to simplify catalyst separation should be developed and the conditions allowing compatibility of photocatalysis with biotreatment should be investigated.

The aim of the study was to develop a method to prepare photocatalytically active and mechanically stable TiO<sub>2</sub> coatings on support material to be applied in photocatalytic suspended-bed reactor, and to couple photocatalytic treatment with activated sludge process for decontamination of pharmaceutical-polluted water.

The primary objectives of the present research were as follows:

- to search for and assess the method of TiO<sub>2</sub> photocatalyst attachment to expanded clay granules used as support material to be applied in suspended-bed photocatalytic reactor
- to optimize the procedure of TiO<sub>2</sub> catalyst synthesis and attachment in order to minimize catalyst washout during suspended-bed reactor operation and maximize photocatalytic activity
- to optimize suspended-bed reactor operation conditions
- to evaluate the efficacy of elimination of micropollutants (AMO, SMZ, DC and PNL separately and in mixture) during photocatalytic treatment
- to determine the applicability of coupling photocatalytic treatment and aerobic bio-oxidation for DC removal.

## **2. MATERIALS AND METHODS**

### **2.1 Catalyst attachment and study of photocatalytic activity of the coatings**

Lightweight expanded clay aggregates (LECA, Saint-Gobain Weber) of 2-3 and 4-5.5 mm in diameter were selected as substrate for TiO<sub>2</sub> attachment. Two

methods of catalyst attachment were studied: adsorption from catalyst suspensions and synthesis and immobilization via sol-gel process. The procedures of fixation of TiO<sub>2</sub> on LECA by adsorption from aqueous or isopropanolic suspensions and via sol-gel process with tetraethyl orthosilicate (TEOS) as a precursor are described in detail in *Paper I*. The procedures of TiO<sub>2</sub> attachment via sol-gel process with tetrabutyl orthotitanate (TBOT) or titanium tetrakisopropoxide (TTIP) as precursors as well as using commercial sols Hombikat XXS 100 and S5-300A are presented in *Paper II*. Dip-coating technique was applied for coating the substrate with TBOT-, TTIP-based solutions and Hombikat XXS 100 and S5-300A sols. The titania source for suspension and TEOS-based methods was P25 TiO<sub>2</sub> nanoparticles (Evonik) while in TBOT- and TTIP-based methods additionally to P25, TiO<sub>2</sub> was also synthesized during the sol-gel process from precursors. All the studied attachment methods can be divided in three groups, adsorption, sol-gel and combination of adsorption with sol-gel. The list of studied coating preparation procedures with the references to a respective article is schematically presented in Fig. 2.1.

Among studied procedures, coatings prepared with TTIP-based sol-gel solution exhibited higher photocatalytic activity and mechanical stability during DC degradation in suspended-bed reactor operation. Therefore, to improve the photocatalytic and mechanical properties of this way prepared coatings, the influence of preparation conditions and sol composition on the performance of the coatings was investigated as described in detail in *Paper II*. The following parameters of the preparation procedure were studied: TiO<sub>2</sub> P25 powder and TTIP precursor concentration in sol were varied in the range of 0 to 5.5 and 9.9 to 15.3 wt%, respectively, withdrawal speed during dip-coating was changed from 0.5 to 2.0 mm s<sup>-1</sup>, heat treatment temperature from 400 to 600°C and duration from 1 to 3 h. The influence of heat treatment in nitrogen or air atmosphere on the properties of photocatalytic coating was also investigated.

The photocatalytic activity and stability of coatings were evaluated by DC (Table 2.1) degradation experiments conducted in two stirred reactors described in *Paper I* or lab-scale borosilicate glass suspended-bed reactors described in *Paper II*. Stirred reactors were equipped with one UV-A light source positioned horizontally over the reactors; lab-scale suspended-bed reactors with air diffusers at the reactor bottom for fluidization of support were irradiated by two UV-A lamps equipped with light reflectors placed vertically around the reactors. To account for the elimination of DC due to its adsorption onto catalyst support one of two reactors was operating in dark conditions (reference experimental runs). In stirred reactors the DC solution with initial concentration of 25 mg L<sup>-1</sup> and volume of 0.2 L was treated under irradiation intensity of 15 W m<sup>-2</sup> at 24 ± 1°C for 5 h in presence of 7 g of coated expanded clay that corresponds to the concentration of 35 g L<sup>-1</sup>. The conditions in suspended-bed reactors were as follows: DC initial concentration and volume of 25 mg L<sup>-1</sup> and of 0.2 L, respectively, irradiation intensity of ca. 9 W m<sup>-2</sup>, temperature 25±2°C, duration

of 3 h, expanded clay loading of 3.5 g (bed loading of 17.5 g L<sup>-1</sup>). Photocatalytic activity was characterized by photocatalytic efficiency  $E$ , mg W<sup>-1</sup> h<sup>-1</sup>, defined as decrease in the amount of target compound divided by the product of irradiation intensity, the irradiated surface of treated solution and treatment time [134]. Mechanical stability was evaluated by the turbidity measurements in solution during photocatalytic treatment. The morphology of coatings was visualized by SEM (see the *Analytical methods* section).

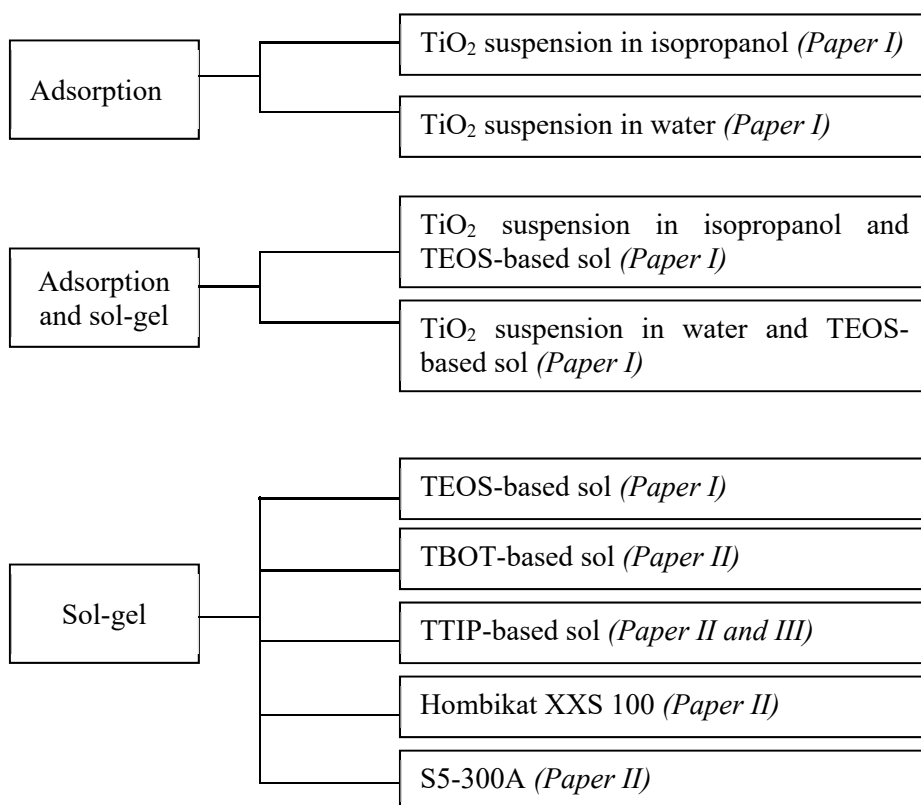


Fig 2.1. Classification of studied attachment methods.

## 2.2 Evaluation of the performance of suspended-bed photocatalytic reactor

The coatings with superior photocatalytic and mechanical properties were applied in larger lab-scale suspended-bed reactor composed of UV-A transmitting Plexiglas® XT to treat 2 L of model solution (*Paper III*). Solution to be treated was fluidized by air supplied through diffusers at the bottom of reactor and UV-A was provided by four lamps placed around the reactor. The influence of reactor operation conditions on pollutant removal was investigated varying air superficial velocity in the range of 4 to 8 cm s<sup>-1</sup> and TiO<sub>2</sub>-coated bed

loading in the range of 7 to 23 g L<sup>-1</sup>. AMO, DC, PNL and SMZ were selected as model water pollutants (Table 2.1) and were used at initial concentration of 25 mg L<sup>-1</sup> separately and at 10 mg L<sup>-1</sup> each in a mixture. Model solutions were treated under irradiation of ca. 29 W m<sup>-2</sup> at 20±4°C from 3 to 4 h. The experimental details and procedures are described in *Paper III*. Performance of the reactor was evaluated by photocatalytic efficiency with adsorption taken into account (reference experimental runs) and turbidity measurements. To evaluate the changes in toxicity during the photocatalytic treatment growth inhibition assay was applied. The tested bacterial strains were *Escherichia coli* 1655, *Staphylococcus aureus* RN4220, *Pseudomonas putida* KT2440, a bacterial strain isolated from activated sludge titled Dev3, or mixed bacterial colonies taken from activated sludge. The toxicity evaluation procedures are described in *Paper III*.

### 2.3 Combination of photocatalytic pre-treatment with aerobic bio-oxidation

Bio-oxidation experiments were conducted in two working in parallel continuous flow stirred-tank reactors (CSTR; aeration basin 7.5 L, clarifier 2.5 L) colonized with activated sludge obtained from a municipal WWTP (Paljassaare WWTP, Tallinn, Estonia). Photocatalytically pre-treated DC solution was directed to one of the CSTRs while another was operating with untreated DC solution (*Paper III*).

Two experimental runs A and B were performed: after the run A was carried out, the conditions were changed according to received results and the run B was performed.

In run A photocatalytic pre-treatment process lasted for 3 h with initial DC concentration of 25 mg L<sup>-1</sup> at previously optimized reactor operating conditions of 5 cm s<sup>-1</sup> air velocity and 19 g L<sup>-1</sup> bed loading (*Paper III*). In run B the initial concentration of DC was lowered to 10 mg L<sup>-1</sup> with treatment duration prolonged to 4.5 h. Additionally to antibiotic-containing solutions, model wastewater as the main carbon source supplemented with nutrients and containing bacteriological peptone, beef extract, urea, Na<sub>2</sub>HPO<sub>4</sub>, NaCl, CaCl<sub>2</sub>, MgSO<sub>4</sub>, and CH<sub>3</sub>COONa was continuously directed to both CSTRs (model wastewater details are presented in *Paper III*). The CSTRs were operating at 20±1°C with dissolved oxygen in the range of 2 to 4 mgO<sub>2</sub> L<sup>-1</sup> and hydraulic retention time (HTR) of 1 day.

Both experimental runs consisted of 3 stages: first, the degradation of model wastewater without DC was studied, then the transition stage took place where DC was introduced to the reactors for activated sludge adaptation and the final stage – investigation of efficiency of combined system to eliminate DC in comparison to conventional aerobic oxidation. The duration of stages in the runs A and B were as follows: the 1<sup>st</sup> stage 138 and 55 days, the 2<sup>nd</sup> stage 39 and 24 days, and the 3<sup>rd</sup> stage 37 and 42 days, respectively.

The performance of each CSTR was evaluated by measurements of activated sludge condition, nutrient removal from influent and DC concentration in effluent and in sludge.

## 2.4 Analytical methods

The list of analytical methods that were used throughout the study is presented in Table 2.2.

The specific surface area of uncoated and TiO<sub>2</sub>-coated LECA was measured by Areameter. The deposition of TiO<sub>2</sub> coating on the surface of LECA was confirmed by depth profile analysis of single elements by secondary neutral mass spectrometer (SNMS) and characterized by field emission scanning electron microscope (FE-SEM). The crystallinity of coatings was measured by X-ray diffraction (XRD).

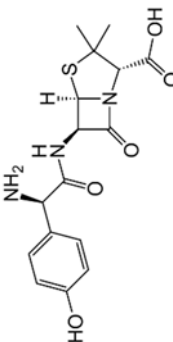
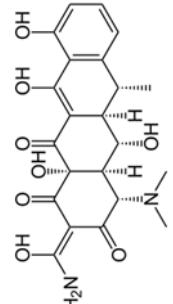
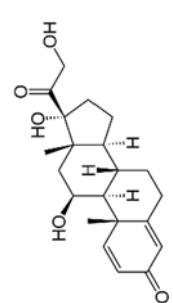
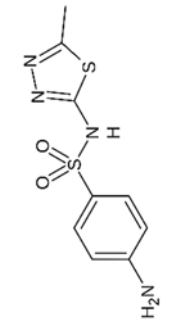
The decrease of pollutant concentration during photocatalytic oxidation experiments was measured by spectrophotometer or high-performance liquid chromatograph equipped with photodiode array detector (HPLC-PDA). The by-products formed during photocatalytic treatment were determined using mass spectrometer (HPLC-MS).

Mineralization was evaluated by dissolved organic carbon (DOC) measurements. Turbidity of treated solution caused by coating detachment due to attrition during fluidization was measured spectrophotometrically.

The activated sludge condition during aerobic bio-oxidation experiments was evaluated by monitoring the concentration of microorganisms in the bioreactor (MLSS, MLVSS), sludge settleability (SVI), turbidity of bioreactor effluent and sludge specific oxygen uptake rate (sOUR). The performance of bioreactor was assessed by monitoring the nutrient conversion and removal (TC, DOC, BOD<sub>7</sub>, COD, NH<sub>4</sub>-N, NO<sub>3</sub>-N, NO<sub>2</sub>-N, TN). The concentration of DC in bioreactor influent, effluent and amount adsorbed on sludge was measured by high-performance liquid chromatography using photodiode array detector and mass spectrometer (HPLC-PDA-MS).

The details of applied methods are described in *Experimental* sections of *Papers I-III*.

Table 2.1. Structures and basic properties of AMO, DC, PNL and SMZ [135, 136].

Properties	Amoxicillin (AMO)	Doxycycline (DC)	Prednisolone (PNL)	Sulfamethizole (SMZ)
IUPAC name	(2S,5R,6R)-6-[[[(2R)-2-amino-2-(4-hydroxyphenyl)acetyl]amino]-3,3-dimethyl-7-oxo-4-thia-1-azabicyclo[3.2.0]heptane-2-carboxylic acid	(4S,4aR,5S,5aR,6R,12aR)-4-(dimethylamino)-1,5,10,11,12a-pentahydroxy-6-methyl-3,12-dioxo-4a,5,5a,6-tetrahydro-4H-tetracene-2-carboxamide	(8S,9S,10R,11S,13S,14S,17R)-11,17-dihydroxy-17-(2-hydroxyacetyl)-10,13-dimethyl-7,8,9,11,12,14,15,16-octahydro-6H-cyclopenta[a]phenanthren-3-one	4-amino-N-(5-methyl-1,3,4-thiadiazol-2-yl)benzenesulfonamide
Classification	Penicillin class antibiotic	Tetracycline class antibiotic	Glucocorticoid	Sulfanilamide class antibiotic
Molecular structure				
Chemical formula	$C_{16}H_{19}N_3O_5S$	$C_{22}H_{24}N_2O_8$	$C_{21}H_{28}O_5$	$C_9H_{10}N_4O_2S_2$
Molar mass, g mol <sup>-1</sup>	365.404	444.44	360.45	270.325
Solubility in water at 25°C, mg L <sup>-1</sup>	3430	630	223	1050*
CAS nr.	26787-78-0	564-25-0	50-24-8	144-82-1
pKa	3.23; 7.43	3.32; 7.97; 9.15	**	2.1; 5.3
Melting point, °C	194	201	235	210

\* solubility at 37°C

\*\* no reference to a pK<sub>a</sub> value was found in the literature

Table 2.2. Analytical methods applied in the study.

<b>Parameter/ Analysis</b>	<b>Analytical method/ Equipment</b>	<b>Paper</b>
Crystallinity	XRD	unpublished
Surface morphology	FE-SEM	I-II
Depth profile	SNMS	unpublished
Specific surface area	Areometer	II
DOC	TOC/TN analyzer	II-III
AMO, DC, PNL, SMZ	Spectrophotometer, HPLC-PDA HPLC-PDA-MS	I-III
Turbidity	Spectrophotometric method	I-III
Toxicity	Growth inhibition assay	III
TC	TOC/TN analyzer	III
TN	TOC/TN analyzer	III
NH <sub>4</sub> -N	Spectrophotometric method	III
NO <sub>2</sub> -N, NO <sub>3</sub> -N	IC-SCD	III
SVI	Standard Method 2710C	III
COD	Standard Method 5220D	III
BOD <sub>7</sub>	Standard Method 5210B	III
MLSS	Standard Method 2540B	III
MLVSS	Standard Method 2540E	III
sOUR	Standard Method 2710B	III

### 3. RESULTS AND DISCUSSION

#### 3.1 Support material

The SEM micrographs of LECA surface and core shown in Fig 3.1 demonstrate the presence of numerous pores on the surface. The measured specific surface area for fraction with average diameter of 2.7 mm is  $0.8 \text{ m}^2 \text{ g}^{-1}$  while the external area with no pores taken into account is  $0.004 \text{ m}^2 \text{ g}^{-1}$ . The core of the granules has a honeycomb structure due to the formation of semi-closed pores during the firing of clay at temperatures up to  $1150 \text{ }^\circ\text{C}$  in rotary kiln [137]. This structure makes the material lightweight with particle density in the range of  $735$  to  $985 \text{ kg m}^{-3}$  [138], which is the beneficial property for suspended-bed reactor application due to lower air velocity needed to fluidize the granules and uniformly distribute them within the treated solution.

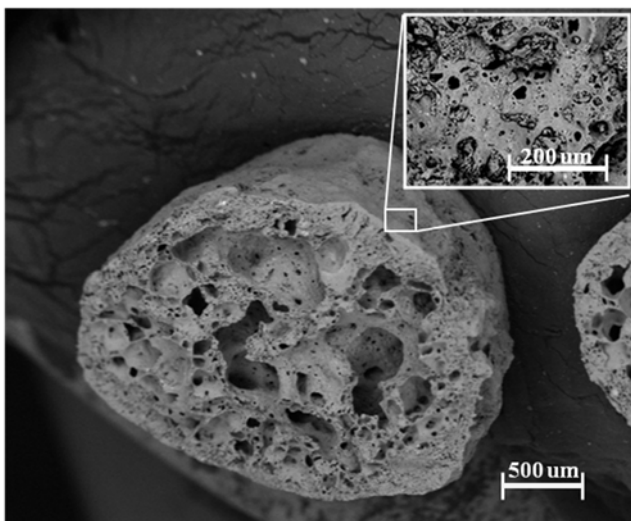


*Fig. 3.1. The SEM images of LECA core and surface (inset).*

Expanded clay granules consist mainly of  $\text{SiO}_2$ ,  $\text{Al}_2\text{O}_3$ ,  $\text{Fe}_2\text{O}_3$ ,  $\text{CaO}$ ,  $\text{MgO}$ ,  $\text{K}_2\text{O}$  and  $\text{Na}_2\text{O}$  [139-141]. Content of sodium, that is known for negative effects on  $\text{TiO}_2$  photocatalytic performance (see section 1.2 Photocatalytic coatings and reactors) is lower than 2 wt% of  $\text{Na}_2\text{O}$ , while for example in soda-lime glass, where the effect of sodium on photocatalytic activity was observed and reported is 12-16 wt% [142]. In present study, the expanded clay granules have been observed to change the pH of water in 8% slurry from ca. 6.5 to 9 that may be related to partial dissolution of soluble compounds present in LECA [143, 144]. Several studies report LECA pH to be equal to 8.4 [144-146] and it may vary depending on raw material composition.

In water treatment applications LECA are predominantly studied as an adsorbent for toxic material and metals removal [139, 141, 145, 147] and the use for photocatalytic processes has not been reported by the time this study was

started and the first article was published (*Paper I*). However, in 2013 another study on the application of expanded clay granules as substrate for the adsorption of titania nanoparticles and their use in photocatalytic degradation of ammonia was concurrently published [140].

### 3.2 Coatings

#### *Adsorption and combination of adsorption with TEOS-based sol-gel method*

The immobilization of TiO<sub>2</sub> nanoparticles by adsorption from aqueous and isopropanolic suspensions was studied. This method allowed to attach higher amount of catalyst onto LECA, if compared to studied sol-gel methods, however, the results of DC degradation experiments revealed poor binding of catalyst to the surface of expanded clay and unacceptable catalyst washout during photocatalytic experimental runs. In order to prevent the detachment of catalyst SiO<sub>2</sub> layer was deposited via TEOS-based sol-gel method on the surface of expanded clay with previously deposited TiO<sub>2</sub> by adsorption from suspension. This approach allowed to reduce the turbidity, caused by catalyst washout, and evaluate the photocatalytic activity of 1.50 and 1.35 mg W<sup>-1</sup> h<sup>-1</sup> for titania adsorbed from its isopropanol and aqueous slurries, respectively.

#### *TEOS-based coatings*

The immobilization of P25 TiO<sub>2</sub> particles by their addition to the TEOS-based sol was studied. The resulted coatings exhibited low adhesion to the substrate and showed high levels of detachment during experimental runs. The increase in TiO<sub>2</sub> content in the sol and number of deposited layers, i.e. the coating thickness, did not lead to essential increase in photocatalytic efficiency and resulted in even higher turbidity in treated solutions (over 100 FAU) (*Paper I*, Fig. 3, right).

The changes in conditions of pre-drying and drying stages of coating preparation had a noticeable effect on coatings morphology that is directly connected to the adhesion of coatings to a substrate. Coatings with cracks exhibit lower adhesion to substrate and thus it is preferable to avoid cracking of the coatings. Thus, the insufficient pre-drying stage (less than 24 h) led to the crack evolution in the coating (*Paper I*, Fig. 3, left), while drying for 24 h resulted in the decrease in turbidity up to 60 FAU and measurable photocatalytic efficiency of 0.75 mg W<sup>-1</sup> h<sup>-1</sup>.

With the preliminary substrate surface acidification (in 1 M HNO<sub>3</sub>) the stability of coatings was significantly improved resulting in decreased turbidity levels (from 60 to 20 FAU), though lowering slightly the coatings' activity from 0.75 to 0.5 mg W<sup>-1</sup> h<sup>-1</sup>.

The coatings with the best photocatalytic activity and adhesion within this series were obtained on preliminary acidified LECA with pre-drying stage of 24 h and subsequent drying of 15 h, showing only 20 FAU of turbidity with photocatalytic efficiency of 0.5 mg W<sup>-1</sup> h<sup>-1</sup> (*Paper I*, Fig. 3, middle).

### *Coatings prepared from TBOT, S5-300A or Hombikat XXS 100 sols*

The coatings prepared using commercial sols Hombikat XXS 100 and S5-300A demonstrated poor mechanical stability causing high levels of turbidity (up to 160 FAU) in treated solutions and therefore were not considered to be effective. The reason for poor binding of the coating to the surface could be the pH sensitivity of the sols. Since the support material shows basic behavior, the shift in the pH of the sol may lead to the development of unfavorable conditions for the sol polymerization and induce particle agglomeration.

Although, the mechanical stability of coatings prepared via TBOT-based sol-gel was higher (turbidity up to 60 FAU), if compared to Hombikat XXS 100 and S5-300A derived coatings, these were still considered to be less suitable for wastewater treatment application than TTIP-based coatings described further.

### *TTIP-based coatings*

The coatings prepared by TTIP-based method without P25 addition showed photocatalytic efficiency of  $1.5 \text{ mg W}^{-1} \text{ h}^{-1}$  accompanied by zero levels of turbidity in treated solution. The photocatalytic activity of this coating is attributed only to the titania formed from TTIP precursor. Clear solution with no titania washout observed indicated good adhesion of coatings to the substrate. The surface of coatings, visualized by SEM, is smooth and uniform with no cracks present (*Paper II*, Fig. 2, right). Due to the preferences of this preparation method, it was selected for the subsequent study and its processing parameters were optimized in order to enhance the photocatalytic activity of thus prepared coatings.

Addition of different amounts of P25 resulted in the increase of photocatalytic activity (up to  $2.3 \text{ mg W}^{-1} \text{ h}^{-1}$ ) and coating washout (up to 28 FAU) (*Paper II*, Table 1, series of exp. I). The addition of  $\text{TiO}_2$  particles also influenced the coating morphology, resulting in non-uniform P25 particle distribution within the coating (*Paper II*, Fig. 3, left). Furthermore, at higher amounts of P25 the evolution of crack was observed due to the increase in sol viscosity and as a consequence increased thickness of deposited  $\text{TiO}_2$  layers. The application of ultrasonication of P25 isopropanol suspension prior to sol addition allowed lowering the turbidity from 17 to 13 FAU, which can be attributed to lowered size of P25 agglomerates and improved particle distribution in coating.

The variation of TTIP concentration, i.e. of isopropanol amount, in the sol influenced the thickness of deposited coatings due to the changes in the sol viscosity (*Paper II*, Table 1, series of exp. II). The decrease in solvent amount led to the deposition of thicker coating with photocatalytic activity of  $2.3 \text{ mg W}^{-1} \text{ h}^{-1}$  while the increase in isopropanol amount resulted in thinner coating with lowered activity of  $1.4 \text{ mg W}^{-1} \text{ h}^{-1}$  (*Paper II*, Fig. 4). The most mechanically stable coatings (27 FAU) were produced with medium solvent amount (12.2 wt% TTIP concentration in the sol), while lower amount led to the coating cracking

and coating detachment and higher to insufficient anchoring of P25 and particle washout.

The changes in the withdrawal speed during substrate dip-coating, similarly to variation in solvent concentration in sol, influence the thickness of deposited coatings (*Paper II*, Table 1, series of exp. III). Higher withdrawal speed ( $2 \text{ mm s}^{-1}$ ) resulted in thicker coatings with efficiency of  $1.9 \text{ mg W}^{-1} \text{ h}^{-1}$  and speed reduction (to  $0.5 \text{ mm s}^{-1}$ ) led to the decrease in layer thickness and photocatalytic efficiency to  $1.6 \text{ mg W}^{-1} \text{ h}^{-1}$  (*Paper II*, Fig. 4). In a similar manner, turbidity increases with the increase in withdrawal speed from 20 to 29 FAU. The withdrawal speed of  $2 \text{ mm s}^{-1}$  lead to coating cracking (*Paper II*, Fig. 5).

The deposition of multiple layers improved the activity, however it weakened the adhesion of coatings.

The temperature and duration of heat treatment influences the process of  $\text{TiO}_2$  crystallization (*Paper II*, Table 1, series of exp. IV and V). The results revealed lower photocatalytic activity of the coatings, when heat treatment at  $400^\circ\text{C}$  was applied, that can be explained by the insufficient temperature for the crystallization of amorphous  $\text{TiO}_2$  to anatase (*Paper II*, Fig. 4). No effect of temperature variation on mechanical stability of the coatings have been observed. The duration of the calcination showed no influence on the activity of coatings, however their adhesion and abrasion resistance reduced with the increase in heat treatment time, pointing to the possible propagation of microcracks.

The application of heat treatment in nitrogen atmosphere instead of air resulted in up to 25% increase in photocatalytic activity accompanied by the decrease in mechanical stability, i.e. increase in turbidity up to 56%.

Depth profile analysis using SNMS confirmed the deposition of  $\text{TiO}_2$  on the surface of expanded clay (Fig. 3.2). The diffusion of the elements from the substrate could not, however, be specified due to the non-uniformity of the coating on the porous surface of clay granules. The XRD analysis proved the formation of anatase crystalline phase in the coatings.

Based on the activity and turbidity measurements the procedure of coating processing was adjusted and resulted in the production of coating with enhanced performance in terms of photocatalytic activity and mechanical stability (*Paper II*, Fig. 6).

The reduction of turbidity over 6.5 times accompanied by only 35% activity loss, as a result of twofold decrease in bed loading, demonstrated essential effect of reactor operation conditions on the performance and lifetime of coatings. Thus, the optimization of bed material loading and fluidization air velocity have been carried out in a larger lab-scale suspended-bed reactor.

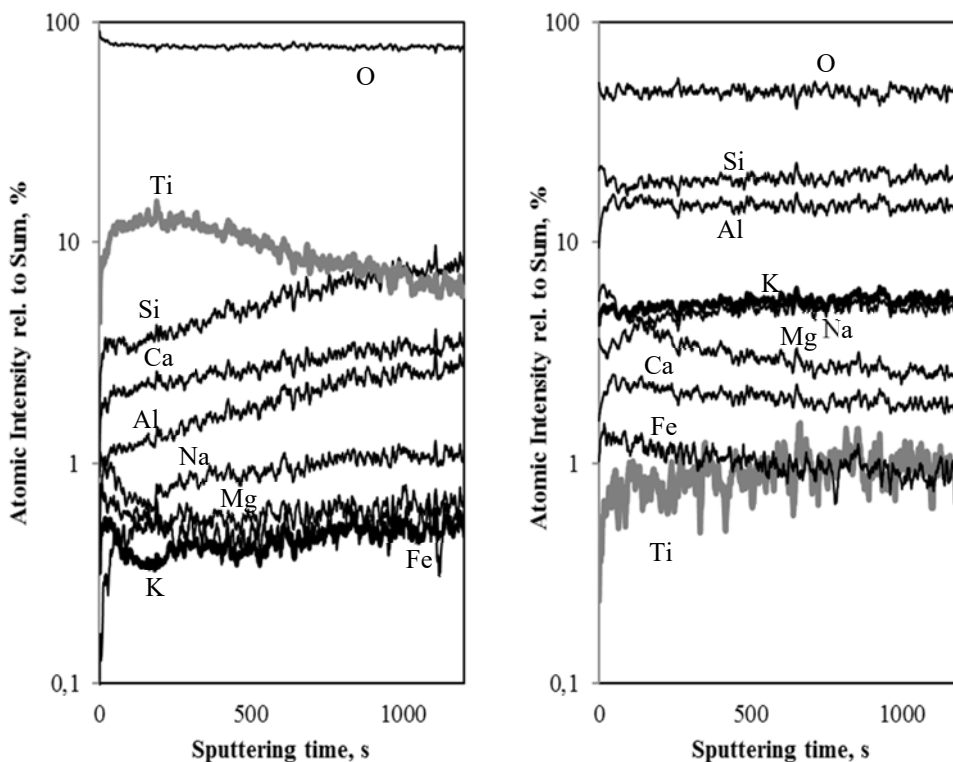


Fig. 3.2. Depth profiles of coated (left) and uncoated (right) LECA.

### 3.3 Performance of suspended-bed photocatalytic reactor

The increase in bed loading in suspended-bed reactor on the one hand raises the amount of catalyst present for the reaction and places the higher mechanical stress on coated granules on the other, i.e. the number of collisions would be increased during operation leading to the detachment of coating, higher turbidity and decreased penetration of UV radiation. Experimental runs showed that at constant air velocity the increase in bed loading results in the increase in photocatalytic efficiency until a certain bed loading value, after which coating detachment and decreased solution transparency deteriorate the photocatalytic process performance (*Paper III*, Fig. 1).

The bed loading also determines the minimal fluidizing air velocity ( $v_{mg}$ ) that allows to fluidize and uniformly distribute the granules in the treated solution. In experiments at velocities lower than  $v_{mg}$ , lower photocatalytic efficiency was observed due to the accumulation of granules at the top and bottom of reactor, while higher velocities, similarly to increase in bed loading, led to the enhanced turbidity and consequently reduction in process efficiency (*Paper III*, Fig. 1).

Based on the measurements of turbidity and calculations of the photocatalytic process efficiency the optimal operating conditions of suspended-bed reactor

were selected and the study on coating reuse was undertaken. The decrease in efficiency of ca. 50% accompanied by ca. 40% reduction in turbidity if compared to the first use were observed during the third cycle of use for coatings prepared via the optimized procedure. In order to prolong the lifetime of coatings further development of the preparations procedures to improve the abrasion resistance of coatings is needed.

Additionally to DC degradation experiments, the photocatalytic degradation of AMO, PNL and SMZ as single compounds and in a mixture was also investigated. Among studied pharmaceuticals, DC occurred to exhibit the highest degradation efficiency, followed by PNL, AMO and SMZ (*Paper III*, Fig. 3). A similar tendency for the adsorption of these model pollutants onto TiO<sub>2</sub>-coated expanded clay granules was observed. The correlation between degradation and adsorption of pollutants could be explained by the direct photocatalytic reaction on the surface of TiO<sub>2</sub>. Thus, compounds having lower adsorption affinity towards TiO<sub>2</sub>/LECA demonstrate lower photocatalytic removal.

The results of DOC measurements in photocatalytic experimental runs with DC did not indicate the noticeable mineralization of initial pollutant. Thus, after elimination of DC its by-products still remain in the solution. The by-products of photocatalytic degradation of DC were determined in *Paper I* (*Paper I*, Fig. 8). Therefore, in applications where photocatalysis is intended to be used as a pre-treatment before bio-oxidation, monitoring the changes of toxicity during the oxidation of initial compound is of great importance.

DC was proven to have antimicrobial activity against studied bacterial strains *E. Coli*, *S. aureus*, *P. putida* and Dev3 (*Paper III*, Fig. 4). The photocatalytic treatment of DC solution allowed reducing the toxicity of DC to *E. coli*, *P. putida* and Dev3, while the growth of *S. aureus* remained inhibited. The antimicrobial effect of DC to investigated bacterial strains was reduced after photocatalytic treatment in the following order: *E. coli*>*P. putida*>Dev3>*S. aureus* (*Paper III*, Fig. 5, left). Samples taken from reference reactor (dark adsorption) have not revealed the reduction in toxicity, as well as model solutions with DC concentrations similar to those measured during the photocatalytic experiment. The difference in antimicrobial activity of photocatalytically treated and untreated model DC solutions with respective concentrations may be attributed to the presence of multivalent cations originating from the catalyst support, i.e. clay granules, such as Al<sup>3+</sup>, Ca<sup>2+</sup>, Fe<sup>2+/3+</sup> and Mg<sup>2+</sup>, that were reported to suppress the activity of tetracyclines against bacteria [148].

### **3.4 Combination of photocatalytic oxidation with biological treatment**

In the experimental run A, the photocatalytic pre-treatment of DC solution with initial concentration of 25 mg L<sup>-1</sup> resulted in decrease in DC concentration up to 10±2 mg L<sup>-1</sup> while the DOC decrease was 20% and COD was 26%.

After the introduction of photocatalytically pre-treated DC solution to the acclimated activated sludge (3<sup>rd</sup> stage), sludge settleability became poor, with

sudden increase in SVI to over 300 mL g<sup>-1</sup> pointing to toxic effect of the influent. Furthermore, the SVI remained high until the end of the experimental run, suggesting that the exposure to DC by-products formed during pre-treatment was greatly affecting sludge settleability. However, the SVI of the control bioreactor increased slowly during the period of the 3<sup>rd</sup> stage accompanied by the increase in turbidity of effluent, pointing to growing toxic effect of DC on microorganisms, probably leading to sludge flock breakup. It is in the accordance with study [149] where authors reported decrease in settling ability of sludge exposed to tetracyclines.

The toxic effect of influent in both reactors was also confirmed by the reduction of sOUR of activated sludge by 13 and 25% during the 3<sup>rd</sup> stage of experimental run in the main and control bioreactor, respectively.

Experimental run A resulted in the elimination of DC from liquid phase up to 90 and 96% during combined (photocatalytic pre-treatment followed by the bio-oxidation) and control experiments while DC concentrations on sludge reached 4.4 and 8.1 mg g<sup>-1</sup>, respectively. The study [150] pointed out that tetracyclines are mostly removed by adsorption and show higher resistance to biodegradation. This was confirmed in our study by observing DC accumulation on activated sludge; the biodegradation yields are expected to be low as tetracyclines are hardly breakable by microorganisms [129, 151-154]. Higher DC concentration in effluent in combined system may be attributed to the different properties and composition of activated sludge in two bioreactors caused by toxic effect of pre-treated and untreated DC solutions.

The run A indicated that the conditions of photocatalytic pre-treatment of DC solution were inappropriate for further biological treatment and for the run B the initial concentration of DC of 10 mg L<sup>-1</sup> and prolonged time of pre-treatment of 4.5 h were selected to ensure the residual organic content with more profound degradation of DC (*Paper III*). By the end of the photocatalytic treatment under newly selected conditions, DOC removal remained unchanged (18%) and COD removal was improved to 35%, while the DC final concentration was not exceeding 1 mg L<sup>-1</sup>.

Experimental run B resulted in the elimination of DC from liquid phase up to 98% during coupled experiment and the operation of bioreactor remained stable in terms of sludge properties and nutrient removal. The elimination of DC during single bio-treatment process (control) was 88% during first weeks of experimental run slowly decreasing to 76% by the end of the experiment. The sOUR of activated sludge in bio-treatment reactor decreased by 40% by the end of the experimental run (*Paper III*).

The concentration of DC on sludge by the end of the experimental run reached approx. 3.4 and 10.5 mg g<sup>-1</sup> in combined and reference process.

The combination of photocatalytic pre-treatment with bio-oxidation for DC removal resulted in enhanced DC elimination from liquid phase without affecting the operation of biological system.

## CONCLUSIONS

The study to develop the photocatalytic water treatment system based on fluidized-bed concept with catalyst immobilized onto support was carried out and the potential to apply this system as pre-treatment prior to activated sludge process was investigated. This study presents one of the first implementations of lightweight expanded clay aggregates as  $\text{TiO}_2$  support and the first application of sol-gel technology for coating of expanded clay granules with  $\text{TiO}_2$ . This approach simplifies the catalyst separation, reduces the cost of treatment process and thus hasten the implementation of photocatalysis.

The main results of the study can be summarized as follows:

- The selection of LECA as a support material for  $\text{TiO}_2$  deposition for the application in suspended-bed photocatalytic reactor demonstrated high potential due to beneficial properties of expanded clay granules.
- Among  $\text{TiO}_2$  immobilization methods studied, sol-gel method based on P25-modified TTIP-sol allowed to prepare  $\text{TiO}_2$  coatings on the surface of LECA with the best performance in terms of photocatalytic oxidation and mechanical stability. The coatings properties are dependent on the preparation conditions and their optimization allowed enhancing the coating performance.
- The process of elimination of pollutants in photocatalytic suspended-bed reactor with  $\text{TiO}_2$  immobilized on LECA is a combination of adsorption and photocatalytic degradation. The efficiency of pollutant removal correlates with the adsorption affinities of pharmaceutical molecules towards the  $\text{TiO}_2$ -coated expanded clay: the pharmaceuticals with higher adsorption demonstrate higher degradation efficiency.
- The choice of suspended-bed reactor operating parameters i.e. fluidizing air velocity and bed loading, allowed to outline the conditions for improved removal of the pollutants, whereas the present state of knowledge could be a good basis for the further development of coating preparation procedures to enhance their abrasion resistance and photocatalytic activity.
- Photocatalytic treatment of doxycycline reduced its antimicrobial activity to tested bacterial strains and allowed the coupling photocatalytic treatment and bio-oxidation with almost complete (98%) doxycycline removal from liquid phase without disruption of biological system operation.

Overall, the results obtained within this study provide information essential for the practical implementation of photocatalysis for treatment of pharmaceutical-containing wastewater separately or in a combination with biological oxidation.

## REFERENCES

1. Fujishima, A., Honda, K. Electrochemical Photolysis of Water at a Semiconductor Electrode. - *Nature*, 1972, 238, 37-38.
2. Fujishima, A., Zhang, X., Tryk, D. A. TiO<sub>2</sub> photocatalysis and related surface phenomena. - *Surface Science Reports*, 2008, 63, 515-582.
3. Ibadon, A. O., Fitzpatrick, P. Heterogeneous Photocatalysis: Recent Advances and Applications. – *Catalysts*, 2013, 3, 189-218.
4. Hashimoto, K., Irie, H., Fujishima, A. TiO<sub>2</sub> photocatalysis: historical overview and future prospects. – *Japanese Journal of Applied Physics*, 2005, 44 (12), 8269-8285.
5. Umar M., Aziz, H. A. Photocatalytic Degradation of Organic Pollutants in Water, Organic Pollutants. - *Monitoring, Risk and Treatment* / ed. M. Nageeb Rashed. InTech, 2013. [WWW] <http://www.intechopen.com/sci-hub.cc/books/organic-pollutants-monitoring-risk-and-treatment/photocatalytic-degradation-of-organic-pollutants-in-water> (28.01.2017).
6. Al-Rasheed, R. A. Water Treatment by Heterogeneous Photocatalysis: An Review. - *Proceedings of the 4th SWCC Acquired Experience Symposium*, Jeddah, Saudi Arabia, 7 May 2005.
7. Kisch, H. Semiconductor Photocatalysis - Mechanistic and Synthetic Aspects. - *Angewandte Chemie International Edition*, 2012, 51, 2-38.
8. Barrera-Díaz, C., Cañizares, P., Fernández, F. J., Natividad, R., Rodrigo, M.A. Electrochemical Advanced Oxidation Processes: An Overview of the Current Applications to Actual Industrial Effluents. - *Journal of the Mexican Chemical Society*, 2014, 58 (3), 256-275.
9. Fagan, R., McCormack, D. E., Dionysiou, D. D., Pillai, S. C. A review of solar and visible light active TiO<sub>2</sub> photocatalysis for treating bacteria, cyanotoxins and contaminants of emerging concern. - *Materials Science in Semiconductor Processing*, 2016, 42, 2-14.
10. Khan, M. M., Adil, S. F., Al-Mayouf, A. Metal oxides as photocatalysts. - *Journal of Saudi Chemical Society*, 2015, 19 (5), 462-464.
11. Hoffmann, M. R., Martin, S. T., Choi, W., Bahnemann, D. W. Environmental Applications of Semiconductor Photocatalysis. - *Chemical Reviews*, 1995, 95, 69-96.
12. Dong, P., Xi, X., Hou, G. Typical Non-TiO<sub>2</sub>-Based Visible-Light Photocatalysts, Semiconductor Photocatalysis. - *Materials, Mechanisms and Applications* / ed. W. Cao, InTech, 2016. [WWW]

<http://www.intechopen.com/books/semiconductor-photocatalysis-materials-mechanisms-and-applications/typical-non-tio2-based-visible-light-photocatalysts> (15.02.2017).

13. Marchelek, M., Diak, M., Kozak, M., Zaleska-Medynska, A., Grabowska, E. Some Unitary, Binary, and Ternary Non-TiO<sub>2</sub> Photocatalysts, Semiconductor Photocatalysis. - *Materials, Mechanisms and Applications* / ed. W. Cao, InTech, 2016. [WWW] <http://www.intechopen.com/books/semiconductor-photocatalysis-materials-mechanisms-and-applications/some-unitary-binary-and-ternary-non-tio2-photocatalysts> (28.02.2017).

14. Ola, O., Maroto-Valer, M. M. Review of material design and reactor engineering on TiO<sub>2</sub> photocatalysis for CO<sub>2</sub> reduction. - *Journal of Photochemistry and Photobiology C: Photochemistry Reviews*, 2015, 24, 16-42.

15. Eskandarloo, H., Badiei, A. Photocatalytic Application of Titania Nanoparticles for Degradation of Organic Pollutants. - *Nanotechnology for optics and sensors* / ed. M. Aliofkhazraei, One Central Press, 2014, 108-128. [WWW] <http://www.onecentralpress.com/photocatalytic-application-of-titania-nanoparticles-for-degradation-of-organic-pollutants/> (27.02.2017).

16. Luttrell, T., Halpegamage, S., Tao, J., Kramer, A., Sutter, E., Batzill, M. Why is anatase a better photocatalyst than rutile? - Model studies on epitaxial TiO<sub>2</sub> films. - *Scientific reports*, 2014, 4043. [WWW] <http://www.nature.com/articles/srep04043> (18.02.2017).

17. Li, Z., Cong, S., Xu, Y. Brookite vs Anatase TiO<sub>2</sub> in the Photocatalytic Activity for Organic Degradation in Water - *ACS Catalysis*, 2014, 4, 3273-3280.

18. Zhang, J., Zhou, P., Liu, J., Yu, J. New understanding of the difference of photocatalytic activity among anatase, rutile and brookite TiO<sub>2</sub>. - *Physical Chemistry Chemical Physics*, 2014, 16, 20382-20386.

19. Kandiel, T. A., Robben, L., Alkaim, A., Bahnemann, D. Brookite versus anatase TiO<sub>2</sub> photocatalysts: phase transformations and photocatalytic activities. - *Photochemical & Photobiological Sciences*, 2013, 12, 602-609.

20. Diaz-Real, J. A., Ma, J., Alonso-Vante, N. Highly photoactive Brookite and Anatase with enhanced photocatalytic activity for the degradation of Indigo Carmine application. - *Applied Catalysis B: Environmental*, 2016, 198, 471-479.

21. Paola, A. D., Bellardita, M., Palmisano, L. Brookite, the Least Known TiO<sub>2</sub> Photocatalyst. - *Catalysts*, 2013, 3, 36-73.

22. Wang, S., Kurepa, J., Smalle, J. A. Ultra-small TiO<sub>2</sub> nanoparticles disrupt microtubular networks in *Arabidopsis thaliana*. - *Plant, Cell and Environment*, 2011, 34, 811-820.

23. Kolarova, H., Tomankova, K., Harvanova, M., Horakova, J., Malohlava, J., Cenklova, V., Bajgar, R., Kejlova, K., Jirova, D. Cell uptake of titanium dioxide nanoparticles - *Int'l Conf. on Medical Genetics, Cellular & Molecular Biology, Pharmaceutical & Food Sciences (GCMBPF-2015): 5-6th June 2015, Istanbul, Turkey*, 2015, 114-116.
24. Hamzeh, M., Sunahara, G. I. In vitro cytotoxicity and genotoxicity studies of titanium dioxide (TiO<sub>2</sub>) nanoparticles in Chinese hamster lung fibroblast cells. - *Toxicology in Vitro*, 2013, 27, 864-873.
25. Gheshlaghi, Z. N., Riazi, G. H., Ahmadian, S., Ghafari, M., Mahinpour, R. Toxicity and interaction of titanium dioxide nanoparticles with microtubule protein. – *Acta Biochim Biophys Sin*, 2008, 40 (9), 777-782.
26. International Agency for Research on Cancer. [WWW] <http://monographs.iarc.fr/ENG/Classification/> (10.02.2017).
27. Purifics. Photo-Cat. [WWW] <http://www.purifics.com/photo-cat-photocatalytic-membrane-system> (27.02.2017).
28. RECAT Technologies. PhotoCREC. [WWW] [http://www.recattechnologies.com/pdf/RECAT\\_photo\\_crec.pdf](http://www.recattechnologies.com/pdf/RECAT_photo_crec.pdf) (27.02.2017).
29. Gyrecat® Core Product. [WWW] <http://www.gyrecat.com/gyrecat-core-product/> (27.02.2017).
30. Serrano Rosales, B., Moreira del Rio, J., Guayaquil. J. F., de Lasa, H. Photodegradation Efficiencies in a Photo-CREC Water-II Reactor Using Several TiO<sub>2</sub> Based Catalysts. - *International Journal of Chemical Reactor Engineering*, 2016, 14 (3), 685-701.
31. Panasonic Newsroom Global. Panasonic Develops 'Photocatalytic Water Purification Technology' - Creating Drinkable Water with Sunlight and Photocatalysts. [WWW] <http://news.panasonic.com/global/stories/2014/30520.html> (27.02.2017).
32. SOWARLA SUN. [WWW] <http://www.sowarla.de/demonstration-plant.html> (27.02.2017).
33. The SOLARDETOX® Technology. [WWW] [https://www.researchgate.net/publication/224987074\\_The\\_SOLARDETOX\\_Technology](https://www.researchgate.net/publication/224987074_The_SOLARDETOX_Technology) (22.02.2017).

34. Hariharan, V. Photocatalysis and its Applications in Water Treatment. [WWW]  
[http://www.academia.edu/6403070/Photocatalysis\\_and\\_its\\_Applications\\_in\\_Water\\_Treatment](http://www.academia.edu/6403070/Photocatalysis_and_its_Applications_in_Water_Treatment) (22.02.2017).
35. Dong, H., Zeng, G., Tang, L., Fan, C., Zhang, C., He, X., He, Y. An overview on limitations of TiO<sub>2</sub>-based particles for photocatalytic degradation of organic pollutants and the corresponding countermeasures. - *Water Research*, 2015, 79, 128-146.
36. Suárez, S. Immobilised Photocatalysts. – *Design of Advanced Photocatalytic Materials for Energy and Environmental Applications* / ed. J. Coronado, F. Fresno, M. D. Hernández-Alonso, R. Portela. London: Springer, 2013, 245-268.
37. Shan, A. Y., Ghazi, T. I. M., Rashid, S. A. Immobilisation of titanium dioxide onto supporting materials in heterogeneous photocatalysis: A review. - *Applied Catalysis A: General*, 2010, 389, 1-8.
38. Karav, S., Cohen, J. L., Barile, D., Leite, J. M., de Moura Bell, N. Recent Advances in Immobilization Strategies for Glycosidases. – *Biotechnology Progress*, 2016, 33 (1), 104-112.
39. Vodyanitskii, Y. N., Yakovlev, A. S. Contamination of Soils and Groundwater with New Organic Micropollutants: A Review. - *Eurasian Soil Science*, 2016, 49 (5), 560-569.
40. Solcova, O., Spacilova, L., Maleterova, Y., Morozova, M., Ezechias, M., Kresinova, Z. Photocatalytic water treatment on TiO<sub>2</sub> thin layers. - *Desalination and Water Treatment*, 2015, 57 (25), 11631-11638.
41. Curcio, M. S., Oliveira, M. P., Waldman, W. R., Sánchez, B., Canela, M. C. TiO<sub>2</sub> sol-gel for formaldehyde photodegradation using polymeric support: photocatalysis efficiency versus material stability. – *Environmental Science and Pollution Research*, 2015, 22, 800-809.
42. Robert, D., Keller, V., Keller, N. Immobilization of a Semiconductor Photocatalyst on Solid Supports: Methods, Materials, and Applications. - *Photocatalysis and Water Purification: From Fundamentals to Recent Applications* / ed. M. Lu, P. Pichat. Weinheim, Germany: Wiley-VCH Verlag GmbH & Co. KGaA, 2013, 145-178.
43. Xie, H., Li, N., Liu, B., Yang, J., Zhao, X. Role of Sodium Ion on TiO<sub>2</sub> Photocatalyst: Influencing Crystallographic Properties or Serving as The Recombination Center of Charge Carriers? - *The Journal of Physical Chemistry C*, 2016, 120 (19), 10390-10399.
44. Espino-Estévez, M. R., Fernández-Rodríguez, C., González-Díaz, O. M., Navío, J. A., Fernández-Hevia, D., Doña-Rodríguez, J. M. Enhancement of

stability and photoactivity of TiO<sub>2</sub> coatings on annular glass reactors to remove emerging pollutants from waters. - *Chemical Engineering Journal*, 2015, 279, 488-497.

45. Chen, Y., Dionysiou, D. D. Sol-gel synthesis of nanostructured TiO<sub>2</sub> films for water purification. – *Sol-Gel Methods for Materials Processing: Focusing on Materials for Pollution control, Water purification, and Soil Remediation*. The Netherlands: Springer, 2007, 67-76.

46. Livage, J., Sanchez, C. Sol-gel chemistry. - *Journal of Non-Crystalline Solids*, 1992, 145, 11-19.

47. Milea, C. A., Bogatu C., Duta, A. The influence of parameters in silica sol-gel process. - *Bulletin of the Transilvania University of Braşov Series I: Engineering Sciences*, 2011, 4 (53), No. 1

48. Brinker, C. J., Hurd, A. Fundamentals of sol-gel dip-coating. - *Journal de Physique III, EDP Sciences*, 1994, 4 (7), 1231-1242.

49. Brinker, C. J., Hurd, A. J., Schunk, P. R., Frye, G. C., Ashley, C. S. Review of sol-gel thin film formation. - *Journal of Non-Crystalline Solids*, 1992, 147-148, 424-436.

50. Birnie, D. P. Spin Coating Technique. - *Sol-Gel Technologies for Glass Producers and Users* / ed. M. Aegerter, M. Mennig. New York: Springer US, 2004, 49-55.

51. Richardson, S. D., Ternes, T. A. Water Analysis: Emerging Contaminants and Current Issues. - *Analytical Chemistry*, 2014, 86, 2813–2848.

52. Clara, M., Strenn, B., Gans, O., Martinez, E., Kreuzinger, N., Kroiss, H. Removal of selected pharmaceuticals, fragrances and endocrine disrupting compounds in a membrane bioreactor and conventional wastewater treatment plants. - *Water Research*, 2005, 39, 4797-4807.

53. Richardson, S. D., Kimura, S. Y. Water Analysis: Emerging Contaminants and Current Issues - *Analytical Chemistry*, 2016, 88, 546-582.

54. Barbosa, M., Moreira, N. F. F., Ribeiro, A. R., Pereira, M. F. R., Silva, A. M. T. Occurrence and removal of organic micropollutants: an overview of the watch list of EU Decision 2015/495. - *Water Research*, 2016, 94, 257-279.

55. Cotruvo, J. A. Organic Micropollutants in Drinking Water: An Overview. – *The Science of the Total Environment*, 1985, 47, 7-26.

56. Mansouri, H., Carmona, R. J., Gomis-Berenguer, A., Souissi-Najar, S., Ouederni A., Ania C. O. Competitive adsorption of ibuprofen and amoxicillin

mixtures from aqueous solution on activated carbons. - *Journal of Colloid and Interface Science*, 2015, 449, 252-260.

57. Richards, S. M., Wilson, C. J., Johnson, D. J., Castle, D. M., Lam, M., Mabury, S. A., Sibley, P. K., Solomon, K. R. Effects of Pharmaceutical Mixtures in Aquatic Microcosms. - *Environmental Toxicology and Chemistry*, 2004, 23 (4), 1035–1042.

58. Oetken, M., Nentwig, G., Löffler, D., Ternes, T., Oehlmann, J. Effects of Pharmaceuticals on Aquatic Invertebrates. Part I. The Antiepileptic Drug Carbamazepine. - *Archives of Environmental Contamination and Toxicology*, 2005, 49, 353-361.

59. Arnold, K. E., Brown, A. R., Ankley, G. T., Sumpter, J. P. Medicating the environment: assessing risks of pharmaceuticals to wildlife and ecosystems. - *Philosophical Transactions of the Royal Society B: Biological Sciences*, 2014, 369: 20130569

60. Ternes, T. A., Giger, W., Joss, A. Human Pharmaceuticals, Hormones and Fragrances. Introduction / ed. T. Ternes, A. Joss. London: IWA Publishing, 2006.

61. Perazzolo, C., Morasch, B., Kohn, T., Magnet, A., Thonney, D., Chevre, N. Occurrence and fate of micropollutants in the Vidy Bay of Lake Geneva, Switzerland. Part I: Priority list for environmental risk assessment of pharmaceuticals. - *Environmental Toxicology and Chemistry*, 2010, 29 (8), 1649-1657.

62. Teixeira, S., Gurke, R., Eckert, H., Kühn, K., Fauler, J., Cuniberti, G. Photocatalytic degradation of pharmaceuticals present in conventional treated wastewater by nanoparticle suspensions. - *Journal of Environmental Chemical Engineering*, 2016, 4 (1), 287-292.

63. Isidori, M., Bellotta, M., Cangiano, M., Parrella, A. Estrogenic activity of pharmaceuticals in the aquatic environment. - *Environment International*, 2009, 35, 826-829.

64. Dietrich, S., Ploessl, F., Bracher, F., Laforsch, C. Single and combined toxicity of pharmaceuticals at environmentally relevant concentrations in *Daphnia magna* – A multigenerational study. - *Chemosphere*, 2010, 79 (1), 60-66.

65. Corcoran, J., Winter, M. J., Tyler, C. R. Pharmaceuticals in the aquatic environment: A critical review of the evidence for health effects in fish - *Critical Reviews in Toxicology*, 2010, 40 (4), 287-304.

66. Gonzalez-Rey M., Mattos J. J., Piazza C. E., Bainy A. C. D., Bebianno M. J. Effects of active pharmaceutical ingredients mixtures in mussel *Mytilus galloprovincialis*. - *Aquatic Toxicology*, 2014, 153, 12-26.
67. Gonzalez-Pleiter, M., Gonzalo, S., Rodea-Palomares, I., Leganes, F., Rosal, R., Boltes, K., Marco, E., Fernandez-Pinas, F. Toxicity of five antibiotics and their mixtures towards photosynthetic aquatic organisms: Implications for environmental risk assessment. - *Water research*, 2013, 47, 2050-2064.
68. Vasquez, M. I., Lambrianides, A., Schneider, M., Kümmerer, K., Fatta-Kassinos, D. Environmental side effects of pharmaceutical cocktails: What we know and what we should know. - *Journal of Hazardous Materials*, 2014, 279, 169-189.
69. Brienza, M., Mahdi Ahmed, M., Escande, A., Plantard, G., Scrano, L., Chiron, S., Bufo, S. A., Goetz, V. Use of solar advanced oxidation processes for wastewater treatment: Follow-up on degradation products, acute toxicity, genotoxicity and Estrogenicity. - *Chemosphere*, 2016, 148, 473-480.
70. Shore, R. F., Taggart, M. A., Smits, J., Mateo, R., Richards, N. L., Fryday, S. Detection and drivers of exposure and effects of pharmaceuticals in higher vertebrates. - *Philosophical Transactions of the Royal Society B: Biological Sciences*, 2014, 369: 20130570.
71. Gothwal, R., Shashidhar, T. Antibiotic Pollution in the Environment: A Review. - *Clean – Soil, Air, Water*, 2015, 43 (4), 479-489.
72. Taggart M. A., Richards N. L., Kinney C. A. Impact of pharmaceuticals on terrestrial wildlife. - *Pharmaceuticals in the Environment* / ed. R. E. Hester, R. M. Harrison, Royal Society of Chemistry, 2016. [WWW] [https://books.google.de/books?id=3wCNCgAAQBAJ&pg=PA233&lpg=PA233&dq=terrestrial+vertebrates+pharmaceuticals+chain&source=bl&ots=BKDs4tr0Nl&sig=V1K7RdUWUF3ahr97widl8PELSis&hl=et&sa=X&ved=0ahUKEwj\\_jszt0tHTAhWjYJoKHSrFD0IQ6AEINDAE#v=onepage&q=terrestrial%20vertebrates%20pharmaceuticals%20chain&f=false](https://books.google.de/books?id=3wCNCgAAQBAJ&pg=PA233&lpg=PA233&dq=terrestrial+vertebrates+pharmaceuticals+chain&source=bl&ots=BKDs4tr0Nl&sig=V1K7RdUWUF3ahr97widl8PELSis&hl=et&sa=X&ved=0ahUKEwj_jszt0tHTAhWjYJoKHSrFD0IQ6AEINDAE#v=onepage&q=terrestrial%20vertebrates%20pharmaceuticals%20chain&f=false) (07.04.17).
73. PubChem. Open Chemistry Database. Amoxicillin. [WWW] <https://pubchem.ncbi.nlm.nih.gov/compound/amoxicillin#section=Top> (03.02.2017).
74. Mutiyar, P. K., Mittal, A. K. Occurrences and fate of an antibiotic amoxicillin in extended aeration-based sewage treatment plant in Delhi, India: a case study of emerging pollutant. - *Desalination and Water Treatment*, 2013, 51 (31-33), 6158-6164.

75. Lamm, A., Gozlan, I., Rotstein, A., Avisar, D. Detection of amoxicillin-diketopiperazine-2', 5' in wastewater samples. - *Journal of Environmental Science and Health Part A*, 2009, 44, 1512–1517.
76. Elizalde-Velázquez, A., Gómez-Oliván, L. M., Galar-Martínez, M., Islas-Flores, H., Dublán-García, O., SanJuan-Reyes, N. Amoxicillin in the Aquatic Environment, Its Fate and Environmental Risk, Environmental Health Risk - *Hazardous Factors to Living Species* / ed. M. Larramendy, InTech, 2016. [WWW] <http://www.intechopen.com/books/environmental-health-risk-hazardous-factors-to-living-species/amoxicillin-in-the-aquatic-environment-its-fate-and-environmental-risk> (28.02.2017).
77. Khan, G. A., Berglund, B., Khan, K. M., Lindgren, P.-E., Fick, J. Occurrence and Abundance of Antibiotics and Resistance Genes in Rivers, Canal and near Drug Formulation Facilities – A Study in Pakistan. – *PLoS One*, 2013, 8 (6), e62712.
78. Li, P.Y., Chang, Y.C., Tzang, B.S., Chen, C.C., Liu, Y.C. Antibiotic amoxicillin induces DNA lesions in mammalian cells possibly via the reactive oxygen species. - *Mutation Research*, 2007, 629 (2), 133–139.
79. Andreozzi, R., Caprio, V., Ciniglia, C., De Champdoré, M., Lo Giudice, R., Marotta, R., Zucatto, E. Antibiotics in the Environment: Occurrence in Italian STPs, fate, and preliminary assessment on algal toxicity of amoxicillin. - *Environmental Science and Technology*, 2004, 38, 6832–6838.
80. Liu, Y., Wang, F., Chen, X., Zhang, J., Gao, B. Cellular responses and biodegradation of amoxicillin in *Microcystis aeruginosa* at different nitrogen levels. - *Ecotoxicology and Environmental Safety*, 2015, 111, 138-145.
81. Oliveira, R., McDonough, S., Ladewig, C.L.J., Soares, M.V.M.A., Nogueira, J.A.A., Domingues I. Effects of oxytetracycline and amoxicillin on development and biomarkers activities of zebrafish (*Danio rerio*). - *Environmental Toxicology and Pharmacology*, 2013, 36, 903–912.
82. González-Pérez, B. K., Sarma, S. S. S., Nandini, S. Effects of selected pharmaceuticals (ibuprofen and amoxicillin) on the demography of *Brachionus calyciflorus* and *Brachionus havanaensis* (Rotifera). - *The Egyptian Journal of Aquatic Research*, 2016, 42 (3), 341-347.
83. Drugs.com. Doxycycline. [WWW] <https://www.drugs.com/pro/doxycycline.html> (23.01.2017).
84. Chopra, I., Roberts, M. Tetracycline Antibiotics: Mode of Action, Applications, Molecular Biology, and Epidemiology of Bacterial Resistance. - *Microbiology and Molecular Biology Reviews*, 2001, 65 (2), 232-260.

85. Xu, D. M., Wang, Y. H., Rao, G. W. Cellular response of freshwater green algae to the toxicity of tetracycline antibiotics. - *Huan Jing Ke Xue*. 2013, 34 (9), 3386-3390.
86. Moullan, N., Mouchiroud, L., Wang, X., Ryu, D., Williams, E. G., Mottis, A., Jovaisaite, V., Frochaux, M. V., Quiros, P. M., Deplancke, B., Houtkooper, R. H., Auwerx, J. Tetracyclines Disturb Mitochondrial Function across Eukaryotic Models: A Call for Caution in Biomedical Research. - *Cell Reports*, 2015, 10, 1681-1691.
87. Vutukuru, P., Kumar Bodapati, A. K., Bhimavarapu, V., Vutukuru, S. S. Doxycycline Induced Alterations in The Glycogen and Protein Content Of The Zebra Fish, *Danio rerio*. - *Asian Journal of Microbiology, Biotechnology & Environmental Sciences*, 2015, 17 (3), 655-660.
88. Khetan, S. K., Collins T. J. Human Pharmaceuticals in the Aquatic Environment: A Challenge to Green Chemistry. - *Chemical Reviews*, 2007, 107, 2319-2364.
89. PubChem. Open Chemistry Database. Sulfamethiyole. [WWW] <https://pubchem.ncbi.nlm.nih.gov/compound/sulfamethizole#section=Pharmacology-and-Biochemistry> (03.02.2017).
90. Białk-Bielińska, A., Kumirska, J., Stepnowski, P. What Do We Know About the Chronic and Mixture Toxicity of the Residues of Sulfonamides in the Environment? - *Organic Pollutants - Monitoring, Risk and Treatment* / ed. M. Nageeb Rashed, InTech, 2013. [WWW] <http://www.intechopen.com/books/organic-pollutants-monitoring-risk-and-treatment/what-do-we-know-about-the-chronic-and-mixture-toxicity-of-the-residues-of-sulfonamides-in-the-enviro> (28.02.2017).
91. Lin, T., Yu, S., Chen, Y., Chen, W. Integrated biomarker responses in zebrafish exposed to sulfonamides. - *Environmental Toxicology and Pharmacology*, 2014, 38, 444-452.
92. Lin, T., Chen, Y., Chen, W. Impact of toxicological properties of sulfonamides on the growth of zebrafish embryos in the water. - *Environmental Toxicology and Pharmacology*, 2013, 36 (3), 1068-1076.
93. Garcia Galan, M. J., Diaz-Cruz, M. S., Barcelo, D. Sulfonamide Antibiotics in Natural and Treated Waters: Environmental and Human Health Risks. - *Emerging Organic Contaminants and Human Health*, 2012, 20, 71-92.
94. Baran, W., Adamek, E., Ziemianska, J., Sobczak, A. Effects of the presence of sulfonamides in the environment and their influence on human health. - *Journal of Hazardous Materials*, 2011, 196, 1-15.

95. United States National Library of Medicine. Corticosteroids. [WWW] <https://livertox.nih.gov/Corticosteroids.htm> (4.02.2017).
96. DellaGreca, M., Fiorentino, A., Isidori, M., Lavorgna, M., Previtiera, L., Rubino, M., Temussi, F. Toxicity of prednisolone, dexamethasone and their photochemical derivatives on aquatic organisms. – *Chemosphere*, 2004, 54, 629-637.
97. McNeil, P. L., Nebot, C., Cepeda, A., Sloman, K. A. Environmental concentrations of prednisolone alter visually mediated responses during early life stages of zebrafish (*Danio rerio*). - *Environmental Pollution*, 2016, 218, 981-987.
98. Baranowska, I., Kowalski, B. A Rapid UHPLC Method for the Simultaneous Determination of Drugs from Different Therapeutic Groups in Surface Water and Wastewater. - *Bulletin of Environmental Contamination and Toxicology*, 2012, 89, 8-14.
99. McNeil, P. L., Nebot, C., Sloman, K. A. Physiological and Behavioral Effects of Exposure to Environmentally Relevant Concentrations of Prednisolone During Zebrafish (*Danio rerio*) Embryogenesis. - *Environmental Science & Technology*, 2016, 50 (10), 5294-5304.
100. Watkinson, A.J., Murby, E.J., Costanzo, S.D. Removal of antibiotics in conventional and advanced wastewater treatment: Implications for environmental discharge and wastewater recycling. – *Water Research*, 2007, 41, 4164-4176.
101. Rúa-Gómez, P.C., Püttmann, W. Occurrence and removal of lidocaine, tramadol, venlafaxine, and their metabolites in German wastewater treatment plants. - *Environmental Science and Pollution Research*, 2012, 19, 689-99.
102. Kasprzyk-Hordern, B., Dinsdale, R. M., Guwy, A. J. The removal of pharmaceuticals, personal care products, endocrine disruptors and illicit drugs during wastewater treatment and its impact on the quality of receiving waters. - *Water Research*, 2009, 43, 363-380.
103. Fatta-Kassinos, D., Meric, S., Nikolaou, A. Pharmaceutical residues in environmental waters and wastewater: current state of knowledge and future research. - *Analytical and Bioanalytical Chemistry*, 2011, 399, 251-275.
104. Kasprzyk-Hordern, B., Dinsdale, R. M., Guwy, A. J. The occurrence of pharmaceuticals, personal care products, endocrine disruptors and illicit drugs in surface water in South Wales, UK – *Water Research*, 2008, 42, 3498-3518.
105. Heeb, F., Singer, H., Pernet-Coudrier, B., Qi, W., Liu, H., Longree, P., Müller, B., Berg, M. Organic Micropollutants in Rivers Downstream of the Megacity Beijing: Sources and Mass Fluxes in a Large-Scale Wastewater Irrigation System. - *Environmental Science & Technology*, 2012, 46, 8680-8688.

106. Gros, M., Petrović, M., Ginebreda, A., Barceló, D. Removal of pharmaceuticals during wastewater treatment and environmental risk assessment using hazard indexes. - *Environment International*, 2010, 36, 15-26.
107. Joss, A., Siegrist, H., Ternes, T. A. Are we about to upgrade wastewater treatment for removing organic micropollutants? - *Water Science & Technology*, 2008, 57 (2), 251-255..
108. Larsen, T. A., Lienert, J., Joss, A., Siegrist, H. How to avoid pharmaceuticals in the aquatic environment. - *Journal of Biotechnology*, 2004, 113, 295-304.
109. Luo, Y., Guo, W., Ngo, H. H., Nghiem, L. D., Hai, F. I., Zhang, J., Liang, S. A review on the occurrence of micropollutants in the aquatic environment and their fate and removal during wastewater treatment. - *Science of the Total Environment*, 2014, 473-474, 619-641.
110. Gadipelly, C., Perez-González, A., Yadav, G. D., Ortiz, I., Ibáñez, R., Rathod, V. K., Marathe, K. V. Pharmaceutical Industry Wastewater: Review of the Technologies for Water Treatment and Reuse - *Industrial & Engineering Chemistry Research*, 2014, 53, 11571–11592
111. EUR-Lex. Commission Implementing Decision (EU) 2015/495 of 20 March 2015 establishing a watch list of substances for Union-wide monitoring in the field of water policy pursuant to Directive 2008/105/EC of the European Parliament and of the Council (notified under document C (2015) 1756). [WWW] <http://eur-lex.europa.eu/legal-content/en/ALL/?uri=CELEX%3A32015D0495> (17.01.2017).
112. Development of the first Watch List Under the Environmental Quality Standards Directive. [WWW] [http://bookshop.europa.eu/sci-hub.bz/en/development-of-the-first-watch-list-under-the-environmental-quality-standards-directive-pbLBNA27142/downloads/LB-NA-27-142-EN-N/LBNA27142ENN\\_002.pdf?FileName=LBNA27142ENN\\_002.pdf&SKU=LBNA27142ENN\\_PDF&CatalogueNumber=LB-NA-27-142-EN-N](http://bookshop.europa.eu/sci-hub.bz/en/development-of-the-first-watch-list-under-the-environmental-quality-standards-directive-pbLBNA27142/downloads/LB-NA-27-142-EN-N/LBNA27142ENN_002.pdf?FileName=LBNA27142ENN_002.pdf&SKU=LBNA27142ENN_PDF&CatalogueNumber=LB-NA-27-142-EN-N) (04.02.2017).
113. Chang, H., Hu, J., Shao, B. Occurrence of Natural and Synthetic Glucocorticoids in Sewage Treatment Plants and Receiving River Waters - *Environmental Science & Technology*, 2007, 41, 3462-3468.
114. Tushara Chaminda, G. G., Furumai, H., Sawaittayotin V. Occurrence of pharmaceutical and personal care products (PPCPs) in wastewaters and surface waters in industrial estates in Thailand. – *Southeast Asian Water Environment* / ed. K. Yamamoto, H. Furumai, H. Katayama, C. Chiemchaisri, U. Puetpaiboon, C. Visvanathan, H. Satoh. London: IWA Publishing, 2014, 159-164.

115. Baresel, C., Cousins, A. P., Hörsing, M., Ek, M., Ejhed, H., Allard, A.-S., Magnér, J., Westling, K., Wahlberg, C., Fortkamp, U., Söhr, S. Pharmaceutical residues and other emerging substances in the effluent of sewage treatment plants. [WWW] [http://vav.griffel.net/filer/C\\_IVL2015-B2226.pdf](http://vav.griffel.net/filer/C_IVL2015-B2226.pdf) (15.02.2017).
116. Ibraheem, J. A., Abdul-Ahad, M. Y. Detection of Tetracycline, Doxycycline, Chlortetracycline, and Oxytetracycline Antibiotics in Nineveha Drug Wastewater. - *Nahrain University, College of Engineering Journal (NUCEJ)*, 2012, 15 (2), 215-221.
117. Bui, X. T., Vo, T. P. T., Ngo, H. H., Guo W. S., Nguyen T. T. Multicriteria assessment of advanced treatment technologies for micropollutants removal at large-scale applications. - *Science of The Total Environment*, 2016, 563–564, 1050-1067.
118. Segneanu, A. E., Orbeci, C., Lazau, C., Sfirloaga, P., Vlazan, P., Bandas, C., Grozescu, I. Waste Water Treatment Methods, Water Treatment / ed. W. Elshorbagy, InTech, 2013. [WWW] <http://www.intechopen.com/books/water-treatment/waste-water-treatment-methods> (28.02.2017).
119. Choi, J., Lee, H., Choi, Y., Kim, S., Lee, S., Lee, S., Choi, W., Lee, J. Heterogeneous photocatalytic treatment of pharmaceutical micropollutants: Effects of wastewater effluent matrix and catalyst modifications. - *Applied Catalysis B: Environmental*, 2014, 147, 8-16.
120. Kanakaraju, D., Glass, B. D., Oelgemöller, M. Titanium dioxide photocatalysis for pharmaceutical wastewater treatment. - *Environmental Chemistry Letters*, 2014, 12, 27-47.
121. Oller, I., Malato, S., Sánchez-Pérez, J. A. Combination of Advanced Oxidation Processes and biological treatments for wastewater decontamination - A review. - *Science of the Total Environment*, 2011, 409, 4141-4166.
122. Khenniche, L., Favier, L., Bouzaza, A., Fourcade, F., Aissani, F., Amrane, A. Photocatalytic degradation of bezacryl yellow in batch reactors – feasibility of the combination of photocatalysis and a biological treatment. - *Environmental Technology*, 2015, 36 (1), 1-10.
123. Klauson, D., Pilnik-Sudareva, J., Pronina, N., Budarnaja, O., Krichevskaya, M., Käkänen, A., Juganson, K., Preis, S. Aqueous photocatalytic oxidation of prednisolone. - *Central European Journal of Chemistry*, 2013, 11 (10), 1620-1633.

124. Klauson, D., Babkina, J., Stepanova, K., Krichevskaya, M., Preis, S. Aqueous photocatalytic oxidation of amoxicillin. - *Catalysis Today*, 2010, 151, 39-45.
125. Klauson, D., Krichevskaya, M., Borissova, M., Preis, S. Aqueous photocatalytic oxidation of sulfamethizole. - *Environmental Technology*, 2010, 31 (14), 1547-1555.
126. Klauson, D., Poljakova, A., Pronina, N., Krichevskaya, M., Moiseev, A., Dedova, T., Preis, S. Aqueous Photocatalytic Oxidation of Doxycycline. - *Journal of Advanced Oxidation Technologies*, 2013, 16 (2), 234-243.
127. Oller, I., Polo-Lopez, I., Miralles-Cuevas, S., Fernandez-Ibanez, P., Malato, S. Advanced Technologies for Emerging Contaminants Removal in Urban Wastewater. - *Advanced Treatment Technologies for Urban Wastewater Reuse*, 2015, 45, 145-169.
128. Cesaro, A., Naddeo, V., Belgiorno, V. Wastewater Treatment by Combination of Advanced Oxidation Processes and Conventional Biological Systems. - *Journal of Bioremediation & Biodegradation*, 2013, 4, 208.
129. Yahiat, S., Fourcade, F., Brosillon, S., Amrane, A. Removal of antibiotics by an integrated process coupling photocatalysis and biological treatment - Case of tetracycline and tylosin. - *International Biodeterioration & Biodegradation*, 2011, 65, 997-1003.
130. Michael, I., Rizzo, L., Mc Ardell, C. S., Manaia, C. M., Merlin, C., Schwartz, T., Dagot, C., Fatta-Kassinos, D. Urban wastewater treatment plants as hotspots for the release of antibiotics in the environment: A review. - *Water Research*, 2013, 47, 957-995.
131. Van Doorslaer, X., Haylamicheal, I. D., Dewulf, J., Van Langenhove, H., Janssen, C. R., Demeestere, K. Heterogeneous photocatalysis of moxifloxacin in water: Chemical transformation and ecotoxicity. - *Chemosphere*, 2015, 119, S75-S80.
132. He, Y. J., Sutton, N. B., Rijnaarts, H. H. M., Langenhoff, A. A. M. Degradation of pharmaceuticals in wastewater using immobilized TiO<sub>2</sub> photocatalysis under simulated solar irradiation. - *Applied Catalysis B: Environmental*, 2016, 182, 132-141.
133. Rizzo, L., Meric, S., Guida, M., Kassinos, D., Belgiorno, V. Heterogenous photocatalytic degradation kinetics and detoxification of an urban wastewater treatment plant effluent contaminated with pharmaceuticals. - *Water Research*, 2009, 43, 4070- 4078.

134. Krichevskaya, M., Malygina, T., Preis, S., Kallas, J. Photocatalytic oxidation of de-icing agents in aqueous solutions and aqueous extract of jet fuel. - *Water Science & Technology*, 2001, 44, 1-6.
135. Drugbank. [WWW] <https://www.drugbank.ca/> (04.02.2017).
136. PubChem. [WWW] <https://pubchem.ncbi.nlm.nih.gov/> (02.02.2017).
137. Weber Saint-Gobain. Leca kergkruus 2-4 mm. [WWW] <https://www.weber.ee/kergkruus/tooted/leca-kergkruus/leca-kergkruus-2-4-mm.html> (20.02.2017).
138. Tootmisohje sertifikaat. Leca kergkruus 2-4 mm. [WWW] [https://www.weber.ee/uploads/tx\\_weberproductpage/Leca\\_2-4mm\\_CE\\_Est\\_Eng.pdf](https://www.weber.ee/uploads/tx_weberproductpage/Leca_2-4mm_CE_Est_Eng.pdf) (20.02.2017).
139. Nkansah, M. A., Christy, A. A., Barth, T., Francis, G. W. The use of lightweight expanded clay aggregate (LECA) as sorbent for PAHs removal from water. - *Journal of Hazardous Materials*, 2012, 217-218, 360-365.
140. Zندهzaban, M., Sharifnia, S., Hosseini, S. N. Photocatalytic degradation of ammonia by light expanded clay aggregate (LECA)-coating of TiO<sub>2</sub> nanoparticles. - *Korean Journal of Chemical Engineering*, 2013, 30 (3), 574-579.
141. Malakootian, M., Nouri, J., Hossaini, H. Removal of heavy metals from paint industry's wastewater using Leca as an available adsorbent. - *International Journal of Environmental Science and Technology*, 2009, 6 (2), 183-190.
142. Dodd, G. Construction Materials: Their Nature and Behaviour, Fourth Edition, Part 9, Glass / ed. P. Domone, J. Illston. Boca Raton: CRC Press, 2010.
143. Shavisi, Y., Sharifnia, S., Zندهzaban, M., Lobabi Mirghavami, M., Kakehazar, S. Application of solar light for degradation of ammonia in petrochemical wastewater by a floating TiO<sub>2</sub>/LECA photocatalyst. - *Journal of Industrial and Engineering Chemistry*, 2014, 20 (5), 2806-2813.
144. Amiri, H., Jaafarzadeh, N., Ahmadi, M., Martínez, S. S. Application of LECA modified with Fenton in arsenite and arsenate removal as an adsorbent. - *Desalination*, 2011, 272, 212-217.
145. Tabase, R. K., Liu, D., Feilberg, A. Chemisorption of hydrogen sulphide and methanethiol by light expanded clay aggregates (Leca). - *Chemosphere*, 2013, 93, 1345-1351.
146. Mohammadi Kalhori, E., Al-Musawi, T. J., Ghahramani, E., Kazemian, H., Zarrabi, M. Enhancement of the adsorption capacity of the light-weight expanded clay aggregate surface for the metronidazole antibiotic by coating with MgO

nanoparticles: studies on the kinetic, isotherm, and effects of environmental parameters. - *Chemosphere*, 2017, 175, 8-20.

147. Dharani, R., Sivalingam, A., Thirumarimurugan, M. Utilization of Light Weight Expanded Clay Aggregate in Waste Water Treatment – A Review. - *International Journal of Emerging Technologies in Engineering Research (IJETER)*, 2016, 4 (4), 26-28.

148. Weinberg, E. D. The mutual effects of antimicrobial compounds and metallic cations. - *Bacteriological Reviews*, 1957, 21, 46-68.

149. Katsou, E., Alvarino, T., Malamis, S., Suarez, S., Frison, N., Omil, F., Fatone, F. Effect of selected pharmaceuticals on nitrogen and phosphorus removal bioprocesses. *Chemical Engineering Journal*, 2016, 295, 509-517.

150. Cirja, M., Ivashechkin, P., Schäffer, A., Corvini, P. F. X. Factors affecting the removal of organic micropollutants from wastewater in conventional treatment plants (CTP) and membrane bioreactors (MBR). - *Reviews in Environmental Science and Bio/Technology*, 2008, 7, 61-78.

151. Prado, N., Monteleon, C., C., Ochoa, J., Amrane, A. Evaluation of the toxicity of veterinary antibiotics on activated sludge using modified Sturm tests – application to tetracycline and tylosine antibiotics. - *Journal of Chemical Technology and Biotechnology*, 2010, 85, 471-477.

152. Prado, N., Ochoa, J., Amrane, A. Biodegradation and biosorption of tetracycline and tylosin antibiotics in activated sludge system. - *Process Biochemistry*, 2009, 44 (11), 1302-1306.

153. Alexy, R., Kümpel, T., Kümmerer, K. Assessment of degradation of 18 antibiotics in the Closed Bottle Test. – *Chemosphere*, 2004, 57, 505-512.

154. Mboula, V. M., Hequet, V., Gru, Y., Colin, R., Andres, Y. Assessment of the efficiency of photocatalysis on tetracycline biodegradation. - *Journal of Hazardous Materials*, 2012, 209-210, 355-364.

## **ACKNOWLEDGMENTS**

I would like to acknowledge the Estonian Research Council (grant G8978), Estonian Ministry of Education and Research (project IUT1-7), Archimedes Foundation (project 3.2.0801.11-0009), UTs and TTUs graduate school „Functional materials and technologies“ and European Regional Development Fund (Dora pluss programm) for financial support.

I would like to express my sincere gratitude to my supervisor Dr. Marina Kritševskaja for thoughtful guidance, valuable advice, permanent support and encouragement through the years of my study. I would also like to thank all my colleagues from Tallinn University of Technology and TU Clausthal especially Dr. Deniss Klauson for his help and for sharing useful suggestions and experience, Dr.-Ing. Gundula Hensch and Dr.-Ing. Anna Moiseev for sharing knowledge regarding sol-gel technology and material characterization, and Dipl.-Ing. Thomas Peter for assistance with SNMS and SEM measurements. The warmest and deepest thanks to my family and friends for their continuous support and endless encouragement throughout the whole period.

## **ABSTRACT**

### **Degradation of Persistent Micropollutants in Suspended-Bed Reactor by Photocatalytic Oxidation and Combination of Biological Treatment with Photocatalysis**

The presence of pharmaceuticals in the water bodies is an important environmental issue due to their negative health and ecological effects. Originating from a variety of sources, such as agricultural, industrial and domestic wastewater, they are entering the environmental matrices passing through conventional wastewater treatment plants. One of the feasible options for the degradation of such a biologically persistent pollutant is the application of advanced oxidation technologies, e.g. photocatalysis. Despite the obvious ability of photocatalysis to effectively degrade recalcitrant water pollutants, the implementation of photocatalytic treatment for water purification is currently limited, mainly due to the costly catalyst separation after treatment. Therefore, there is a need for the elaboration of photocatalyst attachment techniques to apply bed materials in a photoreactor, where the pollutants can be efficiently transferred to the vicinity of UV-A irradiated catalyst surface.

This research is focused on the development of catalyst immobilization procedure onto support to be applied in the photocatalytic treatment system based on fluidized-bed concept. It is also focused on the evaluation of its performance for the removal of pharmaceuticals and estimation of the potential of combining this system with bio-oxidation for enhanced elimination of emerging environmental micropollutants.

The catalyst immobilization procedures were performed using adsorption and the sol-gel method. For sol-gel coating preparation various compositions of sols and conditions of the procedure were examined. The coatings with superior performance in terms of photocatalytic activity and mechanical stability were applied for aqueous photocatalytic degradation of persistent pharmaceuticals, amoxicillin, doxycycline, prednisolone and sulfamethizole, and their mixture in a larger lab-scale suspended-bed reactor. The toxicity reduction against selected bacterial strains during photocatalytic treatment as well as the potential for the coupling photocatalytic pre-treatment and biological activated sludge process was studied.

The immobilization of TiO<sub>2</sub> via sol-gel process onto commercially available lightweight expanded clay aggregates for photocatalytic water decontamination is a novel approach that simplifies the catalyst separation, reduces the cost of treatment process and thus hasten the widespread implementation of photocatalysis. The synthesis and immobilization of titania on lightweight expanded clay aggregates by means of titanium tetraisopropoxide-based sol-gel method resulted in stable and photocatalytically active coatings while TiO<sub>2</sub> deposition via adsorption, tetraethyl orthosilicate- and tetrabutyl orthotitanate-based sol-gel methods and using Hombikat XXS 100 and S5-300A sols resulted

in poor mechanical or photocatalytic properties of coatings. Pharmaceuticals more prone to adsorption on titania coatings have higher photocatalytic oxidation reaction probability, i.e. higher degradation efficiency. The photocatalytic oxidation was accompanied by a significant decrease in the toxicity to several bacterial strains allowing the process application as a pre-treatment prior to biodegradation.

## KOKKUVÕTE

### **Püsivate mikrosaasteainete lagundamine keevkihtreaktoris fotokatalüütilise oksüdatsiooniga ning bioloogilise oksüdatsiooni kombineerimine fotokatalüüsiga**

Ravimite olemasolu looduslikes veekogudes on oluline keskkonnaprobleem selliste ainete negatiivse mõju tõttu tervisele ja keskkonnale. Ravimid pärinevad erinevatest allikatest, nagu näiteks põllumajandus-, tööstus- ja olmereoveest, sattudes keskkonda läbi tavapärase reoveepuhasti. Üks võimalikest lahendustest selliste bioloogiliselt püsivate saasteainete kõrvaldamiseks on kasutada süvaoksüdatsiooniprotsesse nagu fotokatalüüs. Vaatamata fotokatalüüsi ilmsele võimele püsivaid veesaasteaineid tõhusalt lagundada, on fotokatalüütilise töötluste rakendamine vee puhastamiseks praegu piiratud, peamiselt seetõttu, et katalüsaatori eraldamine peale töötlust on kulukas. Seega tuleb täiustada fotokatalüsaatori kinnitamismeetodit, et rakendada seda kihi materjalina fotoreaktoris, milles saab saasteaineid efektiivselt viia UV-A kiiritatud katalüsaatori pinna lähedusse.

Käesolev uurimistöö keskendub katalüsaatori kandjale kinnitamismeetodi leidmisele, et seda rakendada keevkihi põhimõttel töötavas reovee töötlemissüsteemis. Uurimistöö eesmärgiks on ka selle süsteemi toime hindamine ravimite eemaldamiseks ja antud süsteemi biooksüdatsiooniga kombineerimise võimalikkuse hindamine keskkonnas esilekerkivate mikrosaasteainete tõhustatud ärastamiseks.

Katalüsaatori kinnitamiseks kasutati adsorptsiooni ja sool-geel meetodit. Sool-geel meetodi rakendamisel katete valmistamiseks kasutati erineva koostisega lahuseid ja tingimusi. Kõrgeima fotokatalüütilise aktiivsuse ja mehaanilise stabiilsusega katteid kasutati püsivate ravimite fotokatalüütiliseks lagundamiseks suuremõtmelises kolmefaasilises keevkihtreaktoris; uuritavate ainetena kasutati amoksitsilliini, doksütsükliini, prednisolooni ja sulfametisooli eraldi ning segus. Uuriti toksilisuse vähenemist fotokatalüütilise töötlemise ajal valitud bakteritüvede vastu ja võimalust fotokatalüütilise eeltöötluste kombineerimiseks bioloogilise aktiivmudaprotsessiga.

Titaandioksiidi kinnitamine sool-geel meetodiga kaubanduslikult saadavale kergkruusale vee fotokatalüütiliseks puhastamiseks saasteainetest on uudne lähenemine, mis lihtsustab katalüsaatori eemaldamist, alandab töötlemise hinda ja seega soodustab laialdast fotokatalüüsi kasutuselevõttu. Titaandioksiidi süntees ja kinnitamine keramsiidi pinnale kasutades titaan tetraisopropoksiidil põhinevat sool-geel meetodit võimaldas valmistada stabiilseid ja fotokatalüütiliselt aktiivseid katteid. Katted, mis moodustusid TiO<sub>2</sub> kinnitamisel adsorptsiooni teel, tetraetüül ortosilikaatil ja titaan butoksiidil baseeruva sool-geel meetodi abil, ning kasutades Hombikat XXS 100 ja S5-300A lahuseid, olid kehvade mehaaniliste ja fotokatalüütiliste omadustega. Ravimid, mis on aldis TiO<sub>2</sub> katetel adsorbeeruma, omavad suuremat fotokatalüütilise oksüdatsiooni

reaktsiooni tõenäosust, st kõrgemat lagunemise efektiivsust. Fotokatalüütilise oksüdatsiooniga kaasnes oluline toksilisuse langemine mitmete bakteritüvede vastu, võimaldades protsessi rakendust enne bioloogilist töötlust.



## **APPENDIX A**



## PAPER I

Klauson, D., Poljakova, A., **Pronina, N.**, Krichevskaya, M., Moiseev, A., Dedova, T., Preis, S. Aqueous photocatalytic oxidation of doxycycline. - *Journal of Advanced Oxidation Technologies*, 2013, 16 (2), 234–243.

Reproduced with permission from De Gruyter.



# Aqueous Photocatalytic Oxidation of Doxycycline

Deniss Klauson<sup>\*1</sup>, Alissa Poljakova<sup>1</sup>, Natalja Pronina<sup>1</sup>, Marina Krichevskaya<sup>1</sup>, Anna Moiseev<sup>2</sup>, Tatjana Dedova<sup>3</sup>, Sergei Preis<sup>4</sup>

<sup>1</sup>Department of Chemical Engineering, Tallinn University of Technology, Ehitajate tee 5, 19086 Tallinn, Estonia

<sup>2</sup>Institute of Non-Metallic Materials, TU Clausthal, Zehntnerstrasse 2a, 38678, Clausthal-Zellerfeld, Germany

<sup>3</sup>Department of Materials Science, Tallinn University of Technology, Ehitajate tee 5, 19086 Tallinn, Estonia

<sup>4</sup>LUT Chemistry, Lappeenranta University of Technology, P.O. Box 20, 53851 Lappeenranta, Finland

---

## Abstract:

The experimental research into the aqueous photocatalytic oxidation of doxycycline, a tetracycline family antibiotic, was undertaken. The objective of the study was to ensure the feasibility of doxycycline photocatalytic degradation by UVA irradiated titania coatings on granulated media to be used in fluidised bed photocatalytic reactor and by slurries of P25, Evonik, as well as by visible light-sensitive sol-gel synthesized carbon-containing titania. The parameters influencing doxycycline oxidation, like catalyst concentration, initial doxycycline concentration and pH with P25 TiO<sub>2</sub> were studied. The impact of calcination temperature on the catalytic properties of carbon-containing titania and catalytic activity of titania film on expanded clay as bed material towards doxycycline degradation were also studied. Based on the examination of doxycycline photocatalytic oxidation by-products, possible doxycycline degradation pathways were proposed.

**Keywords:** oxidation pathway, tetracycline antibiotics, visible light-sensitive titania, calcinations, granular support

---

## Introduction

Antibiotics in wastewaters, originating mainly from household, medical and veterinary sources, are refractory substances (1-3) that tend to pass the conventional biological treatment plants intact (4), either remaining in the liquid phase or, dependent on their hydrophilicity, adsorbing to the active sludge with subsequent desorption to the environment (5). In the environment, they pose a serious threat to micro-flora and fauna, accumulate in food chains (6, 7), and accelerate the development of resistant micro-organisms, including pathogens (8-11). The accumulation of antibiotics in organisms may cause various health problems, including arthropathy, nephropathy, damages in central nervous system and spermatogenesis, mutagenic effects and light sensitivity (2).

Doxycycline ((4*S*,4*aR*,5*S*,5*aR*,6*R*,12*aS*)-4-(dimethylamino)-3,5,10,12,12a-pentahydroxy-6-methyl-1,11-dioxo-1,4,4a,5,5a,6,11,12a-octahydrotetracene-2-carboxamide; Figure 1) is a widely used tetracycline antibiotic. Besides from the usual antibacterial action doxycycline is also used against protozoa and helminths. Since doxycycline is used as a treatment or prophylactic of some of the most hazardous diseases known to mankind, such as bubonic plague and anthrax (12, 13), its prevention from entering the environment is of great importance.

Photocatalytic oxidation is one of the advanced oxidation processes (AOPs) based on the action of positively charged holes on the surface of illuminated semiconductor, most often titanium dioxide. Water molecules decompose on the holes to form powerful hydroxyl radicals (14); the hole itself also can degrade the pollutant having even higher oxidation potential (15). The electrons, excited by the UV-irradiation, participate in the photocatalysis, reducing adsorbed oxygen resulting in formation of other radical oxidants. The ratio of radical to hole oxidation reactions depends on the adsorptive and reactive properties of the substance to be degraded. Many substances may be degraded by both mechanisms simultaneously (16-18).

Large-scale implementation of photocatalytic processes requires a respective photoreactor with titania nanoparticles fixed on support material, whereas fluidized bed systems are considered to have several advantages such as more uniform exposure of particles to the fluid, i.e. better reactant-catalyst contact, potentially better photons transfer efficiency and high mass and heat transfer rates (19). However, fluidized bed process suffers from the particle attrition (20), thus the stability of the bond between a photocatalyst and its support is crucial for effective operation of such a photocatalytic reactor. Photocatalyst P25 attachment methods incorporating sol-gel derived silica films are reported in present study. Future work will address the properties of sol-gel derived titania films and how

---

\*Corresponding author; E-mail address: [deniss.klauson@ttu.ee](mailto:deniss.klauson@ttu.ee)

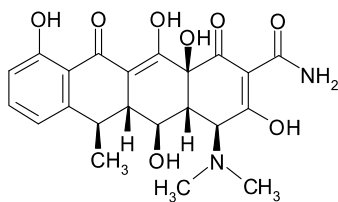


**Figure 1.** Structural formula of doxycycline.

their activity and stability are influenced by the sol-gel process parameters.

Although industrial photocatalytic materials, such as P25 titanium dioxide (Evonik), exhibit a good performance, they can use only an ultraviolet fraction (ca. 4%) of solar radiation reaching the earth surface due to the high energy of its band gap (21). This makes sensitising TiO<sub>2</sub>-based photocatalysts to visible light the potential way of widening of utilised solar spectrum. For this purpose, titanium dioxide can be doped with various metals or non-metals, which can effectively reduce the band-gap (22–28) for excitation of electrons by lower energy photons at greater wavelength up to 540 nm as reported. However, the authors found earlier that the doped titania photocatalysts may, unlike “universal” P25, oxidise only selected pollutants (29) that can be explained by the smaller redox potential and, possibly, higher electron-hole recombination rate of these catalysts (30).

The authors failed to find any available information in the scientific literature considering photocatalytic oxidation by-products of doxycycline. The study on doxycycline photocatalytic oxidation with the elucidation of its oxidation pathways was one of the objectives and novelties of the present research, since the published works on treatment of antibiotics by AOPs mainly focus on the parent compound removal and mineralization, leaving the degradation by-products unexplored. Another objective was characterisation and study of visible light active photocatalysts testing their performance by the degradation of doxycycline. The applicability, i.e. activity towards doxycycline degradation and adhesion degree to the support, of photocatalysts coatings attached to expanded clay by sol-gel silica derived films, not considered before was also studied.

## Materials and Methods

### Experimental Setup and Procedures

Two thermostatted at 20±1 °C 200-mL batch reactors with inner diameter 100 mm, irradiated plane surface 40 m<sup>2</sup> m<sup>-3</sup>, agitated with magnetic stirrers, were used in photocatalytic oxidation experiments: the one

used for the photocatalysis was called “active” and the other containing no photocatalyst was called “reference”. Both reactors were exposed to the identical experimental conditions. The samples from the active reactor were compared to the reference samples to avoid complications caused by water evaporation. An artificial UV-light source, Phillips Actinic BL low pressure luminescent mercury UV-lamp (15 W), having maximum emission around 365-nm, was positioned horizontally over the reactors, providing the irradiance of about 1.5 mW cm<sup>-2</sup> measured at a distance corresponding to the level of the surface of the reactor by the optical radiometer Micropulse MP100 (Micropulse Technology, UK). With artificial daylight fluorescent lamp (Phillips TL-D 15W/33-640), the irradiance could not be directly measured. The illuminance was measured using TES 1332 luxmeter (TES Inc., Taiwan) reaching 3,700 lx (lm/m<sup>2</sup>), which corresponds to the irradiance of 0.6 mW/cm<sup>2</sup>. The irradiance was calculated using lumen to watt ratio of 684, as the response of the human eye to the illuminance of 684 lm equals to that to the irradiance of 1 W (31). The photometric data on Phillips TL-D fluorescent lamp could be found in (32).

Titanium dioxide P25, Evonik, was used as slurry, with its concentration varying from 0.5 to 1.5 g L<sup>-1</sup>. The experiments were carried out with aqueous solutions of doxycycline supplied by Sigma-Aldrich. In the experiments, the initial concentration of doxycycline varied between 10 and 100 mg L<sup>-1</sup>. The influence of the initial pH was studied in the range from 3 to 7, adjusted by 4 N sulphuric acid or 15% sodium hydroxide. The pH was monitored throughout the experiments without adjustment. The treatment time was chosen to be 1 to 4 h (dependent on the initial concentration) under artificial light of the UV and VIS lamps. The experimental time was chosen to achieve at least 50% reduction of the initial doxycycline concentration. The photolytic doxycycline degradation under UVA irradiation and in absence of catalyst was tested at natural pH 4.4 and initial concentration of 25 mg l<sup>-1</sup>. Photolysis was found to be insignificant as doxycycline concentrations varied within 5% from the initial value.

Adsorption experiments were carried out in dark in closed thermostatted flasks equipped with magnetic stirrers at 20±1 °C. The amount of adsorbed substance was derived from the batch mass balance: the concentration of the dissolved substance was determined before and after adsorption. The adsorption equilibrium was experimentally determined to be reached in 2 h. In order to determine doxycycline concentration in the adsorption experiments, the UV-absorbance was used.

All the experiments were carried out for at least three times under identical experimental conditions. The average deviation of data in parallel experiments did not exceed 5%.

### **Synthesis of Photocatalysts**

Six specimens of carbon-doped titania were obtained by the hydrolysis of tetrabutyl orthotitanate (28.6 and 71.4% w/w of tetrabutyl orthotitanate and water, respectively) at room temperature without adjustment of pH being around 5.5 to 6.0, followed by drying and calcination at different temperatures (200 to 800 °C). After calcinations, all the catalysts were washed with hot (70-80 °C) distilled water applied in a sequence of 10 to 15 rinsing rounds (ca. 1 L per 1 g of catalyst) in order to clean the catalyst surface from water-soluble compounds.

### **Preparation of TiO<sub>2</sub> Coatings**

Two procedures of P25 attachment on expanded clay (fractions 2-3 and 4-5.5 mm, Saint-Gobain Leca) were examined as a beginning for the research on fluidized bed support material to be used for photocatalytic degradation of emerging micropollutants. Tetraethyl orthosilicate (TEOS, Merck Schuchardt OHG) was selected as a precursor for the TiO<sub>2</sub> fixation on expanded clay through silica sol-gel process; the P25 titania was either directly added to the sol (first procedure) or silica sol gel coating of the expanded clay with previously fixed P25 was applied (second procedure). For the first procedure 42.6% (w/w) of TEOS and 41% (w/w) of isopropanol (Lach-Ner) with preliminary suspended P25 (0.6, 2.5 or 9% of TiO<sub>2</sub> in isopropanol) were stirred for 5 min. Afterwards 8.2% (w/w) of 1 M HNO<sub>3</sub> as process catalyst and 8.2% (w/w) of H<sub>2</sub>O were added to the mixture, which was then stirred for 24 h. The support was immersed into the sol-gel followed by decantation of reactive colloid; time of the pre-drying at room temperature was varied from 0 to 72 h, drying time at 200 °C was varied from 1 to 15 h, followed by washing with distilled water and drying at 120 °C. In the second preparation procedure granular support material was constantly stirred for 2 h in isopropanolic or periodically in aqueous titania suspensions (0.6 and 1% w/w, respectively); afterwards the suspensions were decanted and support material was dried at 120 °C up to 2 h. To achieve maximum adsorption of titania on porous expanded clay, this was repeated ten times. To avoid catalyst washout, the support was coated with sol-gel derived silica film prepared as described above with the exception of titania addition. The acidification of expanded clay surface was carried out by its immersion in 1 M HNO<sub>3</sub>

solution for 24 h followed by drying either in furnace at 120 °C for 1.5 h or in air at room temperature for 24 h. The photocatalytic activity of the immobilized P25 TiO<sub>2</sub> was evaluated by the degradation of doxycycline (25 mg L<sup>-1</sup>).

### **Analyses**

In order to determine doxycycline concentration, two methods were compared in several photocatalytic oxidation experiments: photometrical determination of specific UV absorption (SUVA) at 346 nm using Helios β spectrophotometer, and the high-performance liquid chromatography combined with diode array detector and mass-spectrometer, (HPLC-PDA-MS, Shimadzu LC-MS 2020) were used for the determination of doxycycline concentration. In both cases, a pre-constructed calibration curve was used. Phenomenex Gemini-NX 5u C18 110A 150×2.0 mm column, inner diameter 1.7 μm, was used with two eluents, 0.1% acetic acid aqueous solution (eluent A), and acetonitrile (eluent B), with total eluents flow of 0.3 mL min<sup>-1</sup>; starting concentration of eluent B was 5%, increased to 48.5% by 23 minutes with linear gradient, held at that concentration for two minutes, and then decreased to 9.5% by 30 minutes, out of 30 minute analysis. Mass spectra were acquired in full scan mode, MS operated in positive ionisation mode with interface voltage of 4.5 kV, and detector voltage of 3.3 kV. Diode array detector was set to scan samples at 190 – 800 nm. The instrument was operated and the results obtained with MS and PDA detectors were handled using Shimadzu LabSolutions software. The by-products of doxycycline photocatalytic oxidation were determined using the described HPLC-MS method. The reason for using two methods was the relative ease of spectrophotometric determination, provided no or little interference of the UV-absorbing doxycycline photocatalytic oxidation by-products will hamper the photometric analysis. UV-absorbance was proved to be applicable with the sufficient accuracy, because the differences between the concentration values obtained by photometrical and HPLC-MS determination were negligible. The by-products of doxycycline photocatalytic oxidation were determined using the same HPLC-MS set.

Chemical oxygen demand (COD) was determined by a standard dichromate method (33), using HACH kits LCK 314 (15 to 150 mg O L<sup>-1</sup>) and LCK 414 (5 to 60 mg O L<sup>-1</sup>). The concentration of ammonium ion was determined photometrically using a modified version of a standard phenate method (33). Nitrate and sulphate anions were determined using Metrohm 761 Compact IC ionic chromatograph.

The crystal structure and phase composition of carbon-containing titanium dioxide were analysed using D 5000 Kristalloflex, Siemens (Cu-K $\alpha$  irradiation source) X-ray diffraction spectroscope (XRD), with the phase composition calculated by Topas R Software. Identified peak positions were compared to the data found in literature (34, 35). The specific surface area (BET and Langmuir adsorption) and the pore volume of the catalysts were measured by the adsorption of nitrogen using KELVIN 1042 sorptometer.

For the optical measurements ethanol-based suspensions (1 g L<sup>-1</sup>) of TiO<sub>2</sub> powders were prepared on microscopic glass substrates and after total ethanol evaporation measurements were carried out with the obtained coatings. Total and diffused reflectance spectra of the coatings were measured in the wavelength range of 250 – 2500 nm on a Jasco V-670 UV-VIS spectrophotometer equipped with an integrating sphere. Obtained data were used to calculate the absorption coefficient ( $\alpha$ ) and optical band gap values ( $E_g$ ). For the titanium dioxide photocatalysts of various crystalline modifications, evidence supporting both direct electron transition (36, 37) and indirect one (34, 36, 38-42) has been published, although the majority of the last decade publications report indirect transition for titanium dioxide. Consequently, band gap values of the new photocatalysts were calculated assuming indirect transition type. A standard expression for transitions between two parabolic bands for the calculation of band gap energy is:

$$(\alpha h\nu)^m = A(h\nu - E_g) \quad (1)$$

where  $m = 1/2$  and  $A$  is a constant.

Band gap values were found from the intercept of the linear fitting curve extrapolated to the zero absorption of  $(\alpha h\nu)^m$  vs.  $h\nu$  plot. Haze factor values were calculated as the relationship of diffused reflectance to total reflectance; it shows the extent of light scattering, and, thus, the relative roughness of the coatings (43).

Field emission scanning electron microscopy (FE SEM, DualBeam Helios Nanolab 600, FEI) was performed to visualize the catalyst coatings. Turbidity of the solutions treated by titania coating attached to expanded clay was measured at 860 nm in Formazin Attenuation Units (FAU turbidity, HACK DR2800).

### Photocatalytic Oxidation Efficiency

In order to express the results of doxycycline photocatalytic oxidation, its concentration decrease rate and the process efficiency  $E$ , defined as the decrease in the amount of the pollutant divided by the amount of energy reaching the surface of the treated sample,

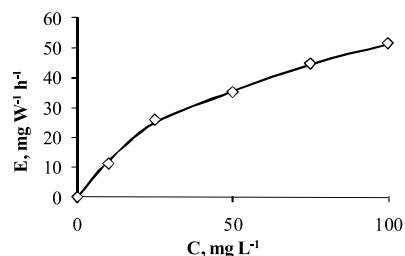


**Figure 2.** The dependence of doxycycline photocatalytic oxidation efficiency on its initial concentration (1 h treatment time, pH 4.4).

were used. The efficiency is calculated according to the following equation (44):

$$E = \frac{1000 \Delta C V}{I S t} \quad (2)$$

where  $E$  – photocatalytic oxidation efficiency, mg W<sup>-1</sup> h<sup>-1</sup>;  $\Delta C$  – the decrease in the pollutant's concentration, mg L<sup>-1</sup>, or COD, mg O L<sup>-1</sup>;  $V$  – the volume of the sample to be treated, L (in this case, 0.2 L);  $I$  – irradiance, mW cm<sup>-2</sup>;  $S$  – irradiated area, cm<sup>2</sup>;  $t$  – treatment time, h.

## Results and Discussion

### Photocatalytic Oxidation with P25

Optimum titanium dioxide dose was determined to be 1 g L<sup>-1</sup> for the degradation of 25 mg L<sup>-1</sup> of doxycycline: with the increase of TiO<sub>2</sub> amount from 0.5 to 1 g L<sup>-1</sup> photocatalytic oxidation efficiency increased, whereas with the subsequent dosage increase up to 1.5 g L<sup>-1</sup>  $E$  has remained the same. The best performance was observed at pH 4.4, occurring naturally in the doxycycline solutions, followed closely by neutral and acidic media, i.e. the observed pH-dependence was rather weakly pronounced.

Figure 2 shows the dependence of photocatalytic oxidation efficiency on the doxycycline initial concentration, calculated for 1 h treatment. It can be seen that  $E$  increases with the increased initial doxycycline concentration within the experimental limits assuming the description of the doxycycline photocatalytic oxidation using Langmuir-Hinshelwood (L-H) model of monomolecular surface reaction, followed by the products desorption (Eq. 3, 4). The equation, derived from the experimental data via the  $1/r_0 = f(1/c_0)$  dependence (plot not shown), has average square deviation  $R^2=0.99$ , supporting the proposed L-H data fit. The reaction rate equation:

$$r_0 = k \frac{K C_0}{1 + K C_0} \quad (3)$$

where  $r_0$  is the reaction rate, mM min<sup>-1</sup>;  $k$  – reaction rate constant, mM<sup>-1</sup> min<sup>-1</sup>;  $K$  – adsorption constant,

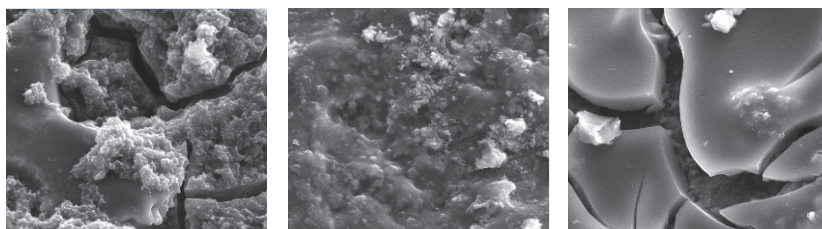


Figure 3. SEM images of silica films with titania inclusions on expanded clay support.

mM;  $c_0$  – initial doxycycline concentration, mM, gives:

$$r_0 = 0.002 \frac{10.2c_0}{1+10.2c_0} \quad (4)$$

With the addition of *tert*-butyl alcohol (TBA) as a radical scavenger to the solution to be treated in the amount equimolar with doxycycline (0.056 mM, i.e. 25 mg L<sup>-1</sup> of doxycycline and 4.2 mg L<sup>-1</sup> of TBA), the doxycycline degradation rate decreased by a very small amount, ca. 5%, comparable to the accuracy limit in parallel experiments, which allows suggesting the dominance of hole oxidation reactions: the radical oxidation should be noticeably affected by the presence of TBA.

The dark adsorption of doxycycline on the surface of P25 titanium dioxide was relatively high from 5.9 mg g<sup>-1</sup> at the initial doxycycline concentration of 10 mg L<sup>-1</sup> to 20 mg g<sup>-1</sup> at 100 mg L<sup>-1</sup>. Within the studied concentration range, the Langmuir equation (Eq. 5, 6), fits well to the adsorption experimental data (R<sup>2</sup>=0.98):

$$q_L = q_{\max} \frac{Kc_0}{1 + Kc_0} \quad (5)$$

where  $q$  – adsorption, mmol g<sup>-1</sup>;  $q_{\max}$  – theoretical maximal adsorption, mmol g<sup>-1</sup>, giving:

$$q_L = 0.08 \frac{9.2c_0}{1 + 9.2c_0} \quad (6)$$

The  $K$ -values obtained from photocatalytic runs and adsorption experiments close to each other indicate the consistency of adsorption and degradation mechanism regularities. Thus, in the photocatalytic oxidation of doxycycline, its adsorption on the catalyst surface is an important factor, as the behaviour of the oxidation efficiency consistent with the adsorption may support the hypothesis of L–H mechanism, where the rate of the reaction of surface-adsorbed doxycycline with holes or electrons is slower, than that of the adsorption obeying a Langmuir isotherm.

The percentage of COD degraded during doxycycline photocatalytic oxidation was reasonably high at smaller concentrations: e.g. at 20–25 mg doxycycline

L<sup>-1</sup>, up to 80% of COD was degraded during two hours of the experiment. With the increased doxycycline concentration COD degradation decreased significantly: with 100 mg doxycycline L<sup>-1</sup>, only 7% of COD was degraded in 4 h. The disproportion between degraded doxycycline and COD at higher initial concentrations can be explained by the accumulation of non-aromatic doxycycline degradation by-products, resulting from the destruction of the aromatic cycle (see Figure 8). This assumption is consistent with the minor discrepancy between the UV-absorbance at 346 nm and the HPLC-MS measurements of the doxycycline concentration in photocatalytic oxidation-treated solutions (see Materials and Methods). Also, the low mineralization degree of the amino nitrogen is consistent with accumulation of organic by-products at higher doxycycline concentrations (see Doxycycline Photocatalytic Oxidation By-Products and Reaction Pathway).

#### Photocatalytic Oxidation of Doxycycline by Catalyst Fixed on Expanded Clay

The activity of P25 titania attached on the granular support was studied varying the procedures of catalyst fixing (see Materials and Methods) and some parameters like pre-drying and drying time, the quantities of titania and the number of sol-gel layers attached; the impact of acidification of expanded clay material on coatings' stability and activity was also investigated. The increase in titania content in sol-gel derived silica film (prepared by the first procedure, Materials and Methods) or in number of film layers, i.e. the coating thickness, (Figure 3c), resulted in high turbidity of treated solutions (over 100 FAU) due to titania washout, weak support - silica film bonds and low photocatalytic efficiency. The coatings were prone to cracking (Figure 3a) if insufficient time of pre-drying was applied so the cracks' propagation was restrained by 24-h time of pre-drying and the efficiency of these materials towards doxycycline degradation raised up to 0.75 mg W<sup>-1</sup> h<sup>-1</sup> along with medium turbidity levels observed (about 60 FAU).

The 24-h pre-drying of coatings on preliminary acidified porous granulated support at room temperature

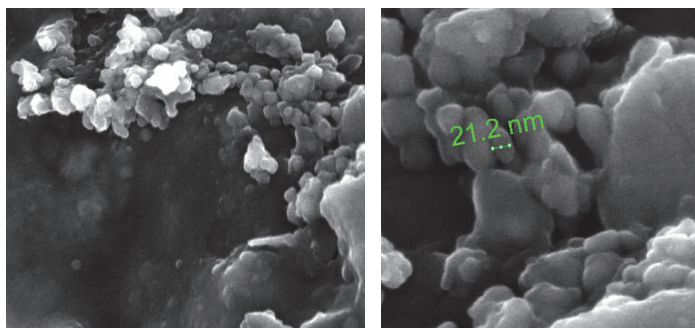


**Figure 4.** SEM images of titania primary particles fixed by silica films on expanded clay support.

and subsequent drying at 200 °C for 15 h lead to stable coatings (Figure 3b) with low turbidity in the solutions to treat (under 20 FAU), though lowering slightly their activity (efficiency up to 0.5 mg W<sup>-1</sup> h<sup>-1</sup>). In present study the highest efficiency in degrading of doxycycline of 1.5 mg W<sup>-1</sup>h<sup>-1</sup> was demonstrated by silica films on non-acidified expanded clay with titania preliminary adsorbed from its isopropanol suspensions (second procedure, Materials and Methods) followed by 1.35 mg W<sup>-1</sup> h<sup>-1</sup> for titania adsorbed from its aqueous slurries, which showed also relatively low turbidity levels, i.e. low catalyst washout and fairly good adhesion of the coating on supporting material. The primary particles of P25 were revealed on the surface of sol-gel films (Figure 4) facilitating the photocatalytic activity of these coatings.

#### **Photocatalytic Oxidation of Doxycycline by Carbon-containing Titania**

Figure 5 shows the X-ray diffraction patterns of carbon-containing titania. With the growth of the calcination temperature, abrupt changes take place in the catalyst crystallographic composition at 600 to 700 °C. Judging from the XRD analysis, at temperatures up to 600 °C the catalysts are composed of both anatase and brookite in relatively constant amounts. For anatase, the (1 0 1) peak was the best pronounced, followed by (1 0 3), (2 0 0), (0 0 4), (1 0 3) and (1 1 2) whereas for brookite, the (1 2 0), (1 2 1), (2 0 1) and (2 3 1) peaks were determined. The catalysts obtained at 700 and 800 °C are pure rutile, as expected for both anatase and brookite transforming directly to rutile starting at temperatures around 500 to 600 °C (45). For rutile, (1 1 0), (1 0 1), (1 1 1), (2 1 0) and (2 2 0) peaks were identified. The exact composition of the photocatalyst, as calculated from the XRD graphs, is given in Table 1.

The specific surface area of the catalysts decreases with the calcination temperature increased from 200 to

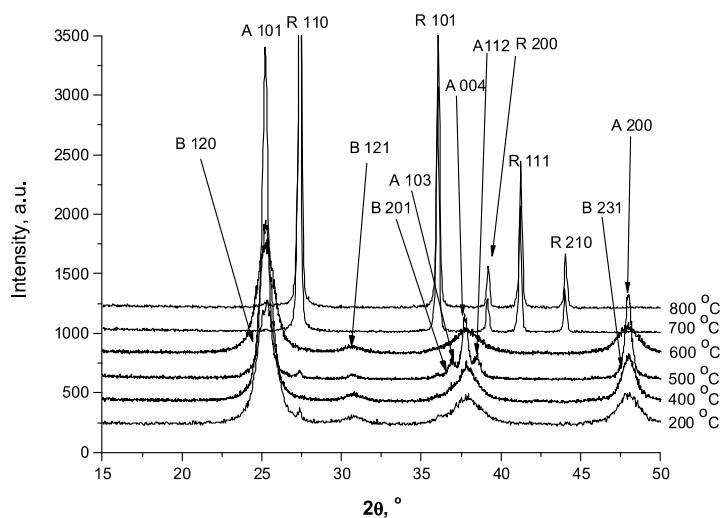
500 °C, whereas micropore volume and area somewhat increased at 400-500 °C, approximating zero at higher temperatures within accuracy of measurements (Table 1). However, since the adsorption of the pollutants by the catalysts was observed to be negligible, surface structure and characteristics of the catalysts can be considered as being of secondary importance for the purposes of this study.

Negligible amount of UV emitted by the visible radiation sources, coupled with observed photocatalytic performance of C-TiO<sub>2</sub> can only indicate visible light activity of the photocatalysts. The calculated band gap values (Table 1), suggesting visible light utilisation, are in good agreement with the observed experimental results. Optical band gap values of C-TiO<sub>2</sub> decreased with the increased calcination temperature, with the biggest changes observed between 500 and 700 °C, coinciding with the TiO<sub>2</sub> phase transformation. The changes in the band gap energy should be viewed with the respect to both dopant incorporation into titanium dioxide and the changes in phase composition. Anatase, brookite and rutile as individual phases were reported to have band-gap energies of 3.34, 3.40 and 2.95 eV respectively (34, 38). Optical band gap of a multi-phase material gives an average value, which takes into account, although not linearly, the band gaps of each phase and their relative amounts.

Diffused reflectance spectra given in Figure 6a shows in general the increase in reflectance with increase in calcination temperature as a result of carbon burning out from the sol along with the agglomeration of particles, i.e. enlargement of the particles average size. With the calcination temperature increased from 200 to 500 °C, total reflectance of the photocatalysts at 400 nm increased from 62 to 74%, and then steadily decreases to 33% at 800 °C. For comparison, total reflectance of P25 at 400 nm was 71%. Thus, with the anatase and brookite phase transformation to rutile,

**Table 1.** Physical characteristics of carbon-containing photocatalysts dependent on the calcination temperature

T(calcination), °C	Crystallographic composition, %			S(BET), m <sup>2</sup> g <sup>-1</sup>	S(Langmuir), m <sup>2</sup> g <sup>-1</sup>	Micropore area, m <sup>2</sup> g <sup>-1</sup>	Micropore volume, mm <sup>3</sup> g <sup>-1</sup>	Total reflectance at 400 nm, %	E <sub>g</sub> , eV	λ <sub>cut-off</sub> , nm
	Anatase	Brookite	Rutile							
200	71.9	28.1	-	202	279	0	0	62	2.81	442
400	78.1	21.9	-	106	145	4.12	1.54	73	2.89	429
500	76.9	18.2	5.0	39	54	3.95	1.39	74	2.89	429
600	74.4	25.6	-	8.8	12.1	0	0	29	2.74	452
700	-	-	100	3.5	4.8	0.20	0.07	30.5	2.77	448
800	0.8	-	99.2	3.7	5.1	0.13	0.05	33	2.78	446

**Figure 5.** X-ray diffraction pattern of the C-TiO<sub>2</sub> photocatalysts.

total reflectance of the catalysts abruptly decreased (see Table 1). Haze factor characterizing light scattering decreased with the increased calcination temperature (Figure 6b), suggesting the surface of the coatings becoming even.

The performance of the carbon-containing titania treated at different calcination temperatures was tested with doxycycline solutions of 25 mg L<sup>-1</sup> at pH 4.4. Under artificial daylight the catalyst thermally treated at 200 °C, having presumably the highest carbon content and the contact surface, showed performance superior to that of P25: if P25 could remove under UV-irradiation 19.5 mg L<sup>-1</sup> during 1 h, C-TiO<sub>2</sub> sample thermally treated at 200 °C degraded 23.2 mg L<sup>-1</sup> under visible light of 2.5 times lower irradiance, making the corresponding photocatalytic oxidation efficiency for

about three times higher. With the increased catalysts' calcination temperature, their performance decreased (see Figure 7).

### ***Doxycycline Photocatalytic Oxidation By-products and Reaction Pathway***

Ammonia and nitrate in small amounts, and traces of nitrite were detected as the doxycycline photocatalytic oxidation by-products indicating the most of nitrogen remaining in organic by-products. A number of organic by-products were determined qualitatively using HPLC coupled with MS.

The determined products allow distinguishing three possible doxycycline photocatalytic oxidation pathways proceeding simultaneously (Figure 8). Two of them (A and C) begin with stepwise oxidation of the terminal

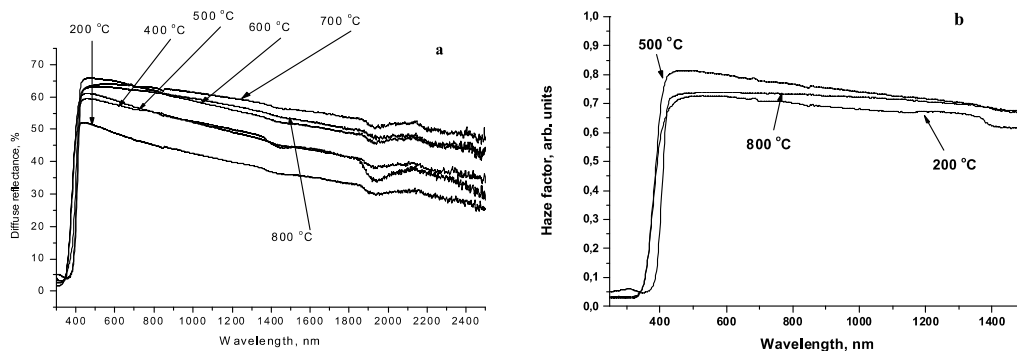


**Figure 6.** The dependence of diffuse reflectance (a) and haze factor (b) on the calcination temperature of C-TiO<sub>2</sub>.

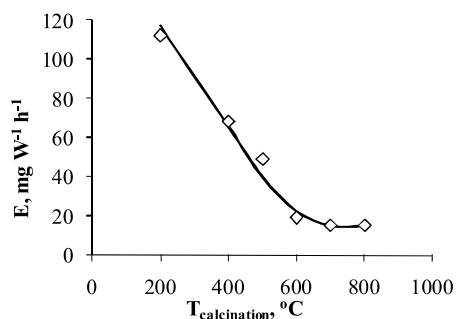


**Figure 7.** The dependence of doxycycline photocatalytic oxidation efficiency on the calcinations temperature of the carbon-modified titania: doxycycline concentration 25 mg L<sup>-1</sup>, pH 4.4.

parts of the doxycycline molecule ( $m/z=445$ ): in pathway A, hydroxyl group adds to aromatic cycle ( $m/z=461$ ), and subsequently aromatic ring and the adjacent cycle are destroyed before finally forming the identified product with  $m/z=409$ , whereas pathway B begins with the subtraction of dimethyl amino- and amino groups and their replacement by hydroxyl group, together with phenolic cycle oxidation ( $m/z=433$ ). Pathway C, on the other hand, proceeds solely through the oxidation of doxycycline molecule starting from the nitrogen-containing side, leading to the formation of product with  $m/z = 291$ . In pathway A, the product with  $m/z=409$  goes through subsequent oxidation of the part of the molecule adjacent to the already degraded phenolic ring, until the formation of mono-cyclic product with  $m/z=415$ . Ammonium and nitrate ions, detected in very small amounts (0.21 mg L<sup>-1</sup>, or 0.012 mM of ammonium, and traces of nitrate) in comparison to the amount of doxycycline degraded under the experimental conditions (19.9 mg L<sup>-1</sup> or 0.045 mM), suggest the predominance of pathway A

over the other ones: about three quarters of doxycycline appear to degrade via pathway A.

## Conclusions

Aqueous photocatalytic oxidation of a widely used tetracycline antibiotic doxycycline was studied using P25 titanium dioxide slurries or supported on expanded clay and visible light-sensitive synthetic sol-gel titania catalysts doped with carbon. The photocatalytic oxidation of doxycycline appeared to be less sensitive towards the solution pH, although proceeding slightly better at unregulated pH 4.4. The efficiency of the doxycycline removal increases with its increasing concentration within the tested limits, up to 100 ppm, although the oxidation by-products tend to accumulate at higher pollutant concentration. The photocatalytic oxidation by-products, determined by HPLC-MS, allow suggesting the reaction pathways. The titania fixation on expanded clay granular support by means of silica sol gel produced stable and photocatalytically active (up to 1.5 mg W<sup>-1</sup> h<sup>-1</sup>) coatings although further development and optimisation are needed to improve their performance. The modified titania sample with the highest carbon content and contact surface showed the performance (ca. 100 mg W<sup>-1</sup> h<sup>-1</sup>) surpassing the one of P25 (ca. 30 mg W<sup>-1</sup> h<sup>-1</sup>). The performance of carbon-containing titania decreased with the increased titania calcination temperature, i.e. decreased carbon content and contact surface.

## Acknowledgements

The authors thank Dr. Mai Uibu, Laboratory of Inorganic Materials, Tallinn University of Technology, for providing specific surface area measurements of the catalysts. The financial support of the Estonian Science Foundation (grants G8978 and GUS10), Estonian Science Agency project IUT1-7, Archimedes Foundation project 3.2.0801.11-0009, Estonian Ministry of

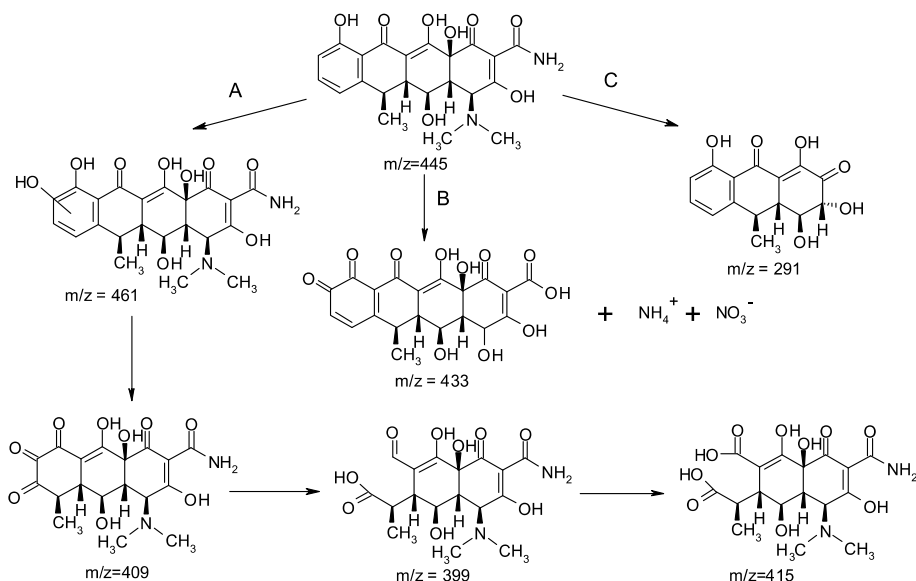


**Figure 8.** Proposed doxycycline photocatalytic oxidation reaction pathways (25 mg L<sup>-1</sup>, natural pH).

Education and Research project SF0140022s10, and the United States Civilian Research and Development Foundation (grant ESC2-2974-TL-09) is greatly appreciated.

## References

- (1) Al-Ahmad, A.; Daschner F.D.; Kummerer K. *Arch. Environ. Con. Tox.* **1999**, *37*, 158-163.
- (2) Kummerer, K.; Al-Ahmad, A.; Mersch-Sundermann, V. *Chemosphere* **2000**, *40*, 701-710.
- (3) Alexy, R.; Kumpel T.; Kummerer K. *Chemosphere* **2004**, *57*, 505-512.
- (4) Heberer, T. *Toxicol. Lett.* **2002**, *131*, 5-17.
- (5) Abellan, M.; Bayarri, B.; Gimenez, J.; Costa, J. *Appl. Catal. B-Environ.* **2007**, *74*, 233-241.
- (6) Halling-Sorensen, B.; Nielsen, S.; Lanzky, P.; Ingerslev, F.; Lutzhoft, H.; Jorgensen, S. *Chemosphere* **1998**, *36*, 357-394.
- (7) Hartig, C.; Storm, T.; Jekel, M. *J. Chromatogr. A* **1999**, *854*, 163-173.
- (8) Kim, S.; Eichhorn, P.; Jensen, J.N.; Weber, A.S.; Aga, D.S. *Environ. Sci. Technol.* **2005**, *39*, 5816-5823.
- (9) Baran, W.; Sochacka, J.; Wardas, W. *Chemosphere* **2006**, *65*, 1295-1299.
- (10) Aarestrup, F.M. *Antimicrobial Resistance in Bacteria of Animal Origin*; ASM Press, 2006.
- (11) Chatzidakis, A.; Berberidou, C.; Paspaltsis, I.; Kyriakou, G.; Sklaviadis, T.; Poullos, I. *Water Res.* **2008**, *42*, 386-394.
- (12) Greenfield, R.A.; Bronze, M.S. *Drug Discov. Today* **2003**, *8*, 881-888.
- (13) Brook, I. *Int. J. Antimicrob. Ag* **2002**, *20*, 320-325.
- (14) Sun, B.; Sato, M.; Clements, J.S. *J. Electrostat.* **1997**, *39*, 189-202.
- (15) Bahnemann, D. *Sol. Energy* **2004**, *77*, 445-459.
- (16) Matthews, R.W. *Water Res.* **1986**, *20*, 569-578.
- (17) Brezova, V.; Vodny, S.; Vesely, M.; Ceppan, M.; Lapcik, L. *J. Photochem. Photobiol. A-Chem.* **1991**, *56*, 125-134.
- (18) Chen, J.; Ollis, D.F.; Rulkens, W.H.; Bruning, H. *Water Res.* **1999**, *33*, 669-676.
- (19) Dong, S.S.; Zhou, D.D.; Bi, X.T. *Particuology* **2010**, *8*, 60-66.
- (20) Wang, R.C.; Fan, K.S.; Chang, J.S. *J. Taiwan Inst. Chem. E.* **2009**, *40*, 533-540.
- (21) Zhang, Y.; Crittenden, J.C.; Hand, D.W.; Perram, D.L. *Environ. Sci. Technol.* **1994**, *28*, 435-442.
- (22) Lettmann, C.; Hildenbrand, K.; Kisch, H.; Macyk, W.; Maier, W.F. *Appl. Catal. B-Environ.* **2001**, *32*, 215-227.
- (23) Arpac, E.; Sayilkan, F.; Asilturk, M.; Tatar, P.; Kiraz, N.; Sayilkan H. *J. Hazard. Mater.* **2007**, *140*, 69-74.
- (24) Ihara, T.; Miyoshi, M.; Iriyama, Y.; Matsumoto, O.; Sugihara S. *Appl. Catal. B-Environ.* **2003**, *42*, 403-409.
- (25) Sharma, S.D.; Singh, D.; Saini, K.K.; Kant, C.; Sharma, V.; Jain, S.C.; Sharma, C.P. *Appl. Catal. A-General* **2006**, *314*, 40-46.

- (26) Li, D.; Haneda, H.; Hishita, S.; Ohashi, N. *Mat. Sci. Eng. B-Solid* **2005**, *117*, 67-75.
- (27) Wang, Z.P.; Cai, W.M.; Hong, X.T.; Zhao, X.L.; Xu, F.; Cai, C.G. *Appl. Catal. B-Environ.* **2005**, *57*, 223-231.
- (28) Ohno, T.; Akiyoshi, M.; Umebayashi, T.; Asai, K.; Mitsui, T.; Matsumura, M. *Appl. Catal. A-General* **2004**, *265*, 115-121.
- (29) Klauson, D.; Portjanskaja, E.; Preis, S. *Environ. Chem. Lett.* **2008**, *6*, 35-39.
- (30) Liu, Z.Y.; Sun, D.D.; Guo, P.; Leckie, J.O. *Chem.-Eur. J.* **2007**, *13*, 1851-1855.
- (31) Kirkpatrick, S.J. *Dent. Mater.* **2005**, *21*, 21-26.
- (32) Philips, TL-D Standard Colours TL-D 15W/33-640 1SL, [http://download.p4c.philips.com/l4b/9/928024803347\\_eu/928024803347\\_eu\\_pss\\_aen.pdf](http://download.p4c.philips.com/l4b/9/928024803347_eu/928024803347_eu_pss_aen.pdf), 2013.
- (33) Clesceri, L.S.; Greenberg, A.E.; Trussel, R.R., Eds. Standard methods for the examination of water and wastewater; APHA, AWWA, WPCF: Washington, DC, 1989.
- (34) Di Paola, A.; Cufalo, G.; Addamo, M.; Bellardita, M.; Camostrini, R.; Ischia, M.; Ceccato, R.; Palmisano, L. *Colloid Surface A* **2008**, *317*, 366-376.
- (35) Sakurai, K.; Mizusawa, M. *Anal. Chem.* **2010**, *82*, 3519-3522.
- (36) Reddy, K.M.; Manorama, S.V.; Reddy, A.R. *Mater. Chem. Phys.* **2003**, *78*, 239-245.
- (37) Magne, C.; Cassaignon, S.; Lancel, G.; Pauporte, T. *Chemphyschem* **2011**, *12*, 2461-2467.
- (38) Koelsch, M.; Cassaignon, S.; Guillemoles, J.F.; Jolivet, J.R. *Thin Solid Films* **2002**, *403*, 312-319.
- (39) Tanemura, S.; Miao, L.; Jin, P.; Kaneko, K.; Terai, A.; Nabatova-Gabain, N. *Appl. Surf. Sci.* **2003**, *212*, 654-660.
- (40) Abdel-Aziz, M.M.; Yahia, I.S.; Wahab, L.A.; Fadel, M.; Afifi, M.A. *Appl. Surf. Sci.* **2006**, *252*, 8163-8170.
- (41) Zallen, R.; Moret, M.P. *Solid State Commun.* **2006**, *137*, 154-157.
- (42) Brezova, V.; Vreckova, Z.; Billik, P.; Caplovicova, M.; Plesch, G. *J. Photoch. Photobio. A* **2009**, *206*, 177-187.
- (43) Lin, C.J.; Yu, W.Y.; Chien, S.H. *Appl. Phys. Lett.* **2007**, *91*, 233120-233120-3.
- (44) Preis, S.; Krichevskaya, M.; Terentyeva, Y.; Moiseev, A.; Kallas, J. *J. Adv. Oxid. Technol.* **2002**, *5*, 77-84.
- (45) Li, J.G.; Ishigaki, T. *Acta Mater.* **2004**, *52*, 5143-5150.

Received for review April 4, 2013. Revised manuscript received May 21, 2013. Accepted May 22, 2013.

## PAPER II

**Pronina, N.**, Klauson, D., Moiseev, A., Deubener, J., Krichevskaya, M. Titanium dioxide sol-gel-coated expanded clay granules for use in photocatalytic fluidized-bed reactor. - *Applied Catalysis B: Environmental*, 2015, 178, 117–123.

Reproduced with permission from Elsevier.





Contents lists available at ScienceDirect

## Applied Catalysis B: Environmental

journal homepage: [www.elsevier.com/locate/apcatb](http://www.elsevier.com/locate/apcatb)

# Titanium dioxide sol–gel-coated expanded clay granules for use in photocatalytic fluidized-bed reactor



Natalja Pronina<sup>a,\*</sup>, Deniss Klauson<sup>a</sup>, Anna Moiseev<sup>b</sup>, Joachim Deubener<sup>b</sup>, Marina Krichevskaya<sup>a</sup>

<sup>a</sup> Department of Chemical Engineering, Tallinn University of Technology, Ehitajate tee 5, 19086 Tallinn, Estonia

<sup>b</sup> Institute of Non-Metallic Materials, TU Clausthal, Zehntnerstrasse 2a, 38678 Clausthal-Zellerfeld, Germany

## ARTICLE INFO

## Article history:

Received 22 June 2014

Received in revised form 9 September 2014

Accepted 5 October 2014

Available online 21 October 2014

## Keywords:

Doxycycline elimination

Photocatalytic coating

Fluidized bed

Expanded clay granules.

## ABSTRACT

An experimental research into the titania coatings on granulated expanded clay to be used in fluidized-bed photocatalytic reactor was undertaken. The preparation procedures were performed via sol–gel method using dip coating techniques. Two sol–gel compositions based on tetrabutyl orthotitanate and titanium tetraisopropoxide as well as two commercial TiO<sub>2</sub> sols were examined. The impacts of titania precursor concentration, modification of sol–gel by industrially available TiO<sub>2</sub> nanoparticles, the substrate withdrawal speed and thermal treatment conditions on the coatings' properties were studied. The photocatalytic activity of expanded clay-supported titania was evaluated by the degradation of an emerging micropollutant, tetracycline family antibiotic doxycycline. Mechanically stable and active coatings with properties dependent on sol–gel processing parameters were obtained. The application of porous titania sol–gel-coated expanded clays could combine pollutants' adsorption and their photocatalytic degradation. The compromise between coatings' improved photocatalytic performance, on the one hand, and their adhesion and attrition properties, significant for fluidized-bed operation, on the other hand, lead to the determination of appropriate processing parameters.

© 2014 Elsevier B.V. All rights reserved.

## 1. Introduction

The presence of pharmaceuticals in the environment has received a lot of attention in the last decades due to their negative health and environmental effects even at low concentrations [1,2]. Particularly, the occurrence of antibiotics in hospital, residential, dairy and livestock effluents and municipal wastewater with these pollutants passing through the conventional wastewater treatment intact causes their emissions and accumulation in the hydrological environment [3,4]. The pharmaceuticals are regularly monitored at low concentrations (mostly detected at ng L<sup>-1</sup> levels) all over the world and the introduction of their obligatory monitoring is currently under discussion [5,6].

The public concern on pharmaceuticals in the environment demands the completion of wastewater treatment plants by the technologies for their removal. One of the options for the

destructive elimination of such biologically persistent pollutants in wastewater is the use of advanced oxidation processes based on the action of reactive oxygen species. Amongst these technologies, the reactive species formed by photoexcitation of titanium dioxide allow degrading antibiotics [7–9]. Photocatalytic oxidation of tetracycline family antibiotic doxycycline was studied by our group [9] using P25 and sol–gel-synthesized titania slurries with oxidation by-products determined by liquid chromatography combined with mass spectrometry allowing to suggest the reaction pathway. Process favoring pH values, adsorption and photocatalytic reaction rate constants were obtained. Despite obvious ability of photocatalysis to degrade recalcitrant water pollutants, there is a need for the development of reactors and techniques for the catalyst attachment to the bed material.

Different materials were applied as titania photocatalyst support including glass, silica, ceramics, zeolites, stainless steel, activated carbon as well as granular materials like quartz sand, polymers, etc. [10–23]. Fixed-bed reactors have an intrinsic advantage of not requiring the catalyst separation operation, whereas fluidized-bed reactors are considered to reduce mass transfer limitations if compared to fixed bed. These, however, require the lightweight granular material with developed surface area.

\* Corresponding author. Tel.: +372 6202851; fax: +372 6202856.

E-mail addresses: [natalja.pronina@ttu.ee](mailto:natalja.pronina@ttu.ee) (N. Pronina), [deniss.klauson@ttu.ee](mailto:deniss.klauson@ttu.ee) (D. Klauson), [anna.moiseev@tu-clausthal.de](mailto:anna.moiseev@tu-clausthal.de) (A. Moiseev), [joachim.deubener@tu-clausthal.de](mailto:joachim.deubener@tu-clausthal.de) (J. Deubener), [marina.krithevskaja@ttu.ee](mailto:marina.krithevskaja@ttu.ee) (M. Krichevskaya).

The present study is focused on the preparation of titania coatings on expanded clay granules to be applied in fluidized-bed reactor for the photocatalytic degradation of doxycycline antibiotic.

The lightweight ceramic expanded clays are rarely used as support material, and its utilization for the titania photocatalyst attachment was studied by our group as reported in [9] and by Zendezhaban et al. [24]. In the last study, the adsorption of titania from its propanolic suspensions on expanded clay granules with those floating on the surface of treated ammonia solutions was investigated. However, our previous study showed that the immobilization of titania on expanded clay from its aqueous or propanolic suspensions had not provided the appropriate adhesion of the catalyst onto the support resulting in a catalyst washout during fluidized bed operation. The application of tetraethyl orthosilicate (TEOS)-based sol-gel as a fixator for industrial photocatalyst nanoparticles showed relatively low activity of the coatings if compared to those obtained later with the titania sol-gel.

Due to the attrition and thus the high level of mechanical stress placed on the coated material, the emphasis on the study of adhesion and abrasion resistance properties of the titania coatings should be firstly done. Secondly, the photocatalytic activity of the bed material should be optimized within the acceptable mechanical properties of the coatings.

In this study, the authors tried to overcome the above-discussed issues by the consecutive investigation of several titania precursors based sol-gel compositions to produce coatings on expanded clay with improved photocatalytic and mechanical properties.

## 2. Experimental

### 2.1. Preparation of coatings

The titania coatings were prepared on preliminary sieved 2–3 mm fraction of lightweight expanded clay aggregates (Saint-Gobain Leca). Four sol-gel coating solutions based on two different titania precursors, such as tetrabutyl orthotitanate (TBOT, Fluka), titanium tetraisopropoxide (TTIP, Alfa Aesar) and two industrial sols Hombikat XXS 100 (Sachtleben Chemie) [25] and S5-300A (Cristal Chemical Company) [26], were examined.

The mixture of Hombikat XXS 100 and ethanol in a mass ratio of 1:4.1, respectively, was used in the Hombikat XXS 100 based coating procedure (procedure 1); S5-300A sol was applied as coating solution either diluted with ethanol (1:1.4, wt%) or as received (procedure 2).

TBOT-based solution (procedure 3) included addition of ethyl acetoacetate (Fluka) in amount of 1.63–5 g of 2-propanol under continuous stirring. TBOT in appropriate amount of 4.25 and 9.12 g of 2-propanol with preliminary dispersed P25 (Evonik) (9 wt% in 2-propanol) were added slowly to the sol-gel solution.

In TTIP-based coating solution (procedure 4), diethanolamine (DEA, Riedel-de-Haen) of 4.2 g was mixed with 5.6 g of 2-propanol. Then 2.84 g of TTIP and 0.72 g of H<sub>2</sub>O were added dropwise under vigorous stirring. Subsequently to 24 h of stirring, 10 g of P25 propanolic suspension were added to the sol-gel solution and final sol was stirred overnight. The sol-gel-coated clay granules without P25 nanoparticles addition to the sol-gel solution were also prepared.

The coatings were prepared by means of dip coating technique. The clay granules were immersed in the sol-gel solution for 10 s and then withdrawn at 1 mm s<sup>-1</sup> (dip coating machine, Vitando OÜ).

Sol-gel-coated clay granules were treated as follows: the pre-drying stage was performed at 120 °C for 1 or 2 h with temperature increasing rate of 30 °C min<sup>-1</sup> (procedures 1–3 and 4, respectively). Afterwards, the coatings were dried at 200 °C for 2 h with temperature increasing rate of 30 °C min<sup>-1</sup> (procedure 1) or calcined

at 500 °C for 2 h with temperature increasing rate of 50 °C min<sup>-1</sup> (procedures 2 and 4) or for 1 h with a rate of 8 °C min<sup>-1</sup> (procedure 3).

The dipping and drying stages (procedures 3 and 4) were repeated also three times to vary the thickness of sol-gel coatings. Following the third drying step, the samples were heated for 2 h at 500 °C.

The coatings obtained by the procedure 4 were found to be the most stable and effective in doxycycline removal (see Section 3.2). Therefore, the influence of following parameters was studied to further improve the coatings properties: substrate withdrawal speed in the range of 0.5–2.0 mm s<sup>-1</sup>, calcination temperature 400–600 °C and duration 1–3 h, P25 nanopowder and TTIP precursor concentration of 0–5.5 and 9.9–15.3 wt% in coating solution, respectively.

### 2.2. Experimental setup of photocatalytic oxidation

Two borosilicate glass tube units with an inner diameter of 30 mm and height of 370 mm with an aperture 146 m<sup>2</sup> m<sup>-3</sup> were used as reaction vessels. Glass air diffusers were installed at the bottom of each reactor providing the clay granules' fluidization by pressurized air. To take into the account the effect of pollutants' adsorption onto the coated porous clay granules, one reactor was irradiated by the UV-A sources and another was operated in the dark (reference). The UV source consisted of two 15 W low-pressure mercury lamps (Philips Actinic BL) with a maximum emission at 365 nm and UV-B/UV-A ratio of less than 0.2%. Radiation loss was prevented by four flat reflectors positioned around the setup. The average UV-A irradiation intensity was ca. 9 W m<sup>-2</sup> measured by fiber-optic spectrometer (USB2000 + UV-VIS-ES, Ocean Optics Inc.). The reaction temperature was maintained at 25 ± 2 °C.

Photocatalytic oxidation of 200 mL of doxycycline hyclate (AppliChem) solution with an initial doxycycline concentration of 25 mg L<sup>-1</sup> was performed with 3.5 g of coated clay granules for 3 h.

The doxycycline concentration was analyzed by the high-performance liquid chromatography combined with diode array detector and mass spectrometer (HPLC-PDA-MS, Shimadzu LC-MS 2020). Phenomenex Gemini-NX 5u C18 110A 150 × 2.0 mm column, inner diameter 1.7 μm, was used with two eluents, 0.1% acetic acid aqueous solution (eluent A), and acetonitrile (eluent B), with total eluents flow of 0.3 mL min<sup>-1</sup>; starting concentration of eluent B was 5%, increased to 48.5% by 23 min with linear gradient, held at that concentration for 2 min, and then decreased to 9.5% by 30 min, out of 30 min analysis. Mass spectra were acquired in full-scan mode, MS operated in positive ionization mode with interface voltage of 4.5 kV, and detector voltage of 1.1 kV. Diode array detector was set to scan samples at 190–800 nm. The instrument was operated and the results obtained with MS and PDA detectors were handled using Shimadzu LabSolutions software.

Scanning electron microscopy (SEM; Zeiss EVO 50 and EVO MA-15) was performed to visualize the catalyst coating. The structural stability and abrasion resistance of the coatings were characterized by the turbidity of the solutions measured during the fluidized-bed treatment process at 860 nm in Formazin Attenuation Units (FAU turbidity, Hach DR2800). The specific surface area of coated and bare expanded clay granules was measured by Areameter Ströhlein.

To express the results of doxycycline degradation and evaluate the activity of obtained sol-gel-coated clay granules, the photocatalytic oxidation efficiency  $E$ , mg W<sup>-1</sup> h<sup>-1</sup> [27], defined as the decrease in the amount of the pollutant in mg, divided by the product of UV-A radiation intensity, in W m<sup>-2</sup>, the surface of the treated solution, in m<sup>2</sup>, and irradiation time, in h, was used. The photocatalytically oxidized amount of doxycycline was calculated as the difference between doxycycline quantities removed in photocatalytic and reference experiments. The first number is taking

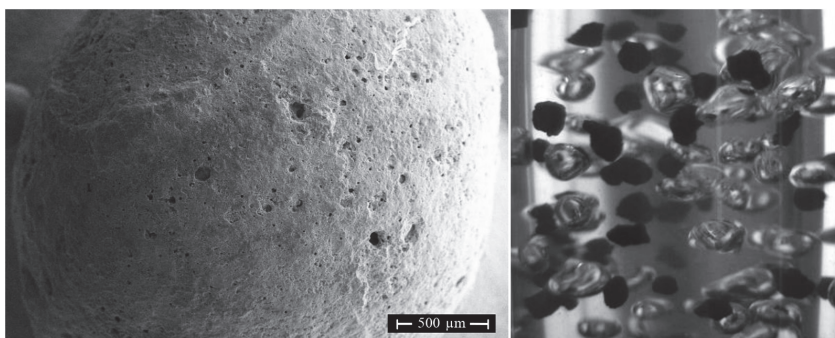


Fig. 1. SEM image of clay granule (left). Fluidized-bed operation of selected fraction of expanded clay granules (right).

into account the doxycycline removal by the net effect of oxidation and adsorption and the second one—removal in the course of dark adsorption. Thus, the effect of adsorption is subtracted from the  $E$ .

### 3. Results

The calculated external surface area of granules (Fig. 1, left) with average diameter of ca. 2.7 mm comprises approximately  $0.004 \text{ m}^2 \text{ g}^{-1}$ , whereas the measured specific surface area of bare expanded clay granules of this particular fraction is ca.  $0.8 \text{ m}^2 \text{ g}^{-1}$ . This porous lightweight granular material could be easily fluidized (Fig. 1, right).

Inorganic expanded clay granules could presumably serve as an adsorbent for the target pollutants and this should be taken into account for the evaluation of photocatalytic functionality of coated materials. For example, the overall doxycycline removal of over 3.4 mg (of initial 5 mg) was observed in 3 h, whereas considering the reference experimental runs (adsorption effects), the amount of doxycycline degraded in photocatalytic reaction reached 1.8 mg. To eliminate the doxycycline dark adsorption, all the reference experiments were carried out with expanded clay granules coated by the respective procedure.

The coatings prepared via procedures 1–4 were thoroughly studied firstly for their mechanical stability and secondly for the photocatalytic activity.

#### 3.1. Industrial sol and TBOT-based sol–gel coatings

The materials prepared using ethanol-diluted Hombikat XXS and S5-300A solutions exhibited the low mechanical stability with high titania washout causing high turbidity levels of treated doxycycline solutions (up to 160 FAU). In the case of coatings obtained from TBOT precursor based sol–gel (procedure 3), sediments and the relatively high levels of turbidity (up to 60 FAU) were also observed presumably as a result of the incomplete hydrolysis and polycondensation reactions in sol and gel during the coating preparation procedure. The more intensive infiltration of low-viscose TBOT sol–gel solutions in the porous ceramic support, as possible explanation, could require the prolonged pre-drying step after dip coating and has led to the discarding of this sol–gel composition in the subsequent study.

Thus, the coatings with Hombikat XXS 100, S5-300A and TBOT used as titania sources (procedures 1–3) were not considered to be long-term effective mostly due to higher detachment levels of coatings' layers if compared with those prepared from different compositions of TTIP/DEA route described further. Although the photocatalytic efficiency of a number of materials prepared via 1–3 procedures approximated to the values of TTIP-based coatings

efficiency, the higher turbidity and thus the shorter potential operating lifetime in fluidized-bed photocatalytic reactor narrowed down the choice of the most promising coating synthesis procedure to TTIP route. TTIP sol–gel-based dip coating resulted in materials of significantly higher abrasion resistance with the turbidity levels observed in the range of 0–40 FAU.

#### 3.2. TTIP-based sol–gel coatings

The SEM micrographs of bare and TTIP-based sol–gel-coated expanded clay granules are shown in Fig. 2. The sol–gel coatings are smoothing the surface if compared to uncoated materials with no cracks observed if the particular (as described further) sol–gel solutions' composition and dip coating process parameters are in use.

Further, the adhesion and abrasion properties and photocatalytic activity of TTIP-based coatings were studied varying components' proportions in the sol–gel solutions and process parameters: 2-propanol content, amount of P25 nanoparticles to increase the photocatalyst weight, the substrate withdrawal speed as well as the temperature and duration of calcination step (Table 1).

The coatings with titania crystallized from TTIP showed explicitly measurable photocatalytic activity of up to  $1.5 \text{ mg W}^{-1} \text{ h}^{-1}$  with zero levels of turbidity in treated solutions.

The addition of P25 to the TTIP sol–gel as nanocrystalline photocatalyst source resulted in higher photocatalytic activities (up to  $2.3 \text{ mg W}^{-1} \text{ h}^{-1}$ ) along with different levels of nanoparticles washout causing the increase in solutions' turbidity in the range between 17 and 28 FAU (see Table 1; series of experiments I). The specific surface area of coated and bare expanded clay was measured to be very close:  $1.0$  and  $0.8 \text{ m}^2 \text{ g}^{-1}$ , respectively, as well as the dark adsorption showed almost no difference in the respective amount of doxycycline adsorbed. The use of ultrasonication of P25 2-propanol suspension before its addition to the sol–gel solution lowered washout of nanoparticles (from 17 to 13 FAU) showing no changes in the coatings activity. The morphology of clay coated with P25 modified sol–gel composition is shown in Fig. 3. The primary particles of P25 titania could be distinguished on the micrograph with higher magnification, while the coating's surface is non-uniform: regions with P25 embedded in the sol–gel are alternating with smooth ones (Fig. 3, left).

The decrease in DEA to 2-propanol mass ratio (Table 1, Series II) lowered the activity of coated expanded clay ( $2.3$ – $1.4 \text{ mg W}^{-1} \text{ h}^{-1}$ , Fig. 4). At the same time, the highest mechanical stability (lowest turbidity during fluidized-bed operation), within the series, was observed with the coated materials prepared from the sol with DEA to 2-propanol ratio of 0.29 (27 FAU). In a similar manner, the faster withdrawal speed (Table 1, Series III) had the positive effect on the coated clay's activity raising this up to  $1.9 \text{ mg W}^{-1} \text{ h}^{-1}$  (Fig. 4)

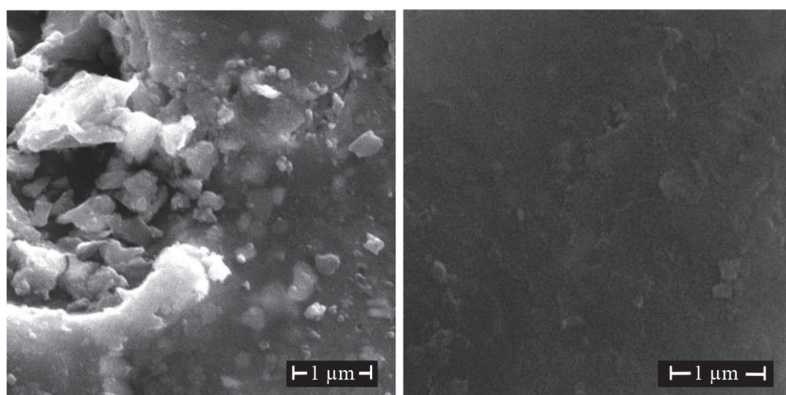


Fig. 2. SEM images of bare (left) and TTIP-based sol-gel-coated (right) expanded clay.

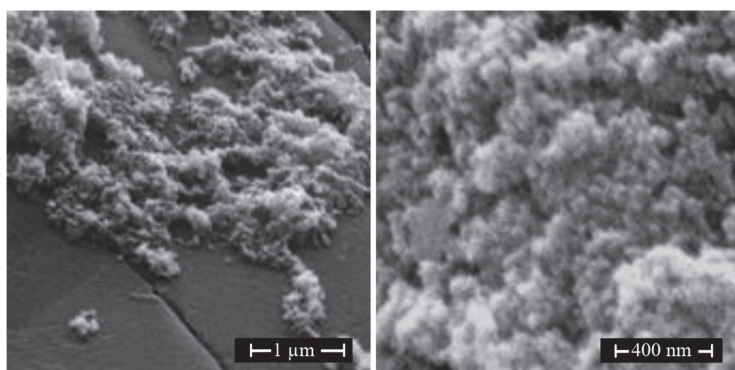


Fig. 3. SEM images of P25-modified sol-gel coatings at different magnifications.

with turbidity levels growing up to 29 FAU. The repetitive dip coating steps applied resulted in higher activity ( $1.7\text{--}2.1\text{ mg W}^{-1}\text{ h}^{-1}$ ), but also weakened the coatings' adhesion followed by the increase in turbidity of up to 40 FAU. However, the effect of intermediate

calcination procedure could improve the mechanical stability of thicker TTIP based coatings (not studied here).

The variations in sol viscosity due to the changes in 2-propanol content, in the support withdrawal speed and in the number of

**Table 1**  
Consolidated data on TTIP-based coatings (numbers in bold were considered to be the optimum).

Series of exp.	Sol-gel composition		Process parameters			Coatings performance	
	P25 (wt%)	2-Propanol (g)	Withdrawal speed ( $\text{mm s}^{-1}$ )	Calcination temperature ( $^{\circ}\text{C}$ )	Calcination time (h)	Photocat. eff. ( $\text{mg W}^{-1}\text{ h}^{-1}$ )	Turbidity (FAU)
I	0.0	14.7	1.0	500	2	1.5	0
	2.0					<b>1.6</b>	<b>17</b>
	3.9					1.7	27
	5.5					2.3	28
II	3.9	9.8	1.0	500	2	<b>2.3</b>	<b>32</b>
		14.7				1.7	27
		19.7				1.4	36
III	3.9	14.7	0.5	500	2	1.6	20
			1.0			<b>1.7</b>	<b>27</b>
			2.0			1.9	29
IV	3.9	14.7	1.0	400	2	1.4	29
				500		<b>1.7</b>	<b>27</b>
				600		1.7	27
V	3.9	14.7	1.0	500	1	<b>1.8</b>	<b>23</b>
					2	1.7	27
					3	1.9	31

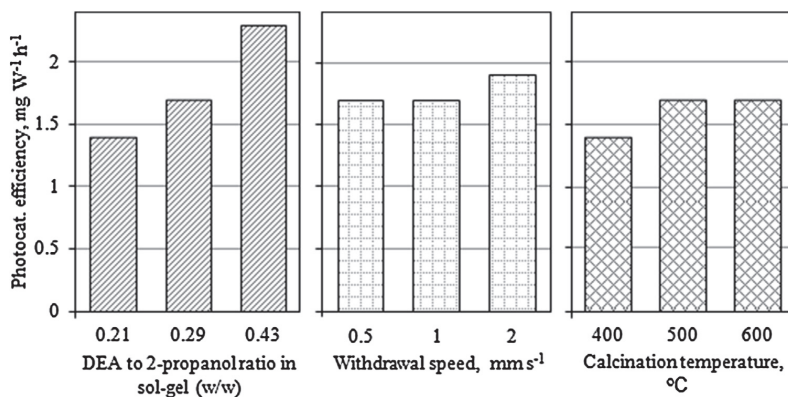


Fig. 4. The impact of DEA to 2-propanol ratio, withdrawal speed and calcination temperature on the photocatalytic activity of sol–gel coatings.

repeated dippings influence the thickness of the coatings and this could be followed in the SEM micrographs.

The increase, for example, in the substrate withdrawal speed from 1 to 2 mm s<sup>-1</sup> contributing to the coating layer thickening is leading to the sequential development of cracks observed in Fig. 5. The deterioration of coating integrity is reflected in the drop of abrasion resistance characterized by the higher levels of turbidity (Table 1, Series III).

The impact of thermal treatment (Table 1, Series IV and V) showed that mechanical stability of the coatings was not altered by the temperature variations between 400 and 600 °C. The activity of the coated clay, however, was positively influenced by the increase in temperature from 400 to 500 °C (Fig. 4) indicating the possible improvements in titania crystallinity.

The duration of thermal treatment varied from 1 to 3 h, on the opposite, had no effect on the activity of the coatings. However, the prolonged treatment lowered the coated clay's abrasion resistance as the turbidity increased in the course of fluidized operation with every additional hour of calcination (from 23 to 31 FAU) pointing out the changes in coatings microstructure.

The coatings' attrition was also studied varying such fluidized-bed reactor operation parameter as loading of coated clay granules in the reactor: twofold decrease in the amount of coated bed material per volume of treated solution from 17.5 to 8.8 g L<sup>-1</sup> led to the decrease in turbidity for over 6.5 times (from 27 to 4 FAU), whereas the 35% loss in activity was observed (from 1.7 to 1.1 mg W<sup>-1</sup> h<sup>-1</sup>). The optimal bed material loading at the particular UV-A light intensity is currently under study in the larger-scale fluidized-bed reactor.

## 4. Discussion

### 4.1. Industrial sols and TBOT-based sol–gel coatings

Low adhesion of the industrial sols on the bed material could be attributed to two factors: the surface of such supporting material as expanded clay is not absolutely inert (towards the coatings solution), because the presence of typical ceramic components, like CaO or Fe<sub>2</sub>O<sub>3</sub>, influences the acid–base equilibrium (a), and the nanoparticles' sols are very pH-sensitive (b). For example, the XXS 100 sol stability (in terms of nanoparticles agglomeration) was previously found to be pH-dependent [28], whereas expanded clay granules shift the pH of ethanol-diluted XXS solution, for example, from ca. 1.95 to 2.3 (in ca. 40% expanded clay slurry in 2 min contact time); moreover, expanded clay granules shift the pH of

water noticeably (e.g. from ca. pH 6.5 to 9 in 8% slurry in 30 min). As a result, the agglomerated TiO<sub>2</sub> nanoparticles could not be firmly fixed on the support material and are washed out. The TTIP-based sol–gel solution with DEA included in its composition allowed to avoid these issues.

### 4.2. TTIP-based sol–gel coatings

#### 4.2.1. TTIP-based coatings without P25 addition

Zero levels of turbidity of doxycycline solutions treated in a fluidized bed mode, in the case of TTIP-based coatings without P25 addition, indicate that *sol per se* has good adhesion to such material as expanded clay with no cracks formation as was confirmed by the SEM study. The photocatalytic activity of these coatings (Table 1, Series I) is attributed only to the titania formed from TTIP precursor (with no photolysis of doxycycline observed and with the adsorption being previously withdrawn). The temperature of coatings thermal treatment (500 °C) is high enough for the anatase crystallization [29] (see Supplementary materials, Fig. S1, peak of anatase on XRD diagram at 2θ = 25.3). The need to enhance the coatings activity was expectedly met by the addition of P25 to the sol–gel solution.

#### 4.2.2. TTIP-based coatings modified by P25

The SEM micrographs of modified sol–gel coatings on expanded clay displayed clearly the change in surface morphology and the appearance of cracks with the increase in P25 particles loading. The addition of P25 to the sol–gel enhancing the coatings activity increases, on the other side, the turbidity of treated solutions with cracks being observed in SEM micrographs at higher P25 contents (5.5 wt%). The improvements in coatings' mechanical properties due to ultrasonication of P25 2-propanol suspension before its addition to the sol–gel solution could be explained by break-up of the largest nanoparticles' agglomerates into the smaller fragments. As a consequence of the more even distribution of P25 powder in sol–gel, less cracking and catalyst washout were achieved. The increase in sol–gel viscosity with the raise of P25 powder content causes also presumably the formation of coatings with increased thickness analogously to the observations in the case of DEA/2-propanol ratio variation in TTIP sol–gel discussed further.

#### 4.2.3. Influence of variations in TTIP-based coatings processing parameters

The variations in sol viscosity, the support withdrawal speed and the number of bed material dippings in the sol–gel are foreseen

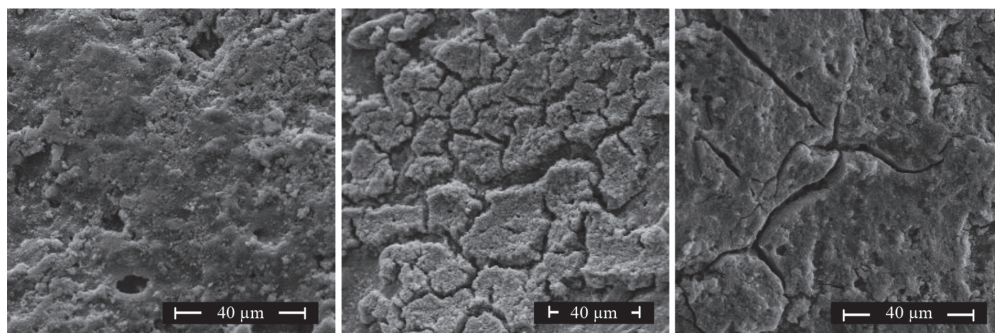


Fig. 5. SEM images of the TTIP-based coatings prepared with substrate withdrawal speed  $1 \text{ mm s}^{-1}$  (left),  $2 \text{ mm s}^{-1}$  (middle) and with DEA to 2-propanol ratio of 0.43, w/w (right).

to influence the coatings' properties [30]. However, the texture of substrate material is also determining the quality and properties of coatings resulting in different morphologies and adhesion on various substrates (Shan et al., 2010).

The dilution of P25-modified sol-gel solution, i.e. the decrease in DEA to 2-propanol ratio with P25 content remained constant, caused the reduction in sol-gel viscosity and in the TTIP content inducing the drop in photocatalytic activity of coated clay. While the trend in turbidity changes with a minimum observed with the average DEA to 2-propanol ratio (Table 1, Series II) could be attributed to the variations in the morphology of sol-gel coatings. The SEM study shows the formation and propagation of cracks within the coatings from the sol-gel solution of higher viscosity (Fig. 5), thus favoring the coatings detachment and P25 particles washout. The coatings from the sol-gel solutions of lower viscosity, on the contrary, show the increase in turbidity because of insufficient anchoring of P25 agglomerates with no formation of cracks observed.

The higher withdrawal speed and the repetitive number of dippings of expanded clay in sol-gel result in the increase in the coatings' thickness, thus contributing to the formation of cracks responsible for the enhanced levels of turbidity and deterioration of coated bed material long-term performance in fluidized bed reactor.

The temperature increase from 500 to 600 °C did not alter the activity of coatings, while lower temperature (400 °C) was considered to be not sufficient for the sol-gel thermal treatment with a decrease in activity observed (Fig. 4).

The formation of cracks jeopardizes the long-term efficiency of coated clay, to be used as the bed for fluidization, and the routes to obtain more intact coatings, including intensive deagglomeration of P25 in sol-gel with its subsequent dilution, could be established. Whereas, specific set-up proportions are relevant only for particular material of support, as for stainless steel, for example, Chen and Dionysiou [31] found the optimal concentration of P25 in the sol-gel to be higher than this for expanded clay settled in present study.

The intact coatings with additional titania crystallites evenly distributed within the sol-gel films of optimized thickness meet the requirements for coatings with good mechanical properties and satisfactory photocatalytic antibiotic oxidation efficiency. Search for the optimum between these two characteristics (activity vs. adhesion and attrition) based on the results of doxycycline photocatalytic degradation efficiency and turbidity measurements suggests the following preparation procedure: TTIP/DEA/2-propanol mass ratio of 1:1.5:3.5, P25 content of 2.0 wt%, withdrawal speed of  $1 \text{ mm s}^{-1}$ , thermal treatment at 500 °C for max 1 h with heating gradient to be optimized. This way

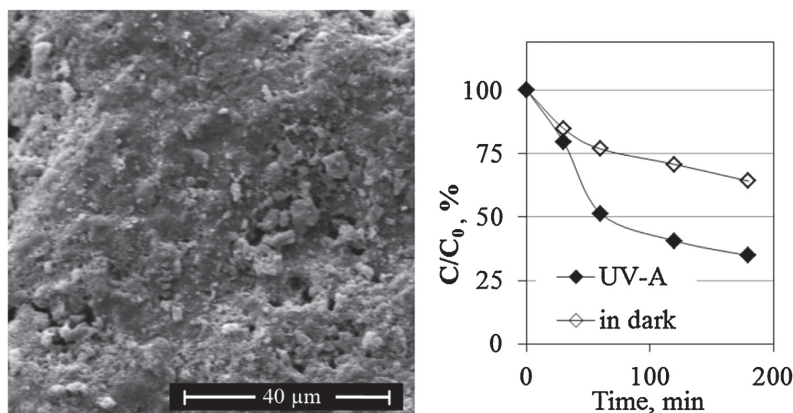


Fig. 6. SEM image and performance of TTIP-based coating prepared using optimized processing parameters.

prepared coatings revealed intact structures characterized also by low turbidity levels (not exceeding 14 FAU) and distinct photocatalytic activity (Fig. 6).

## 5. Conclusions

The prerequisite for the photocatalytic fluidized-bed reactor development is the elaboration of the coated lightweight materials of satisfactory abrasion resistance and activity as these are subjected to the attrition during the reactor operation.

The implementation of titania sol–gel-coated porous expanded clay granules as support material allows using the benefits of water treatment methods' combination successfully adsorbing pollutants with their subsequent photocatalytic oxidation.

Within the variety of studied sol–gel compositions, based on TTIP and TBOT titania precursors and Hombikat XXS 100 and S5-300A industrial sols, titania coatings on expanded clay prepared using TTIP were found to be the most mechanically stable.

The measurable degradation of doxycycline with zero turbidity in treated solutions is an indicator of photocatalytic activity of intact coatings formed from starting TTIP based sol–gel composition. The increase in the coating thickness deteriorates their quality entailing the formation of cracks and causing the detachment and turbidity raise. The addition of P25 enhances the coatings activity changing also distinctly their morphology as the appearance of cracks with the increase in P25 content is observed, whereas the better P25 particles deagglomeration in the sol–gel is contributing to the coatings properties improvement.

It could be concluded that titania fixation on lightweight expanded clay aggregates by means of sol–gel produced stable and active coatings with properties dependent on the processing parameters. The final choice of fluidized-bed material coatings' preparation parameters is a compromise between coatings' photocatalytic activity, on the one hand, and their adhesion and attrition properties, on the other hand. The interrelation of these characteristics will be further influenced by the operation parameters of fluidized-bed reactor.

## Acknowledgements

The financial support from the Estonian Research Council (grant G8978, projects SF0140022s10 and IUT1-7), European Social Fund's Doctoral Studies and Internationalisation Programme DoRa and Archimedes Foundation project 3.2.0801.11-0009 is greatly appreciated. The authors express their gratitude to the Deutsche Forschungsgesellschaft (DFG) (grants DE 598/26-1 and WE 2331/17-1). We thank Tatjana Rudenko for assistance in the laboratory, Juri Pronin for assistance with laboratory apparatus, Thomas Peter and Dr. Mart Viljus for SEM and Adelheid Lürer for BET analyses.

## Appendix A. Supplementary data

Supplementary data associated with this article can be found, in the online version, at <http://dx.doi.org/10.1016/j.apcatb.2014.10.006>.

## References

- [1] K.D. Brown, J. Kulis, B. Thomson, T.H. Chapman, D.B. Mawhinney, *Sci. Total Environ.* 366 (2006) 772–783.
- [2] Z. Dong, D.B. Senn, R.E. Moran, J.P. Shine, *Regul. Toxicol. Pharm.* 65 (2013) 60–67.
- [3] K. Ikehata, N.J. Naghashkar, M.G. El-Din, *Ozone Sci. Eng.* 28 (2006) 353–414.
- [4] A. Nikolaou, S. Meric, D. Fatta, *Anal. Bioanal. Chem.* 387 (2007) 1225–1234.
- [5] S. Mompelat, B. Le Bot, O. Thomas, *Environ. Int.* 35 (2009) 803–814.
- [6] PAN, Demands for Improved Protection of the Environment from the Adverse Effects of Veterinary Medical Products, Veterinary Pharmaceuticals, PAN Germany, 2013.
- [7] D. Klauson, J. Babkina, K. Stepanova, M. Krichevskaya, *S. Preis, Catal. Today* 151 (2010) 39–45.
- [8] D. Klauson, M. Krichevskaya, M. Borissova, S. Preis, *Environ. Technol.* 31 (2010) 1547–1555.
- [9] D. Klauson, A. Poljakova, N. Pronina, M. Krichevskaya, A. Moiseev, T. Dedova, S. Preis, *J. Adv. Oxid. Technol.* 16 (2013) 234–243.
- [10] Y. Zhang, J.C. Crittenden, D.W. Hand, D.L. Perram, *Environ. Sci. Technol.* 28 (1994) 435–442.
- [11] T. Torimoto, S. Ito, S. Kuwabata, H. Yoneyama, *Environ. Sci. Technol.* 30 (1996) 1275–1281.
- [12] H.Y. Ha, M.A. Anderson, *J. Environ. Eng.-ASCE* 122 (1996) 217–221.
- [13] N.J. Peill, M.R. Hoffmann, *J. Sol. Energ.-T ASME* 119 (1997) 229–236.
- [14] S. Preis, M. Krichevskaya, A. Kharchenko, *Water Sci. Technol.* 35 (1997) 265–272.
- [15] P.S. Mukherjee, A.K. Ray, *Chem. Eng. Technol.* 22 (1999) 253–260.
- [16] R.L. Pozzo, J.L. Giombi, M.A. Baltanas, A.E. Cassano, *Catal. Today* 62 (2000) 175–187.
- [17] L. Zhang, Y.F. Zhu, Y. He, W. Li, H.B. Sun, *Appl. Catal. B* 40 (2003) 287–292.
- [18] S. Gelover, P. Mondragon, A. Jimenez, *J. Photochem. Photobiol. A* 165 (2004) 241–246.
- [19] T. Kanki, S. Hamasaki, N. Sano, A. Toyoda, K. Hirano, *Chem. Eng. J.* 108 (2005) 155–160.
- [20] J.M. Kwon, Y.H. Kim, B.K. Song, S.H. Yeom, B.S. Kim, J.B. Im, *J. Hazard. Mater.* 134 (2006) 230–236.
- [21] A.Y. Shan, T.I.M. Ghazi, S.A. Rashid, *Appl. Catal. A* 389 (2010) 1–8.
- [22] J.W. Shi, H.J. Cui, J.W. Chen, M.L. Fu, B. Xu, H.Y. Luo, Z.L. Ye, *J. Colloid. Interf. Sci.* 388 (2012) 201–208.
- [23] D.S. Selishchev, P.A. Kolinko, D.V. Kozlov, *J. Photochem. Photobiol. A* 229 (2012) 11–19.
- [24] M. Zendezhaban, S. Sharifnia, S.N. Hosseini, *Kor. J. Chem. Eng.* 30 (2013) 574–579.
- [25] X.X.S. Hombikat, 100, Product Information, Sachtleben Chemie GmbH, 2006.
- [26] CristalACTIV S5-300A, Product Data Sheet, Cristal (2012).
- [27] S. Preis, M. Krichevskaya, Y. Terentyeva, A. Moiseev, *J. Kallas, J. Adv. Oxid. Technol.* 5 (2002) 77–84.
- [28] A. Matthias, Lichtwellenleitung in TiO<sub>2</sub>-Schichten aus dispergierten Nanopartikeln auf Glas, PhD Thesis, TU Clausthal, 2014.
- [29] S.H. Oh, J.S. Kim, J.S. Chung, E.J. Kim, S.H. Hahn, *Chem. Eng. Commun.* 192 (2005) 327–335.
- [30] C.J. Brinker, A.J. Hurd, P.R. Schunk, G.C. Frye, C.S. Ashley, *J. Non-Cryst. Solids* 147–148 (1992) 424–436.
- [31] Y.J. Chen, D.D. Dionysiou, *Appl. Catal. B* 62 (2006) 255–264.



## PAPER III

**Pronina, N.**, Klauson, D., Rudenko, T., Künnis-Beres, K., Kamenev, I., Kamenev, S., Moiseev, A., Deubener, J., Krichevskaya, M. Elimination of persistent emerging micropollutants in suspended-bed photocatalytic reactor: influence of operating conditions and combination with aerobic biological treatment. - *Photochemical and Photobiological Sciences*, 2016, 12, 1492–1502.

Reproduced with permission from the European Society for Photobiology, the European Photochemistry Association, and the Royal Society of Chemistry.





Cite this: *Photochem. Photobiol. Sci.*, 2016, **15**, 1492

## Elimination of persistent emerging micropollutants in a suspended-bed photocatalytic reactor: influence of operating conditions and combination with aerobic biological treatment†

N. Pronina,<sup>a</sup> D. Klauson,<sup>a</sup> T. Rudenko,<sup>a</sup> K. Künnis-Beres,<sup>b</sup> I. Kamenev,<sup>a</sup> S. Kamenev,<sup>a</sup> A. Moiseev,<sup>c</sup> J. Deubener<sup>c</sup> and M. Krichevskaya<sup>\*a</sup>

A larger, lab-scale photocatalytic suspended-bed reactor using TiO<sub>2</sub> sol-gel-coated expanded clay granules as a bed material was evaluated for oxidative removal of the persistent pharmaceuticals doxycycline, prednisolone, amoxicillin, and sulfamethizole, as well as their mixture, in ppm concentrations. The photocatalytic degradation potential of drug molecules increases as their adsorption affinity increases towards TiO<sub>2</sub>-containing coatings. The performance of the photocatalytic reactor in the removal of drugs was improved by optimizing the fluidization process parameters. The reactor operation at high bed loadings is determined by the abrasion resistance of the catalyst coating. The long-term stability of the coated bed was enhanced by optimal loading, achieving a higher removal rate while placing moderate mechanical stress on the coated granules. The photocatalytic pretreatment decreased the toxicity of doxycycline solutions to several bacterial strains, including the environmental bacterium *Pseudomonas putida* and bacterial strains freshly isolated from the activated sludge. The treatment of doxycycline-containing water with a combination of photocatalytic treatment and bio-oxidation resulted in 98% removal of the target in the bioreactor outlet, with no deterioration in the operation of the biological process.

Received 31st August 2016,  
Accepted 23rd October 2016

DOI: 10.1039/c6pp00319b

www.rsc.org/pps

## Introduction

Traces of pharmaceutical drugs in the environment,<sup>1</sup> especially antibiotics,<sup>2</sup> are gradually accumulating in water and soil and are generally resistant to conventional biological wastewater treatment; thus, the study of advanced oxidation processes for degrading these micropollutants into biodegradable intermediates is important.<sup>3,4</sup> For example, photocatalytic treatment resulted in increased biodegradability of the initial refractory compounds during oxidation of aromatic amines found in rocket fuel-polluted groundwater<sup>5</sup> and model solutions of antibiotic sulfamethizole.<sup>6</sup>

In this study, four widely used pharmaceuticals, doxycycline, prednisolone, amoxicillin and sulfamethizole, were chosen as model aqueous pollutants. Doxycycline is a broad-

spectrum tetracycline antibiotic that is used against a wide range of microorganisms, protozoa and helminths. Prednisolone is a broadly used glucocorticoid anti-inflammatory agent. Amoxicillin is a moderate-spectrum penicillin group antibiotic that is employed to treat a high number of bacterial infections. Sulfamethizole is a sulfonamide antibiotic that is extensively utilized in human and veterinary medicine against a number of microorganisms and protozoa. Consequently, it is very important to prevent the entry of these substances into the environment.

The feasibility of the photocatalytic oxidation of doxycycline, amoxicillin, prednisolone and sulfamethizole in a slurry-type reactor has previously been demonstrated; the formation of oxidation by-products observed in these studies could be a basis for the integration of photocatalysis into wastewater treatment processes, *i.e.* in combination with biological treatment.<sup>6–9</sup>

Bio-oxidation of antibiotics has been previously studied; for example,<sup>10–14</sup> it was found that adsorption is the primary mechanism for removal of tetracyclines in an activated sludge system, while biodegradation appears to be dependent on operation conditions and has been reported to remove antibiotics from negligible amounts to rates up to 63%.<sup>15–18</sup>

<sup>a</sup>Department of Chemical Engineering, Tallinn University of Technology, Ehitajate tee 5, 19086 Tallinn, Estonia. E-mail: marina.kritsevskaja@ttu.ee; Tel: +372 6202851

<sup>b</sup>Institute of Marine Systems, Tallinn University of Technology, Ehitajate tee 5, 19086 Tallinn, Estonia

<sup>c</sup>Institute of Non-Metallic Materials, TU Clausthal, Zehntnerstrasse 2a, 38678 Clausthal-Zellerfeld, Germany

† Electronic supplementary information (ESI) available. See DOI: 10.1039/c6pp00319b

The photocatalytic oxidation of tetracycline as a pretreatment method resulted in the reduction of toxicity of treated antibiotic solution; however, further optimization of the experimental conditions is necessary to generate more biodegradable by-products.<sup>19–21</sup> However, a study focusing on the combination of photocatalytic pretreatment with bio-oxidation to eliminate tetracycline resulted in tetracycline by-products with low biodegradability due to their toxicity and low degradation rates during biotreatment.<sup>22</sup> Decreased toxicity of the oxidation by-products and ease of TiO<sub>2</sub> catalyst separation should, however, be prerequisites for this combination of processes.

When utilizing immobilized photocatalysts, the suspended- or fluidized-bed concept benefits from the high efficiency of both light utilization and mass transfer.<sup>23</sup> Fluidized-bed reactors have found application in numerous chemical industries due to their inherent advantages, such as high mass transfer rates, easy handling and transport of solids, and ability to process large volumes of fluid.<sup>24</sup> Satisfactory mechanical stability of the photocatalytic coating on the bed material, *i.e.* good adhesion and abrasion resistance, enables the catalyst separation stage to be simplified or even eliminated, providing a clear benefit compared to slurry-type reactors. However, despite all these advantages, the bed material is subjected to high levels of mechanical stress, causing detachment of the photocatalyst.<sup>25</sup> Entrained solids bubble columns, where the solid is fluidized by bubble action, are preferable over fluidized-bed columns when catalytic coatings are subject to disintegration.<sup>26</sup> The objective of the present study was to overcome the limitation of the fluidized-bed concept by appropriate choices of support material, coating method and reactor operating conditions. The application of expanded natural clay granules from industrial manufacture as a support for photocatalytic coatings is a novel choice of lightweight inorganic material. The potential of the coatings to be reused was also evaluated.

The growth inhibition assay was applied to study the toxicities of model and photocatalytically treated doxycycline solutions.<sup>27–29</sup> The fact that doxycycline acts by slowing the growth of bacteria additionally supports the choice of this analysis method, which also allows high-throughput screening of antibiotics.<sup>30</sup> The potential of the combination of photocatalytic oxidation with a biological activated sludge process for the treatment of antibiotic-containing water was investigated.

## Results

### Influence of bed loading and air superficial velocity on suspended-bed reactor performance

The influence of the (suspended-bed) reactor operating conditions on the process performance, *i.e.* the photocatalytic oxidation efficiency  $E$  and turbidity of treated model doxycycline solutions, is presented in Fig. 1.

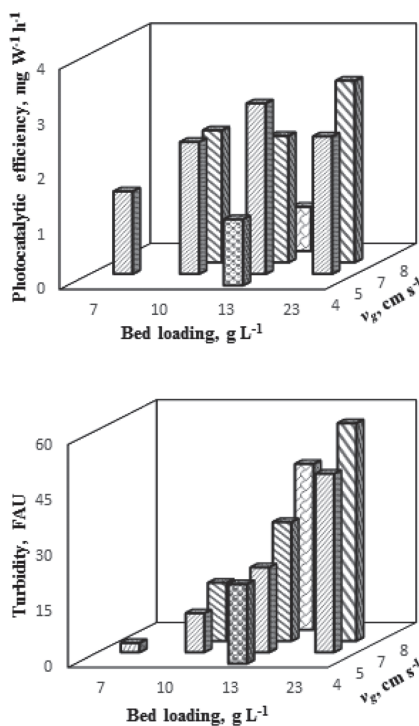


Fig. 1 The effects of bed loading and air superficial velocity,  $v_g$ , on doxycycline photocatalytic oxidation efficiency  $E$  (upper) and solution turbidity (lower).

The critical air velocity, *i.e.* the minimum velocity necessary to fluidize a bed of coated clay granules using an air flow,  $v_{mg}$ , was empirically found to be 5 cm s<sup>-1</sup>; thus, the range of  $v_g$  from 5 to 7 cm s<sup>-1</sup> was studied more profoundly, with additional experimental runs carried out for lower (4 cm s<sup>-1</sup>) and higher (8 cm s<sup>-1</sup>)  $v_g$ .

At a bed loading of 13 g L<sup>-1</sup>, insufficient bed fluidization ( $v_g \leq 4$  cm s<sup>-1</sup>) decreases the photocatalytic oxidation efficiency, whereas higher  $v_g$  values that are sufficient for fluidization ( $v_g \geq 7$  cm s<sup>-1</sup>) also do not improve the process performance. The highest  $E$  was obtained for the minimum fluidization velocity,  $v_{mg}$ . At a higher bed loading of 23 g L<sup>-1</sup>, a higher  $v_{mg}$  was expectedly obtained, leading to improvement in the process at a higher  $v_g$  value.

At a constant  $v_g$  of 5 cm s<sup>-1</sup>, the efficiency increased with increasing catalyst-coated bed loading up to 13 g L<sup>-1</sup>, with a subsequent decrease at higher bed loadings. The intensification of bed fluidization, *i.e.* a further increase in  $v_g$ , and increased bed loading can provide certain improvements in the oxidation process; however, this places higher mechanical stress on the coatings. The coated-bed abrasion resistance was previously found to satisfy the process requirements, provided that the turbidity levels during experimental runs remained in

the range of 0 to 40 FAU.<sup>25</sup> The abrasion resistance of the coatings, expressed as the turbidity measured in the course of the photocatalytic experimental runs under different operating conditions, is shown in Fig. 1 (lower). Increases in bed loading and  $v_g$  within the studied range result in a steady increase in turbidity. Under the process operating conditions of bed loading  $\geq 23 \text{ g L}^{-1}$  and  $v_g \geq 7 \text{ cm s}^{-1}$ , the turbidity exceeded 40 FAU. To minimize the mechanical stress on the coatings, the operating parameters used for further studies, which included catalyst-coated bed reuse, changes in toxicity of model pollutant solutions due to photocatalytic treatment, and oxidation of mixtures of pharmaceuticals, were chosen as follows:  $v_g = 5 \text{ cm s}^{-1}$ , bed loading  $10 \text{ g L}^{-1}$ .

### Influence of the preparation method of the coatings on their reuse potential

In our previous studies, TTIP-based coatings without added  $\text{TiO}_2$  P25 exhibited zero levels of turbidity; however, their photocatalytic activity was lower compared to coatings containing P25 particles.<sup>25</sup> The performance of coated beds without P25 addition compared with those prepared according to an earlier optimized procedure was studied in this paper using a scaled-up suspended-bed reactor (reactor volume increased from 0.2 to 2 L) requiring higher energy input, *i.e.* higher  $v_g$ .<sup>25</sup> With  $v_g = 5 \text{ cm s}^{-1}$  and a bed loading of  $10 \text{ g L}^{-1}$ , no difference in turbidity was observed (turbidity value: *ca.* 16 FAU). Variations in the drying and hardening conditions, *i.e.* dip-coated bed calcination in nitrogen instead of oxidizing air atmosphere, were also studied. Thus-prepared coatings indeed showed up to a 25% increase in photocatalytic activity; however, this was accompanied by a decrease in adsorption capacity of up to 30%. Moreover, the mechanical stability of these coatings was somewhat lower than that of the coatings prepared by the previously optimized procedure, as shown by higher turbidity levels of *ca.* 25 FAU. Therefore, it was decided to carry out the drying and calcination step in air atmosphere.

The results of the reuse study of the coatings prepared with and without P25 addition are presented in Fig. 2. Under more rigorous conditions in the scaled-up reactor, the use of sol-gel without P25 did not provide any improvements in the integrity (adhesion and formation of cracks) or the activity of the coatings: no changes were observed in the turbidity (turbidity columns, Fig. 2), and *ca.* 45% and 70% decreases in the adsorption and photocatalytic activity (absolute values are not shown in Fig. 2), respectively, were observed. The initial photocatalytic efficiencies in the first cycle of the reuse study were 2.5 and  $1.7 \text{ mg W}^{-1} \text{ h}^{-1}$  for coatings with and without addition of P25 to the sol-gel, respectively; a turbidity of 16 FAU was measured for both coatings.

Comparison of the relative efficiencies presented in Fig. 2 also demonstrates a decrease in coated bed performance depending on the preparation method. The photocatalytic efficiency of the coatings used for the third time demonstrated only 30% of the efficiency obtained with the freshly coated bed for the sol-gel without P25 addition, while 50% efficiency was observed for the coatings containing P25.

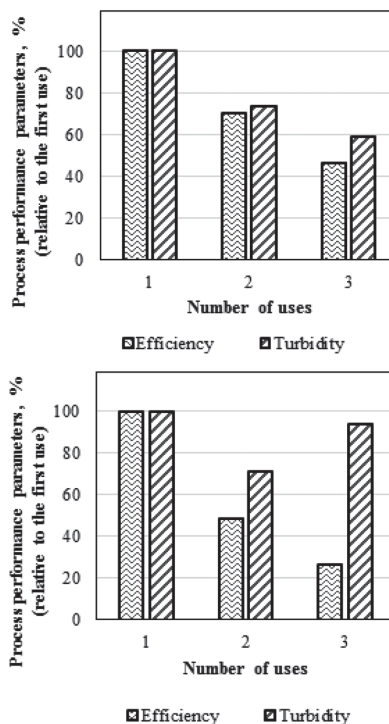


Fig. 2 The performance of catalyst coatings prepared by the optimized procedure with (upper) and without (lower) addition of P25 to the sol-gel throughout 3 reuse cycles in the photocatalytic oxidation of doxycycline.

The bed coated with sol-gel containing P25 particles exhibited a continuous decrease in turbidity, from 16 to *ca.* 8 FAU, when the same portion of the bed was reused for photocatalytic oxidation of doxycycline. In the case of the coatings without P25, low levels of turbidity were also observed, while the turbidity values remained practically unchanged (*ca.* 16 FAU).

### Photocatalytic oxidation of a mixture of pharmaceuticals

The performance of the photocatalytic oxidation process towards the degradation of doxycycline, amoxicillin, prednisolone and sulfamethizole was studied for a mixture of pollutants and for each individual pollutant (Fig. 3).

The photocatalytic degradation of doxycycline alone showed the highest efficiency. If this is taken as 100%, the relative photocatalytic efficiencies of the other pharmaceuticals are as follows: 58%, 33% and 8% for prednisolone, sulfamethizole and amoxicillin, respectively (Fig. 3, diagonal brick pattern). The established sequence, *i.e.* doxycycline > prednisolone > sulfamethizole > amoxicillin, also corresponds to the adsorption affinities of the respective pharmaceuticals towards the sol-gel-coated expanded clay granules. The overall

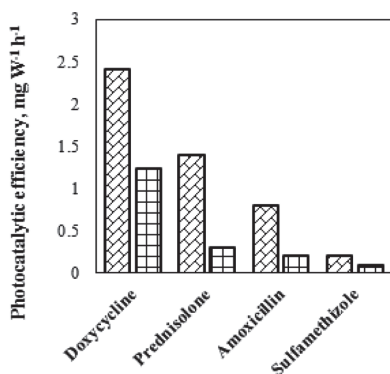


Fig. 3 Photocatalytic oxidation of pharmaceuticals alone (diagonal brick) and in a mixture (solid squares);  $v_g$  5 cm s<sup>-1</sup>, bed loading 10 g L<sup>-1</sup>.

deterioration of the photocatalytic process performance when degrading a mixture of four compounds can be observed in Fig. 3 (columns with solid square pattern).

### Influence of photocatalytic pretreatment on the antimicrobial activity of doxycycline

The results of the growth inhibition assay, which aimed to evaluate the antimicrobial activity of doxycycline toward *E. coli*, *S. aureus*, *P. putida* and Dev3, are presented in Fig. 4.

The assay confirmed the sensitivity of the four tested bacterial strains to doxycycline. The highest impact of doxycycline was observed on *S. aureus*, resulting in an MIC of <0.25 mg L<sup>-1</sup> and an LC<sub>100</sub> of 1 mg L<sup>-1</sup>. While the MICs for Dev3, *P. putida* and *E. coli* were determined to be identical, their LC<sub>100</sub> values were 1, 2.5 and 5 mg L<sup>-1</sup>, respectively.

The changes in bacterial growth inhibition of the four test bacteria in contact with doxycycline solution after experimental photocatalytic oxidation runs are demonstrated in Fig. 5 (left).

The bacterial growth (expressed as OD<sub>600</sub>) of the test bacteria cultures added to the photocatalytically treated doxycycline solutions was measured immediately after mixing, followed by measurements at 3, 16 and 20 h. The OD<sub>600</sub> values showed that moderate concentrations of doxycycline (0.25 to 1.0 mg L<sup>-1</sup>) increased the lag phase (adaptive phase) of bacterial growth. Slight growth was measured after 3 h for

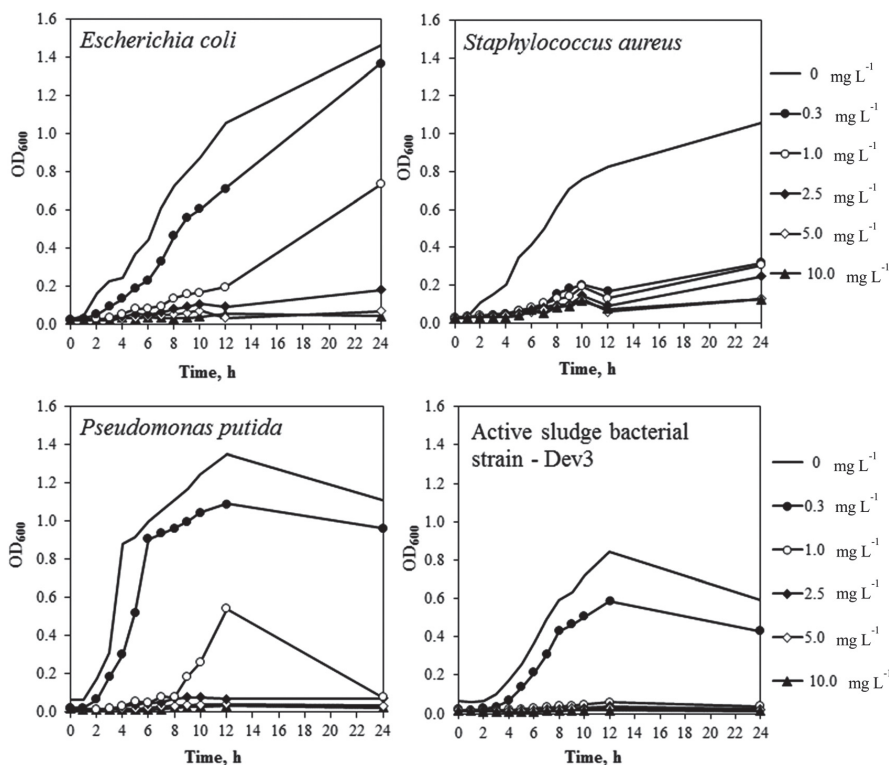


Fig. 4 The antibacterial effects of doxycycline on the test bacteria measured by growth inhibition assay (doxycycline concentration up to 10 mg L<sup>-1</sup>).

*S. aureus*. *S. aureus* did not reach the exponential growth phase and remained inhibited when the doxycycline concentration in the photocatalytically treated sample decreased to  $3.2 \text{ mg L}^{-1}$  after 4 h of treatment and dilution during the growth inhibition assay (Fig. 5). On the other hand, *E. coli*, *P. putida* and the Dev3 strain reached the exponential growth phase after

16 h incubation with doxycycline solutions that were photocatalytically treated for 2.5 h or longer (Fig. 5). The antimicrobial effects of doxycycline solution on the studied bacterial strains decreased during the photocatalytic experimental runs in the following order: *E. coli* (80% in terms of MIC) > *P. putida* > Dev3 > *S. aureus* (33%).

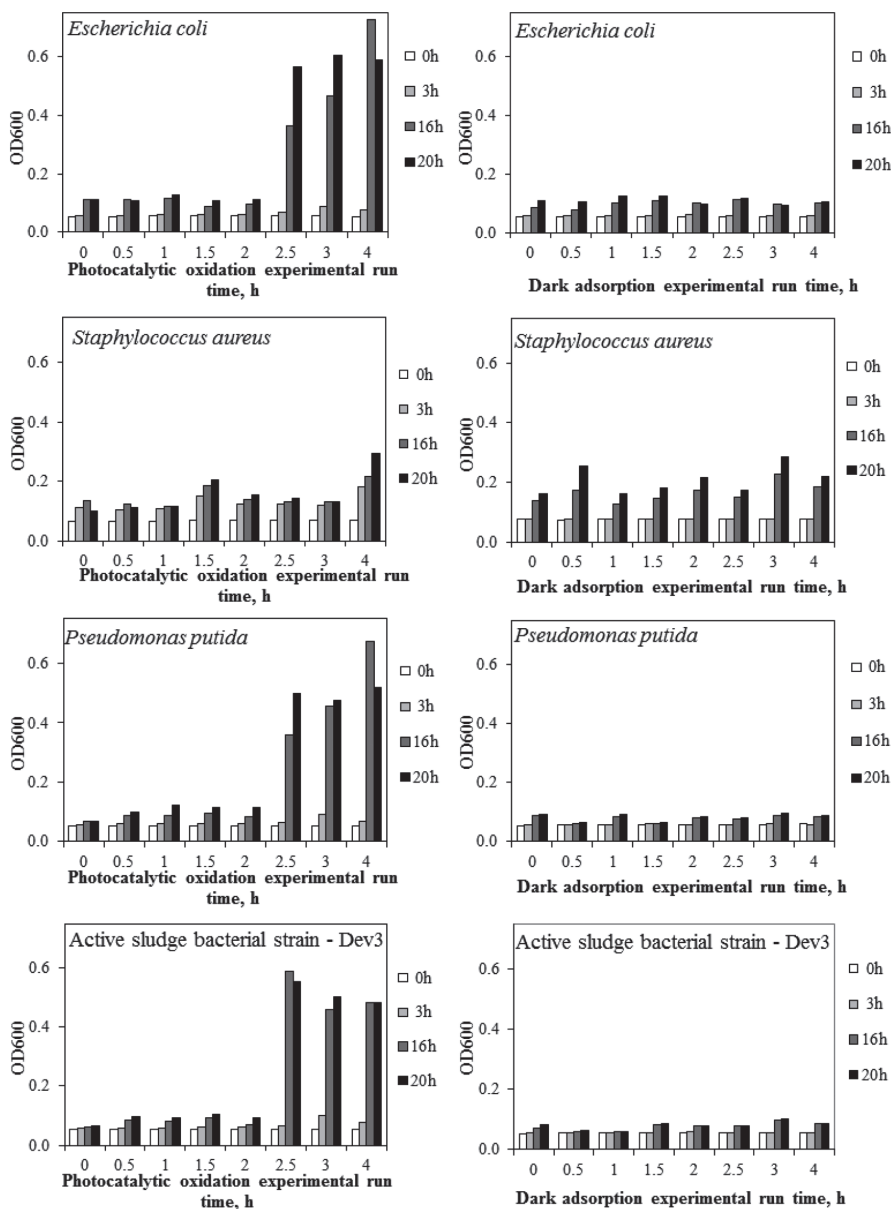


Fig. 5 The antimicrobial effects of treated doxycycline solution on four test bacteria (incubation time up to 20 h).

The antimicrobial effects of doxycycline solution after 4-h dark adsorption on the photocatalyst-coated expanded clay granules remained almost unchanged (Fig. 5, right).

### Combination of photocatalytic oxidation with biological treatment

The 4.5 h oxidation of 10 mg L<sup>-1</sup> doxycycline solution in the suspended-bed photocatalytic reactor resulted in 18% and 35% removal of DOC and COD, respectively, while the concentration of doxycycline did not exceed 1 mg L<sup>-1</sup> at the end of the pretreatment. No changes in AOS were observed after 3 h of photocatalytic treatment; meanwhile, after 4.5 h, an overall increase of AOS from -0.1 to 0.7 was observed, suggesting the formation of more oxidized organic intermediates. The inhibition of the growth of the mixed bacterial colonies by the initial doxycycline solution was 93% compared to the blank samples; the inhibition decreased to 84% and 63% after 3 and 4.5 h of photocatalytic pretreatment, respectively.

During biotreatment combined with photocatalytic oxidation, up to 98% of doxycycline was removed from the liquid phase; no increases in SVI or the turbidity of the effluent were observed. In the reference bio-reactor, however, only 88% of doxycycline was eliminated in the first weeks of the experimental run, with a slow decrease to 76% by the end of the experiment. The sOUR of the activated sludge did not reveal significant changes in the course of the experimental run. Likewise, the initial concentration of activated sludge in the active reactor remained stable throughout the experiment at 2.3 g L<sup>-1</sup>. No significant impact of doxycycline addition on BOD<sub>7</sub> removal was observed; thus, the process remained sustainable for a DOC removal efficiency of ca. 90%. In the reference reactor, decreases in the activated sludge concentration (to 1.8 g L<sup>-1</sup>) and sOUR (by 40%) were observed by the end of the experimental run; however, the BOD<sub>7</sub> and DOC removal remained unchanged (99% and 90%, respectively). In both cases, the main doxycycline removal route during biotreatment was adsorption on the activated sludge; by this method, the doxycycline concentrations on activated sludge reached 3.4 and 10.5 mg g<sup>-1</sup> for the active and reference bio-reactors, respectively.

## Discussion

The specific requirements for the operation of a suspended-bed photocatalytic reactor are the adhesion and attrition properties of the bed materials; these determine the choice of process operating parameters that provide low levels of turbidity of the treated solutions along with maximized doxycycline degradation rates. Furthermore, the compromise between the abrasion resistance of the TiO<sub>2</sub> coatings (*i.e.* low turbidity after 3 h of fluidization) and their photocatalytic activity influenced the choice of the coating preparation procedure in our previous study; different coated-bed preparation methods resulted in turbidity variations from 0 to 160 FAU and photocatalytic efficiency variations from negligible values to

2.3 mg W<sup>-1</sup> h<sup>-1</sup>.<sup>25</sup> In this study, the application of previously optimized TTTP-based sol-gel titania-coated expanded clay granules enabled narrowing of the accepted turbidity range to 0 to 20 FAU.

During suspended-bed reactor operation, the bed loading determines the minimum fluidization velocity,  $v_{mg}$ , whereas an increase in  $v_g$  over  $v_{mg}$  decreases the overall photocatalytic efficiency. The increase in shear force results in enhanced attrition of the coatings. Thus, elevated turbidity levels, along with an increased amount of fluidization medium (air bubbles) in the solution, lead to shielding of UV-A irradiation, reducing the overall efficiency of photocatalytic oxidation. Under a range of operating conditions, the photocatalytic efficiency decreased proportionally to the increase in turbidity of the solutions (Fig. 1); UV-A shielding due to abrasion of the coated granules is believed to be the dominant factor.

In a similar manner, increasing the bed loading, the other defining operating parameter of the process performance, improves the photocatalytic efficiency by intensifying the mass transfer up to a specific bed-loading value. Further increase in the bed loading deteriorates the photocatalytic oxidation performance because of higher mechanical stress on the coatings, resulting in higher turbidity levels of the treated solutions.

Further improvement of the abrasion resistance of the coating should facilitate the overall performance of suspended- or fluidized-bed photocatalytic reactors, allowing higher bed loadings to be applied.

The solution turbidity caused by the attrition of non-coated expanded clay granules did not exceed 18 FAU; thus, solution turbidities surpassing this value during operation with coated bed materials (Fig. 1 lower) should be attributed to attrition of the sol-gel coating.

When studying the preparation of the coatings,<sup>25</sup> the addition of P25 to the sol-gel improved the photocatalytic activity of the coatings; however, the turbidity increased. The importance of the ability to reuse catalytic materials is directly related to the mechanical stability of the coatings. To improve this, we investigated the reuse potential of the coatings with previously optimized compositions in comparison with that of the coatings without P25, which previously demonstrated zero turbidity levels. The difference in shear forces applied in the course of bed fluidization in small (0.2 L) and larger-scale (2 L) laboratory reactors determines the attrition between the coatings prepared by previously optimized (with P25) and modified (without P25) methods.

The abrasion resistance of the coatings was not influenced by changes in the drying and calcination preparation step, where nitrogen atmosphere was applied instead of air. Calcination in nitrogen atmosphere, however, slightly increased the photocatalytic activity of the coatings, probably due to the different interactions of expanded clay, a complex material of natural origin, with sol-gel under inert and oxidative conditions. However, the lower adsorption capacity of the coated bed toward doxycycline, resulting from these changes in chemism, deteriorated the overall performance of the coatings.

In experimental runs with repeated use of the sol-gel-coated expanded clay granules, a more profound decrease in solution turbidity was obtained with the P25-containing coatings in three cycles (Fig. 2). The addition of P25 to the sol-gel affects the viscosity of the coating solution, thus presumably influencing the permeability of the sol-gel into the porous support material (specific surface area of *ca.*  $0.8 \text{ m}^2 \text{ g}^{-1}$ , external surface area of *ca.*  $4 \times 10^{-4} \text{ m}^2 \text{ g}^{-1}$ ).<sup>25</sup> Therefore, the abrasion of granules containing higher amounts of sol-gel coating may cause the higher level of turbidity observed in the third cycle of the experimental run.

The decreases in photocatalytic activity observed in the study of the reuse of coated granules prepared with and without P25 powder can be attributed to both attrition of the support material and abrasion of the coatings. However, the changes in the solution matrix due to the presence of expanded clay were examined earlier by monitoring changes in the pH of distilled water after addition of the granules. In the experimental runs, the pH increased from 4.1 to 6.8 due to the elution of inorganic compounds into the solution (also due to some extent to doxycycline degradation and adsorption on the bed material); thus, the accumulation of these inorganic ions at the support material surface could decrease the photocatalytic activity of the coatings. However, the photocatalytic activity of coatings containing higher amounts of titanium dioxide, *i.e.* with added P25 powder, maintained higher photocatalytic efficiency during the reuse cycles.

The photocatalytic oxidation efficiency of doxycycline, prednisolone, amoxicillin and sulfamethizole as single pollutants correlated with their adsorption onto the sol-gel-coated expanded clay granules. The results are also in agreement with the data on photocatalytic oxidation of these pharmaceuticals in P25 slurry, where doxycycline and prednisolone were degraded faster than amoxicillin and sulfamethizole due to their different molecular structures and higher adsorption affinities to  $\text{TiO}_2$ .<sup>6–9</sup> Higher adsorption affinities of the pollutants were accompanied by higher photocatalytic oxidation efficiencies, presumably due to direct reactions on the surface of  $\text{TiO}_2$ . Higher adsorption on the coated-bed materials is a prerequisite for superior elimination of pollutants by the combination of photocatalytic oxidation and adsorptive removal processes. Consequently, pharmaceuticals less prone to adsorption have lower reaction probabilities and thus demonstrate lower degradation efficiencies and lower overall removal. In the case of simultaneous photocatalytic oxidation, the sequence of the oxidation efficiencies of the individual compounds remains the same: under the conditions of competitive adsorption and oxidation, doxycycline, which has the highest adsorption on the coated expanded clay granules, has also the highest oxidation efficiency.

The lower toxicity of photocatalytically treated doxycycline solution compared to that of a solution treated in the dark can be explained by partial decomposition of doxycycline and the absence of toxic by-products (Fig. 5).

The concentrations of doxycycline decreased during adsorption and photocatalytic oxidation; however, they still exceeded

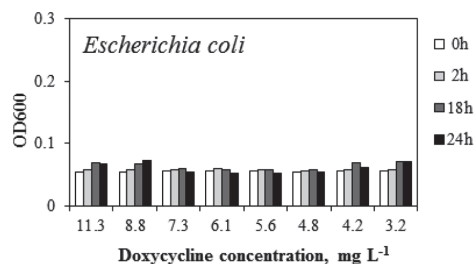


Fig. 6 The growth inhibition of *E. coli* by model doxycycline solutions.

the MIC concentrations measured for the studied bacterial strains. The antimicrobial activity (toxicity) of model doxycycline solutions with concentrations equal to those in samples that were photocatalytically pretreated for 0, 0.5, 1, 1.5, 2, 2.5, 3 and 4 h (11.3 to 3.2 mg L<sup>-1</sup>, respectively) was measured with *E. coli* (Fig. 6), *S. aureus*, *P. putida* and Dev3 (not shown).

In contrast, model doxycycline solutions with concentrations identical to those of the photocatalytically pretreated samples exhibited no decrease in toxicity.

When comparing the antimicrobial properties of the photocatalytically pretreated solution, where antimicrobial activity decreased, and the model solution, with a doxycycline concentration corresponding to that in the photocatalytically pretreated solution, the antimicrobial activity remained unchanged; this may be due to the net effects of the change in pH and the presence of multivalent cations in the solution. In aqueous medium, leaching from the expanded clay bed material leads to the accumulation of metal ions in the solution. At the same time, it has been reported that the presence of multivalent cations, such as  $\text{Fe}^{2+/3+}$ ,  $\text{Mg}^{2+}$ ,  $\text{Al}^{3+}$  and  $\text{Ca}^{2+}$ , markedly suppresses the antimicrobial activity of tetracyclines due to the formation of chelate complexes.<sup>31</sup>

The combination of the photocatalytic pretreatment of doxycycline solution with biological oxidation has been demonstrated to result in both the accumulation of antibiotics on the activated sludge and their removal from the water; the operation of the biological system was not considerably affected by the presence of partially photocatalytically degraded pharmaceuticals.

## Experimental

### Photocatalytic oxidation

**Suspended catalyst bed reactor setup.** A photocatalytic suspended-bed 2 L reactor composed of UV-A-transmitting Plexiglas® XT (Evonik) with an inner diameter of 144 mm was the basis of the experimental setup, as shown in Fig. 7. The bed was fluidized by pressurized air supplied through a diffuser installed in the bottom of the reactor.

The pressurized air was humidified in a pre-column in order to minimize water losses in the treated solution during operation. Four 24-W low-pressure UV-A lamps (Philips PL-L)

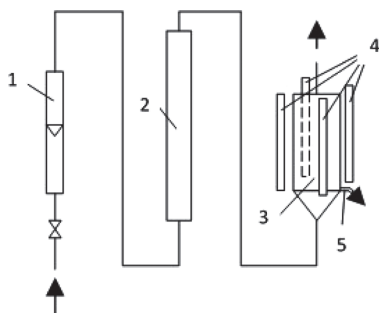


Fig. 7 Experimental setup: 1 – rotameter, 2 – air humidifier, 3 – reactor, 4 – UV-A-lamps, 5 – sample port.

with maximum emission at 365 nm placed around the reactor were used as the UV source; the average UV-A light intensity of ca.  $2.9 \text{ mW cm}^{-2}$  inside the reactor was measured by a fibre-optic spectrometer (USB-2000 + UV-VIS-ES, Ocean Optics Inc.). Periodic measurements of the UV-A transmittance of the reactor walls showed that it remained virtually unchanged during the reactor operation.

The influence of the operating parameters on the reactor performance was studied by varying the air superficial velocity,  $v_g$ , in the range of 4 to  $8 \text{ cm s}^{-1}$  (corresponding to a volumetric airflow range of  $2.5$  to  $4.5 \text{ m}^3 \text{ h}^{-1}$ ) and by varying the coated bed loading from 7 to  $23 \text{ g L}^{-1}$ . The temperature of the solution in the reactor was not additionally regulated; equilibrium was reached between the surrounding temperature, heating by the UV-A lamps, and cooling by the air fluidizing of the bed, resulting in temperatures  $20 \pm 4 \text{ }^\circ\text{C}$ . The experimental runs lasted from 3 to 4 hours (for details, see the Results section). To account for the effects of adsorption of the pollutants onto the coated bed, all the experimental runs were repeated under the same process conditions in the dark (reference experiments), with the reactor shielded from UV-A irradiation to maintain the same temperature range.

**Materials and analysis.** Doxycycline hydrochloride (AppliChem Panreac), sulfamethizole, amoxicillin and prednisolone 21-hemisuccinate sodium salt (Sigma) were used as model water micropollutants at initial concentrations of  $25 \text{ mg L}^{-1}$  as single compounds and at  $10 \text{ mg L}^{-1}$  each in a mixture.

The concentrations of amoxicillin, doxycycline, prednisolone and sulfamethizole were analyzed by high-performance liquid chromatography combined with a diode array detector and mass spectrometer (HPLC-PDA-MS, Shimadzu LC-MS 2020). A Phenomenex Gemini-NX 5u C18 110A  $150 \times 2.0 \text{ mm}$  column, inner diameter  $1.7 \mu\text{m}$ , was used with two eluents, 0.1% acetic acid aqueous solution (eluent A) and acetonitrile (eluent B), with a total eluent flow of  $0.3 \text{ mL min}^{-1}$ ; the starting concentration of eluent B was 5%, increased to 48.5% over 23 minutes with a linear gradient, maintained at that concentration for two minutes, and then decreased to 5% over 30 minutes, during a 30-minute analysis. Mass spectra were

acquired in full scan mode; the MS was operated in positive ionization mode with an interface voltage of 4.5 kV and a detector voltage of 1.1 kV. A diode array detector was set to scan samples at 190 to 800 nm. The instrument was operated and the results obtained from the MS and PDA detectors were processed using Shimadzu LabSolutions software.

To express the micropollutant degradation results, the photocatalytic oxidation efficiency  $E$ ,  $\text{mg W}^{-1} \text{ h}^{-1}$ , was used; this is defined as the decrease in the amount of the pollutant in  $\text{mg}$  divided by the product of UV-A radiation intensity in  $\text{W m}^{-2}$ , the surface of the treated solution, in  $\text{m}^2$ , and the irradiation time, in  $\text{h}$ .<sup>32</sup> The photocatalytically oxidized amount of micropollutant was calculated as the difference between the quantities removed in the photocatalytic and reference experiments. The first number accounts for the removal of the compound by the net effects of oxidation and adsorption, and the second number accounts for the removal in the course of dark adsorption. Thus, the effect of adsorption is subtracted from the  $E$ .

**Preparation of titania coatings.** The titania coatings were deposited on lightweight expanded clay aggregates (Saint-Gobain Leca) 2 to 3 mm in diameter. The catalyst was attached onto these granules via a sol-gel method using a dip coating technique, as described in our previous study.<sup>25</sup> The titanium tetraisopropoxide-based (TTIP-based) coating was prepared according to a procedure optimized earlier.<sup>25</sup> Two procedure modifications were also used in the present research: (a) the coating was prepared without the addition of P25  $\text{TiO}_2$  (Evonic) powder; (b) the drying and the calcination of the coating were carried out in an atmosphere of nitrogen instead of air.

The structural stability and abrasion resistance of the coatings were monitored by turbidity measurements of the treated solutions at 860 nm in Formazin Attenuation Units (FAU turbidity, Hach DR2800).

To study the potential reuse of the catalysts, expanded clay coated granules used in an experimental run were collected and regenerated for 5 hours in water under UV-A irradiation. Two 15 W low-pressure mercury lamps (Philips) with maximum emission at 365 nm were applied in this procedure. The losses of bed material during three cycles of granule reuse were negligible.

### Evaluation of the antibacterial activity of doxycycline solutions

**Single bacterial strain colonies.** In order to evaluate the antibacterial properties (toxicity) of the samples, growth inhibition assays of bacteria with different origins were applied. *Escherichia coli* 1655 (*E. coli* K12BW30270; intestinal bacterium, Gram<sup>-</sup>), *Staphylococcus aureus* RN4220 (opportunistic pathogenic bacterium, Gram<sup>+</sup>), *Pseudomonas putida* KT2440 (environmental bacterium, Gram<sup>+</sup>), and a bacterial strain freshly isolated from the activated sludge (Dev3; Fig. S1 in the ESI†) were used as the test bacteria. The initial concentrations of the bacteria, measured by the conventional plate counting method, in the tests were as follows: *E. coli* –  $5 \times 10^6$  bacterial cells  $\text{mL}^{-1}$ , *S. aureus* –  $4 \times 10^7$  bacterial cells  $\text{mL}^{-1}$ , *P. putida* and strain Dev3 –  $1 \times 10^6$  bacterial

cells mL<sup>-1</sup>. The pure cultures of bacteria, stored frozen in 15% glycerol at -70 °C, were pre-grown overnight in 3 mL of Mueller–Hinton (M–H) broth (Sigma-Aldrich Inc.; composition, g L<sup>-1</sup>: beef infusion solids - 2.0, casein hydrolysate, 17.5 g, starch - 1.5 g) at a temperature of 30 °C on a rotary shaker (200 rpm). After overnight incubation, a second transfer was performed from the tubes into 30 mL of fresh M–H broth (with 1:50 dilution). These second cultures were grown for 2 to 3 h to attain the exponential growth stage; the optical density 0.30 at 600 nm (OD<sub>600</sub> = 0.30) was detected by a Multiskan Spectrum microplate spectrophotometer (Thermo Electron Corporation, Finland). The bacterial cultures were then harvested by centrifugation at 3500g for 7 min (Sigma 3-16PK, Germany) and washed twice with fresh M–H broth. The washed cells were suspended and diluted with the same broth to optical density OD<sub>600</sub> = 0.10. The assay was performed in 96-well polypropylene microplates (Falcon) with a 200 µL final volume per well. Each well contained 100 µL of the serially diluted sample and 100 µL of the test bacteria culture (OD<sub>600</sub> = 0.10) in M–H broth. The OD<sub>600</sub> of the bacterial and test sample mixtures (the model antibiotic solution and solutions treated in either photocatalytic or dark adsorption (reference) experimental runs) in the wells was recorded initially and then after 1, 2, 3, 16, 18, 20 and/or 24 h of incubation at 30 °C on a microplate shaker (Titramax 1000, Heidolph). The minimal inhibitory concentrations (MICs) were determined as the lowest concentration of the antibiotic doxycycline at which no turbidity from microbial growth could be observed.

The Mueller–Hinton (M–H) medium used for the time-dependent growth study of test bacteria is recommended by the Food and Drug Administration, the World Health Organization and the Clinical Laboratory Standard Institute for testing the most commonly encountered aerobic and facultative anaerobic bacteria in food and clinical materials. This medium shows good batch-to-batch reproducibility; it is low in sulfonamide, trimethoprim, and tetracycline inhibitors and yields satisfactory growth of heterotrophic bacteria.

**Mixed bacterial colonies from activated sludge.** The growth inhibition activities of photocatalytically pretreated doxycycline solutions were also evaluated using the traditional plate colony counting method of aerobic sludge bacteria. Activated sludge was diluted 100 times in physiological saline (0.9% NaCl) to obtain a reasonable number of colonizing bacteria on plates; 200 µL of this bacterial solution were mixed with 5 mL of sample containing an antibacterial agent. After 24 h, the 50 µL were transferred to and spread on a plate containing Plate Count Agar (Vegitone, Sigma-Aldrich) and immediately incubated at 21 ± 1 °C for 72 h. Control plates were produced identically, using deionized water instead of antibiotic solution; the tests were performed in triplicate. All plates were counted, and the inhibition *I* in % was calculated as  $I = ((N_0 - N)/N_0) \times 100\%$ , where  $N_0$  and  $N$  are the mean numbers of counted colonies on the non-exposed and antimicrobial-treated agar plates at the end of the incubation period, respectively.<sup>33</sup>

## Aerobic bio-oxidation

**Reactor setup and procedure.** Two continuous flow stirred-tank reactors (CSTR; aeration basin 7.5 L, clarifier 2.5 L) with automatically controlled supporting equipment were colonized by activated sludge obtained from a municipal wastewater treatment plant (Paljassaare WWTP, Tallinn, Estonia). On the basis of preliminary experimental runs (not described in this manuscript for the sake of brevity), the following combination of photocatalytic and biological processes was studied: 4.5 h photocatalytic treatment of 10 mg L<sup>-1</sup> of doxycycline solution (air velocity in photocatalytic reactor: 5 cm s<sup>-1</sup>, catalyst coated bed loading: 19 g L<sup>-1</sup>) followed by biological treatment. The hydraulic retention time (HTR) in the CSTR reactor was 24 h. The activated sludge used in the experiments was acclimated for 55 days to model wastewater and for another 24 days to wastewater containing doxycycline. Subsequently, the photocatalytically pretreated model doxycycline solution was directed to one of two reactors for 42 days, while another reactor was operated as a reference with untreated model solution to acquire conventional aerobic biological treatment data. The model wastewater (bacteriological peptone 0.16 g L<sup>-1</sup>, beef extract 0.11 g L<sup>-1</sup>, urea 0.03 g L<sup>-1</sup>, Na<sub>2</sub>HPO<sub>4</sub>·12H<sub>2</sub>O 0.057 g L<sup>-1</sup>, NaCl 0.007 g L<sup>-1</sup>, CaCl<sub>2</sub> 0.003 g L<sup>-1</sup>, MgSO<sub>4</sub>·7H<sub>2</sub>O 0.002 g L<sup>-1</sup>, CH<sub>3</sub>COONa 0.06 g L<sup>-1</sup>) was continually directed to both bio-reactors;<sup>34</sup> the streams were not mixed with antibiotic-containing solution to prevent loss of the target compound due to its (target compound) adsorption on the materials of the model wastewater delivery system. The reactors were operated at room temperature (20 ± 1 °C), and the dissolved oxygen levels remained between 2 and 4 mgO<sub>2</sub> L<sup>-1</sup>. The concentration ratio of mixed liquor suspended solids to mixed liquor volatile suspended solids (MLVSS/MLSS) remained in the range of 0.79 to 0.91. The CSTR reactors were operated with organic loadings, expressed as chemical oxygen demand (COD), of 210 ± 15 mg COD day<sup>-1</sup> L<sup>-1</sup>.

**Analysis.** The 7-day biochemical oxygen demand (BOD<sub>7</sub>), COD, turbidity, MLSS, MLVSS, sludge volume index (SVI), and specific oxygen uptake rate (sOUR) were determined according to standard methods for water and wastewater analysis.<sup>35</sup>

The turbidity, NH<sub>4</sub>-N, NO<sub>3</sub>-N, NO<sub>2</sub>-N, total nitrogen (TN) and dissolved organic carbon (DOC) concentration were also measured in the effluent and influent samples. The DOC and TN were measured by a total organic carbon (TOC/TN) analyzer (Multi N/C 3100, Analytik Jena); the lowest calibration value of the respective methods was 0.5 mg L<sup>-1</sup>. The concentrations of total ammonia were measured spectrophotometrically by ammonium cuvette tests (Hach Lange DR 2800, LCK 302). NO<sub>2</sub>-N and NO<sub>3</sub>-N were determined by ion chromatography (Metrohm 761 Compact IC).

The effluent average oxidation state (AOS) was calculated as  $AOS = 4 \times (DOC-COD)/DOC$ , where DOC and COD are expressed in molar concentration.<sup>36</sup>

**Determination of doxycycline in the effluent.** The samples were purified and concentrated before analysis using Strata WC-XL (500 mg per 6 mL) extraction cartridges. Prior to

sample loading, the cartridges were activated with 6 ml methanol followed by 6 ml deionized water. After loading the sample with 0.005 g L<sup>-1</sup> dissolved Na<sub>2</sub>EDTA and adjusting the pH to 5 to 6 using H<sub>2</sub>SO<sub>4</sub>, the cartridges were washed with 6 mL of deionized water and 6 mL of methanol. The cartridges were dried under vacuum for 25 min; then, the cartridge was eluted using 5% formic acid in methanol. The eluate was evaporated to dryness on a water bath under a moderate stream of nitrogen and re-diluted in the initial mobile phase for HPLC analysis (0.3% formic acid, 5% acetonitrile in deionized water). Matrix-matched standards were used for calibration (detector – MS). Linear calibration ranged from 0.01 to 0.5 mg L<sup>-1</sup>. All calibration curves were essentially linear, with determination coefficients greater than 0.99.

**Determination of doxycycline adsorbed on activated sludge.** 80 mL of sample from the bioreactor were centrifuged (2600 rpm); the liquid was then separated, and 15 mL of Mellvaine/EDTA extraction solution (pH 5) were added. Extraction was performed for 20 min in an ultrasound bath. After ultrasonication, the samples were centrifuged for 30 min (2600 rpm). After the extract was separated, the extraction cycle was repeated (up to 8 times). The extract was collected and filtered through an Express Plus® Membrane. The concentrations were measured using HPLC with a previously calibrated PDA detector for quantification (an MS detector was used for the *m/z* control). Linear calibration ranged from 0.5 to 50 mg L<sup>-1</sup>, with determination coefficients greater than 0.99; the recovery ratio of the described method was 81 ± 6%.

**HPLC-PDA-MS (section 2.1.2) settings.** Eluent A – 0.3% formic acid aqueous solution, eluent B – 0.3% formic acid in acetonitrile; a binary gradient was used with a flow rate of 0.30 mL min<sup>-1</sup>, where the starting concentration of eluent B was 5% for the first 3 min, increased to 95% by 12 min, held for 2 min and then decreased to 5% by 20 min, followed by 3 min for re-equilibration. Mass spectra were acquired in full scan mode and selected ion mode (SIM) by positive ion electrospray ionization (ESI). The nebulizing and the drying gas flow rates were set to 1.1 and 20 L min<sup>-1</sup>, respectively; the heat block and desolvation line temperatures were 100 °C and 250 °C, respectively; the interface voltage was 3.1 kV.

## Conclusions

A photocatalytic suspended-bed reactor utilizing TiO<sub>2</sub>-coated expanded clay granules as bed material for the degradative removal of pharmaceuticals was successfully scaled up by an order of magnitude in comparison to the authors' previous studies. The efficiency of photocatalytic pretreatment is related to the adsorption affinities of the drug molecules towards the coated expanded clay, and the following sequence was obtained for the studied compounds: doxycycline > prednisolone > amoxicillin > sulfamethizole.

Despite the considerable shear forces typical of a fluidized-bed regime, the choice of operating parameters can provide satisfactory pollutant removal, ensuring the effective

performance of photocatalytic coatings. These sol-gel-coated expanded clay granules could be a good basis for the further development of coating preparation procedures, resulting in coatings with improved abrasion resistance and photocatalytic properties.

The toxicity of antibiotics, using doxycycline as an example, to model and environmental bacterial strains noticeably decreased during the photocatalytic pretreatment in the following order: *E. coli* > *P. putida* > Dev3 (activated sludge bacterium strain) > *S. aureus*, indicating that no toxic oxidation by-products formed.

The decrease in antimicrobial activity is an essential prerequisite for the implementation of photocatalytic processes as a pretreatment stage prior to biological treatment of water polluted by drug molecules, or as a post-treatment; this implementation would substantially decrease the micropollutant load in the environment.

## Acknowledgements

The financial support from the Estonian Research Council (grant G8978, project IUT1-7) and Archimedes Foundation project 3.2.0801.11-0009 is greatly appreciated. The authors express their gratitude to the Deutsche Forschungsgesellschaft (DFG) (grant DE 598/26-1). We thank Pille Laas and Anastasia Laidna for assistance in the laboratory.

## Notes and references

- 1 S. Mompelat, B. Le Bot and O. Thomas, Occurrence and fate of pharmaceutical products and by-products, from resource to drinking water, *Environ. Int.*, 2009, **35**, 803–814.
- 2 K. Kummerer, Antibiotics in the aquatic environment - A review - Part I, *Chemosphere*, 2009, **75**, 417–434.
- 3 K. Ikehata, N. J. Naghashkar and M. G. Ei-Din, Degradation of aqueous pharmaceuticals by ozonolysis and advanced oxidation processes: A review, *Ozone: Sci. Eng.*, 2006, **28**, 353–414.
- 4 A. Nikolaou, S. Meric and D. Fatta, Occurrence patterns of pharmaceuticals in water and wastewater environments, *Anal. Bioanal. Chem.*, 2007, **387**, 1225–1234.
- 5 A. Rozkov, I. Vassiljeva, M. Kurvet, A. Kahru, S. Preis, A. Kharchenko, M. Krichevskaya, M. Liiv, A. Kaard and R. Vilu, Laboratory study of bioremediation of rocket fuel-polluted groundwater, *Water Res.*, 1999, **33**, 1303–1313.
- 6 D. Klauson, M. Krichevskaya, M. Borissova and S. Preis, Aqueous photocatalytic oxidation of sulfamethizole, *Environ. Technol.*, 2010, **31**, 1547–1555.
- 7 D. Klauson, J. Babkina, K. Stepanova, M. Krichevskaya and S. Preis, Aqueous photocatalytic oxidation of amoxicillin, *Catal. Today*, 2010, **151**, 39–45.
- 8 D. Klauson, A. Poljakova, N. Pronina, M. Krichevskaya, A. Moiseev, T. Dedova and S. Preis, Aqueous Photocatalytic

- Oxidation of Doxycycline, *Journal of Advanced Oxidation Technologies, J. Adv. Oxid. Technol.*, 2013, **16**, 234–243.
- 9 D. Klauson, J. Pilnik-Sudareva, N. Pronina, O. Budarnaja, M. Krichevskaya, A. Kaekinen, K. Juganson and S. Preis, Aqueous photocatalytic oxidation of prednisolone, *Cent. Eur. J. Chem.*, 2013, **11**, 1620–1633.
- 10 P. Drillia, S. N. Dokianakis, M. S. Fountoulakis, M. Kornaros, K. Stamatelatou and G. Lyberatos, On the occasional biodegradation of pharmaceuticals in the activated sludge process: The example of the antibiotic sulfamethoxazole, *J. Hazard. Mater.*, 2005, **122**, 259–265.
- 11 N. Prado, J. Ochoa and A. Amrane, Biodegradation by activated sludge and toxicity of tetracycline into a semi-industrial membrane bioreactor, *Bioresour. Technol.*, 2009, **100**, 3769–3774.
- 12 B. Li and T. Zhang, Biodegradation and Adsorption of Antibiotics in the Activated Sludge Process, *Environ. Sci. Technol.*, 2010, **44**, 3468–3473.
- 13 Y. J. Shi, X. H. Wang, Z. Qi, M. H. Diao, M. M. Gao, S. F. Xing, S. G. Wang and X. C. Zhao, Sorption and biodegradation of tetracycline by nitrifying granules and the toxicity of tetracycline on granules, *J. Hazard. Mater.*, 2011, **191**, 103–109.
- 14 S. F. Yang, C. F. Lin, A. Y. C. Lin and P. K. A. Hong, Sorption and biodegradation of sulfonamide antibiotics by activated sludge: Experimental assessment using batch data obtained under aerobic conditions, *Water Res.*, 2011, **45**, 3389–3397.
- 15 S. Kim, P. Eichhorn, J. N. Jensen, A. S. Weber and D. S. Aga, Removal of antibiotics in wastewater: Effect of hydraulic and solid retention times on the fate of tetracycline in the activated sludge process, *Environ. Sci. Technol.*, 2005, **39**, 5816–5823.
- 16 N. Prado, J. Ochoa and A. Amrane, Biodegradation and biosorption of tetracycline and tylosin antibiotics in activated sludge system, *Process Biochem.*, 2009, **44**, 1302–1306.
- 17 M. H. Huang, Y. D. Yang, D. H. Chen, L. Chen and H. D. Guo, Removal mechanism of trace oxytetracycline by aerobic sludge, *Process Saf. Environ.*, 2012, **90**, 141–146.
- 18 P. N. Carvalho, A. Pirra, M. C. P. Basto and C. M. R. Almeida, Activated sludge systems removal efficiency of veterinary pharmaceuticals from slaughterhouse wastewater, *Environ. Sci. Pollut. Res.*, 2013, **20**, 8790–8800.
- 19 C. Reyes, J. Fernandez, J. Freer, M. A. Mondaca, C. Zaror, S. Malato and H. D. Mansilla, Degradation and inactivation of tetracycline by TiO<sub>2</sub> photocatalysis, *J. Photochem. Photobiol. A*, 2006, **184**, 141–146.
- 20 V. M. Mboula, V. Hequet, Y. Gru, R. Colin and Y. Andres, Assessment of the efficiency of photocatalysis on tetracycline biodegradation, *J. Hazard. Mater.*, 2012, **209**, 355–364.
- 21 E. Adamek, W. Baran and A. Sobczak, Photocatalytic degradation of veterinary antibiotics: Biodegradability and antimicrobial activity of intermediates, *Process Saf. Environ.*, 2016, **103**, 1–9.
- 22 S. Yahiat, F. Fourcade, S. Brosillon and A. Amrane, Removal of antibiotics by an integrated process coupling photocatalysis and biological treatment - Case of tetracycline and tylosin, *Int. Biodeterior. Biodegrad.*, 2011, **65**, 997–1003.
- 23 A. V. Vorontsov, E. N. Savinov and P. G. Smirniotis, Vibrofluidized- and fixed-bed photocatalytic reactors: case of gaseous acetone photooxidation, *Chem. Eng. Sci.*, 2000, **55**, 5089–5098.
- 24 J. Werther, Fluidized-Bed Reactors, in *Ullmann's Encyclopedia of Industrial Chemistry*, ed. B. Elvers, Wiley-VCH, Weinheim, 2007.
- 25 N. Pronina, D. Klauson, A. Moiseev, J. Deubener and M. Krichevskaya, Titanium dioxide sol-gel-coated expanded clay granules for use in photocatalytic fluidized-bed reactor, *Appl. Catal., B*, 2015, **178**, 117–123.
- 26 R. H. Perry and D. H. Green, *Perry's Chemical Engineers' Handbook*, McGraw-Hill, 1997.
- 27 J. D. Brewster, A simple micro-growth assay for enumerating bacteria, *J. Microbiol. Methods.*, 2003, **53**, 77–86.
- 28 M. Novak, T. Pfeiffer, M. Ackermann and S. Bonhoeffer, Bacterial growth properties at low optical densities, *Anton Leeuw. Int. J. G.*, 2009, **96**, 267–274.
- 29 S. Suppi, K. Kasemets, A. Ivask, K. Kunnis-Beres, M. Sihtmae, I. Kurvet, V. Aruoja and A. Kahru, A novel method for comparison of biocidal properties of nanomaterials to bacteria, yeasts and algae, *J. Hazard. Mater.*, 2015, **286**, 75–84.
- 30 J. J. Li and E. J. Corey, *Drug Discovery: Practices, Processes, and Perspectives*, Wiley, 2013.
- 31 E. D. Weinberg, The mutual effects of antimicrobial compounds and metallic cations, *Bacteriol. Rev.*, 1957, **21**, 46–68.
- 32 M. Krichevskaya, T. Malygina, S. Preis and J. Kallas, Photocatalytic oxidation of de-icing agents in aqueous solutions and aqueous extract of jet fuel, *Water Sci. Technol.*, 2001, **44**, 1–6.
- 33 Y. L. Yao, J. Guan, P. Tang, H. P. Jiao, C. Lin, J. J. Wang, Z. M. Lu, H. Min and H. C. Gao, Assessment of toxicity of tetrahydrofuran on the microbial community in activated sludge, *Bioresour. Technol.*, 2010, **101**, 5213–5221.
- 34 M. Bajaj, C. Gallert and J. Winter, Biodegradation of high phenol containing synthetic wastewater by an aerobic fixed bed reactor, *Bioresour. Technol.*, 2008, **99**, 8376–8381.
- 35 L. S. Cleceri and A. E. Greenberg and R. R. Trussel, *Standard methods for the examination of water and wastewater*, APHA, AWWA, WPCF, Washington, DC, 1989.
- 36 V. Sarria, S. Parra, N. Adler, P. Peringer, N. Benitez and C. Pulgarin, Recent developments in the coupling of photo-assisted and aerobic biological processes for the treatment of biorecalcitrant compounds, *Catal. Today*, 2002, **76**, 301–315.



## **APPENDIX B**



# ELULOOKIRJELDUS

## 1. Isikuandmed

Ees- ja perekonnanimi: Natalja Pronina  
Sünniaeg ja -koht: 05.05.1988, Tallinn  
Kodakondsus: Eesti  
E-posti aadress: natalja.pronina@mail.ee

## 2. Hariduskäik

Õppeasutus	Lõpetamise aeg	Haridus (eriala/kraad)
Tallinna Tehnikaülikool	2013	tehnikateaduste magistrikraad
Tallinna Tehnikaülikool	2011	tehnikateaduste bakalaureusekraad
Tallinna Juhkentali Gümnaasium	2007	keskharidus

## 3. Keelteoskus (alg-, kesk-, või kõrgtase)

Keel	Tase
Eesti keel	kõrgtase
Vene keel	kõrgtase (emakeel)
Inglise keel	kõrgtase
Saksa keel	algtase

## 4. Teenistuskäik

Töötamise aeg	Tööandja nimetus	Ametikoht
2016-2017	Tallinna Tehnikaülikool	nooremteadur
2014-2015	Tallinna Tehnikaülikool	insener
2012-2013	Tallinna Tehnikaülikool	projektitäitja

## 5. Kaitstud lõputööd

Tehnikateaduste magistrikraad: Titaandioksiidi kinnitamine keramsiidi pinnale: katete fotokatalüütilise aktiivsuse määramine doksütsükliini lagundamisel ning kinnitusmeetodi optimeerimine, Tallinna Tehnikaülikool, Keemia ja materjalitehnoloogia teaduskond, Keemiatehnika instituut, 2013.

Juhendajad: Marina Kritševskaja; Deniss Klauson.

## 6. Teadustöö põhisuunad

1. Bio- ja keskkonnateadused; 1.9. Keskkonnaohtlike aineid käsitlevad uuringud; CERCS ERIALA: P305 Keskkonnakeemia

4. Loodusteadused ja tehnika; 4.11. Keemia ja keemiatehnika; CERCS ERIALA: P402 Fotokeemia

4. Loodusteadused ja tehnika; 4.11. Keemia ja keemiatehnika; CERCS ERIALA: T350 Keemiatehnoloogia ja -masinaehitus

## 7. Uurimisprojektid

IUT1-7 Keemiatehnikapõhine lähenemisviis prioriteetsete saasteainete ja uute esilekerkivate mikrosaasteainete kõrvaldamisele veest/reoveest ja pinnasest: täiustatud oksüdatsioonitehnoloogiate kasutamine ja optimeerimine.

ETF8978 Toksiliste keskkonnaohtlike ainete lagundamine vees fotokatalüüsi ja bioloogilise oksüdatsiooni kombineerimisel ning õhus fotokatalüüsiga.

AR12046 Uus tehnoloogia keskkonnaohtlike mikrosaasteainete lagundamiseks vesifaasis: molekulaarselt jäljendatud polümeeridest analüütiliste sensoritega varustatud fotokatalüütiline puhastusseade.

## 8. Juhendatud väitekirjad

Anastasia Laidna, magistrikraad, 2016, (juh) Natalja Pronina; Inna Kamenev, Fotokatalüütiliselt töödeldud antibiootikume sisaldava reovee aeroobse biooksidatsiooni uurimine, Tallinna Tehnikaülikool, Keemia ja materjalitehnoloogia teaduskond, Keemiatehnika instituut.

Tatjana Rudenko, magistrikraad, 2015, (juh) Marina Kritševskaja; Deniss Klauson; Natalja Pronina, Fotokatalüütilise keevkihi reaktori uurimine mikrosaasteainete lagundamisel vees, Tallinna Tehnikaülikool, Keemia ja materjalitehnoloogia teaduskond, Keemiatehnika instituut.

Pille Laas, magistrikraad, 2015, (juh) Natalja Pronina; Inna Kamenev, Doksütsükliini määramine vees ja reoveesettes, Tallinna Tehnikaülikool, Keemia ja materjalitehnoloogia teaduskond, Keemiatehnika instituut.

# CURRICULUM VITAE

## 1. Personal data

Name: Natalja Pronina

Date and place of birth: 05.05.1988, Tallinn

Citizenship: Estonian

E-mail address: natalja.pronina@mail.ee

## 2. Education

Educational institution	Graduation year	Education (field of study/degree)
Tallinn University of Technology	2013	M. Sc. in Engineering
Tallinn University of Technology	2011	B. Sc. in Engineering
Tallinn Juhkentali Gymnasium	2007	High school education

## 3. Language competence/skills (fluent, average, basic skills)

Language	Level
Estonian	fluent
Russian	fluent (mother tongue)
English	fluent
German	basic

## 4. Professional employment

Period	Organization	Position
2016-2017	Tallinn University of Technology	early stage researcher
2014-2015	Tallinn University of Technology	engineer
2012-2013	Tallinn University of Technology	project worker

## 5. Defended theses

M.Sc. thesis: Immobilization of titanium dioxide on the surface of expanded clay: measurements of coatings' photocatalytic activity by doxycycline degradation and attachment method optimization, Tallinn University of Technology, Faculty of Chemical and Materials Technology, Department of Chemical Engineering, 2013.

Supervisors: Marina Kritševskaja; Deniss Klauson.

## 6. Main areas of scientific work

1. Biosciences and Environment; 1.9. Research into Substances Hazardous to the Environment; CERCS SPECIALTY: P305 Environmental chemistry

4. Natural Sciences and Engineering; 4.11. Chemistry and Chemical Technology; CERCS SPECIALTY: P402 Photochemistry

4. Natural Sciences and Engineering; 4.11. Chemistry and Chemical Technology; CERCS SPECIALTY: T350 Chemical technology and engineering

## 7. Research projects

IUT1-7 Chemical engineering approach to removal of priority pollutants and emerging micropollutants from water/wastewater and soil: implementation and optimization of advanced oxidation technologies.

ETF8978 Degradation of environmentally toxic refractory compounds in water by combination of photocatalysis and biological treatment and in air by photocatalysis.

AR12046 The New Technology for Wastewater Treatment by Photocatalytic Oxidation Combined with Molecularly Imprinted Polymers as Analytical Sensors.

## 8. Supervised dissertations

Anastasia Laidna, Master's Degree, 2016, (sup) Natalja Pronina; Inna Kamenev, Bio-oxidation of photocatalytically pretreated antibiotic containing wastewater, Tallinn University of Technology, Faculty of Chemical and Materials Technology, Department of Chemical Engineering.

Tatjana Rudenko, Master's Degree, 2015, (sup) Marina Kritševskaja; Deniss Klauson; Natalja Pronina, Performance of photocatalytic fluidized-bed reactor in the degradation of aqueous-phase environmental micropollutants, Tallinn University of Technology, Faculty of Chemical and Materials Technology, Department of Chemical Engineering.

Pille Laas, Master's Degree, 2015, (sup) Natalja Pronina; Inna Kamenev, Determination of Doxycycline in Water and Activated Sludge, Tallinn University of Technology Faculty of Chemical and Materials Technology, Department of Chemical Engineering.

**DISSERTATIONS DEFENDED AT  
TALLINN UNIVERSITY OF TECHNOLOGY ON  
CHEMISTRY AND CHEMICAL ENGINEERING**

1. **Endel Piiraja**. Oxidation and Destruction of Polyethylene. 1993.
2. **Meili Rei**. Lihatehnoloogia teaduslikud alused. Fundamentals of Food Technology. 1995.
3. **Meeme Põldme**. Phase Transformations in Hydrothermal Sintering Processing of Phosphate Rock. 1995.
4. **Kaia Tõnsuaadu**. Thermophosphates from Kovdor and Siilinjärvi Apatites. 1995.
5. **Anu Hamburg**. The Influence of Food Processing and Storage on the N-Nitrosamines Formation and Content in Some Estonian Foodstuffs. 1995.
6. **Ruth Kuldvee**. Computerized Sampling in Ion Chromatography and in Capillary Electrophoresis. 1999.
7. **Külliki Varvas**. Enzymatic Oxidation of Arachidonic Acid in the Coral *Gersemia fruticosa*. 1999.
8. **Marina Kudrjašova**. Application of Factor Analysis to Thermochromatography and Promotion Studies. 2000.
9. **Viia Lepane**. Characterization of Aquatic Humic Substances by Size Exclusion Chromatography and Capillary Electrophoresis. 2001.
10. **Andres Trikkel**. Estonian Calcareous Rocks and Oil Shale Ash as Sorbents for SO<sub>2</sub>. 2001.
11. **Marina Kritševskaja**. Photocatalytic Oxidation of Organic Pollutants in Aqueous and Gaseous Phases. 2003.
12. **Inna Kamenev**. Aerobic Bio-Oxidation with Ozonation in Recalcitrant Wastewater Treatment. 2003.
13. **Janek Reinik**. Methods for Purification of Xylidine-Polluted Water. 2003.
14. **Andres Krumme**. Crystallisation Behaviour of High Density Polyethylene Blends with Bimodal Molar Mass Distribution. 2003.
15. **Anna Goi**. Advanced Oxidation Processes for Water Purification and Soil Remediation. 2005.
16. **Pille Meier**. Influence of Aqueous Solutions of Organic Substances on Structure and Properties of Pinewood (*Pinus sylvestris*). 2007.
17. **Kristjan Kruusement**. Water Conversion of Oil Shales and Biomass. 2007.

18. **Niina Kulik**. The Application of Fenton-Based Processes for Wastewater and Soil Treatment. 2008.
19. **Raul Järviste**. The Study of the Changes of Diesel Fuel Properties a its Long Term Storage. 2008.
20. **Mai Uibu**. Abatement of CO<sub>2</sub> Emissions in Estonian Oil Shale-Based Power Production. 2008.
21. **Valeri Gorkunov**. Calcium-Aluminothermal Production of Niobium and Utilization of Wastes. 2008.
22. **Elina Portjanskaja**. Photocatalytic Oxidation of Natural Polymers in Aqueous Solutions. 2009.
23. **Karin Reinhold**. Workplace Assessment: Determination of Hazards Profile using a Flexible Risk Assessment Method. 2009.
24. **Natalja Savest**. Solvent Swelling of Estonian Oil Shales: Low Temperature Thermochemical Conversion Caused Changes in Swelling. 2010.
25. **Triin Märtsen**. Methodology and Equipment for Optical Studies of Fast Crystallizing Polymers. 2010.
26. **Deniss Klauson**. Aqueous Photocatalytic Oxidation of Non-Biodegradable Pollutants. 2010.
27. **Oliver Järvi**. Intensification of Activated Sludge Process – the Impact of Ozone and Activated Carbon. 2011.
28. **Triinu Poltimäe**. Thermal Analysis of Crystallization Behaviour of Polyethylene Copolymers and Their Blends. 2011.
29. **Mariliis Sihtmäe**. (Eco)toxicological Information on REACH-Relevant Chemicals: Contribution of Alternative Methods to *in vivo* Approaches. 2011.
30. **Olga Velts**. Oil Shale Ash as a Source of Calcium for Calcium Carbonate: Process Feasibility, Mechanism and Modeling. 2011.
31. **Svetlana Jõks**. Gas-Phase Photocatalytic Oxidation of Organic Air Pollutants. 2012.
32. **Aleksandr Dulov**. Advanced Oxidation Processes for the Treatment of Water and Wastewater Contaminated with Refractory Organic Compounds. 2012.
33. **Aleksei Zaidentsal**. Investigation of Estonian Oil Shale Thermo-bituminization in Open and Closed System. 2012.
34. **Dmitri Šumigin**. Composites of Low-Density Polyethylene and Poly(Lactic Acid) With Cellulose and Its Derivatives. 2014.
35. **Aleksandr Käkinen**. The Role of Physico-chemical Properties and Test Environment on Biological Effects of Copper and Silver Nanoparticles. 2014.

36. **Ada Traumann.** Improvement of Work Environment through Modelling the Prevention of Health Risks Focusing on Indoor Pollutants. 2014.
37. **Marika Viisimaa.** Peroxygen Compounds and New Integrated Processes for Chlorinated Hydrocarbons Degradation in Contaminated Soil. 2014.
38. **Olga Budarnaja.** Visible-light-sensitive Photocatalysts for Oxidation of Organic Pollutants and Hydrogen Generation. 2014.
39. **Jelena Hruļjova.** Role of Specifically Interacting Solvents in Solvent Swelling of Kukersite Oil Shale Kerogen. 2014.
40. **Irina Klimova.** Modification of Ammonium Nitrate Fertilizer. 2014.
41. **Julia Krasulina.** Upgrading of Liquid Products from Estonian Kukersite Oil Shale by Catalytic Hydrogenation. 2015.
42. **Irina Epold.** Degradation of Pharmaceuticals by Advanced Oxidation Technologies in Aqueous Matrices. 2015.
43. **Kadriann Tamm.** Leaching of the Water-Soluble Calcium Components of Oil Shale Waste Ash. 2016.
44. **Galina Sharajeva.** Thermochemical Destruction of Graptolite Argillite. 2016.
45. **Juri Bolubajev.** Effects of Organic Reducing Agents on the Fenton-like Degradation of Contaminants in Water with a Ferric Sludge Reuse. 2016.
46. **Can Rüstü Yörük.** Experimental and Modeling Studies of Oil Shale Oxy-fuel Combustion. 2016.
47. **Liina Kanarbik.** Ecotoxicological Evaluation of Shale Fuel Oils, Metal-Based Nanoparticles and Glyphosate Formulations. 2017.

